University of Cincinnati

Date: 6/20/2018

I, Huan Liu, hereby submit this original work as part of the requirements for the degree of Doctor of Philosophy in Pathobiology & Molecular Medicine.

It is entitled:

Discover the Role of Dendritic Cell in Pulmonary Langerhans Cell Histiocytosis And Respiratory Syncytial Virus Infection

Student's name: **Huan Liu**

This work and its defense approved by:

Committee chair: Michael Borchers, Ph.D.

Committee member: Ian Paul Lewkowich, Ph.D.

Committee member: Francis McCormack, M.D.

Committee member: William Miller, Ph.D.

Committee member: Kathryn Wikenheiser-Brokamp, M.D., Ph.D.

30440

The Role of Dendritic Cells in Pulmonary Langerhans Cell Histiocytosis And Respiratory Syncytial Virus Infection

Dissertation submitted to the
Division of Graduate Studies and Research of the University of Cincinnati
In partial fulfillment of the requirements for the degree of

DOCTORATE OF PHILOSOPHY (Ph.D.)

In the Graduate Program of Pathobiology and Molecular Medicine
of the College of Medicine

June 2018
By

Huan Liu

B.S., Hebei North University, China, 2013

Committee chair: Dr. Michael T Borchers., Ph.D.

Thesis Abstract

Dendritic cells (DCs) are the most efficient antigen presentation cells and execute a pivotal role in the onset and regulation of innate and adaptive immune responses and the recruitment of a variety of leukocytes to the site of inflammation or injury. To counter the challenge of continual exposure to exogenous pathogens, the lungs posess a complex immunological defense that is often initiated by DC activation. An increasing volume of research on DCs in recent years clearly shows that the disruption of DC equilibrium in the lung may may be at the root of several varied pulmonary diseases. In these studies, we used two different disease models to elucidate the importance of DCs in response to the control of natural killer cells (NK) in viral infection and the pivotal role of DCs in Pulmonary Langerhans Cell Histiocytosis (PLCH), a disease with a clear gene-environment axis.

Respiratory syncytial virus (RSV) is a common cause of respiratory tract infection in vulnerable populations. Natural killer (NK) cells and DC are important for the effector functions of inflammatory cells following infection. To investigate the importance of NKG2D pathway in regulating RSV infection, wild type and NKG2D deficient mice were infected with RSV. We found that NKG2D deficient mice exhibited greater lung pathology, marked by the accumulation of DCs following RSV infection. DCs isolated from NKG2D deficient mice had

impaired responses towards TLR ligands. DCs expressed NKG2D ligands on their surface, which was further increased in NKG2D deficient mice and during RSV infection. Adoptive transfer of DCs isolated from WT mice into the airways of NKG2D deficient mice ameliorated the enhanced inflammation in NKG2D deficient mice after RSV infection. In summary, we discovered that the NKG2D-dependent interactions with DCs control the phenotype and function of DCs and play a critical role in pulmonary host defenses against RSV infection.

PLCH is a rare interstitial lung disease characterized by focal DC accumulation, bronchiolocentric nodule formation, and cystic remodeling of the lung and occurs predominantly in active smokers. Approximately 50% of PLCH patients harbor somatic BRAF-V600E mutations identified mainly within the DC lineage. However, the rare nature of the disease and lack of animal models impedes the study of the pathogenic mechanisms of PLCH. We have established the first mouse model that recapitulates the hallmark characteristics of PLCH. In addition, we show that the BRAF-V600E mutation is associated with increased DC responsiveness towards multiple stimuli including the DC-chemokine CCL20. We provide evidence that DC accumulation in the lung is due to both increased viability and enhanced recruitment. Further evidence indicates that the accumulation of other inflammatory cells in PLCH is a secondary event driven by CCL7 secreted from DCs in a BRAF-V600E-dependent manner. Moreover, we

demonstrate that the PLCH-like phenotype in the mouse model can be attenuated following smoking cessation and removal of BRAF-V600E DCs. Furthermore, we show PBMCs isolated from PLCH patients harboring the BRAF-V600E mutation produce CCL7. Collectively, our studies provide the first mechanistic insights into the role of DC BRAF-V600E mutation and CS exposure that mediate PLCH pathogenesis.

Collectively, these results support the concept that the delicacy of DC-mediated lung equilibrium can be affected by both innate defects (BRAF-V600E mutation) and interaction of other cells in the local lung microenvironment (NKG2D-dependent editing). Our findings not only provide insights into the pathogenesis of PLCH and severe RSV infection but also broaden the knowledge of basic DC biology and shed light upon other DC-related diseases.

Acknowledgement

I would first like to acknowledgement my mentors Drs. Michael Borchers and Francis McCormack. To Dr. Borchers, your humor, kindness, generousity and passion connect everyone in the lab and create a perfect research environment. Thank you for always being available to me and reminding me to step back and focus on the big picture. To Dr. McCormack, your work ethic, broad interests, and curiosity in science set a perfect example of what an excellent physician scientist should be. You encouraged me to be independent in research yet provided help and advice whenever I needed it. Thank you for being a perfect captain and you will always be my role model. I would also like to thank my committee members, Drs. Kathryn Wikenheiser-Brokamp, Ian Lewkowich and William Miller for all the help you provided along the way. My thesis research was not an easy ride but it was your encouragement and constructive idea-inspiring feedback that made sure it arrived at its destination. To people in the Borchers' lab: Andrew, thank you for being my big brother in science, answering millions of my questions and lighting up the lab environment. Jennifer, thank you for being the back-bone of the lab and I will always cherish our fun animal surgery memories. Most of all, my deepest appreciation to my family. Thank you mom for your unconditional love and support. To my wife Ran. Thank you for taking care of my life and believing in me. You are the color of my life and the source of my courage.

Table of content

List of figures

List of abbreviation

DC - dendritic cell
APC - antigen-presenting cell
HEV - high endothelial venule
HSC - hematopoietic stem cell
CMP - common myeloid progenitor
FLT3 - FMS-related tyrosine kinase 3
MDP - macrophage and DC progenitor
pre-DC - precursor DC
pDC - plasmacytoid DC
cDC - conventional DC
mDC - myeloid DC
cMoP - common monocyte progenitor
moDC - monocyte-derived DC
Batf3 - basic leucine zipper transcription factor ATF-like 3
Irf4 - interferon regulatory factor 4
LN - lymph node
mLN – Mediastinal lymph node
CCR - chemokine receptor
TLR - toll-like receptor
Mtb - Mycobacterium tuberculosis
PLCH - Pulmonary Langerhans cell histiocytosis
MAPK - mitogen-activated protein kinase
COPD - chronic obstructive pulmonary disease
Th1 - T helper type 1 T cell
IFN-γ - interferon-gamma
HP - hypersensitivity pneumonitis
IIP - idiopathic interstitial pneumonia
IPF - idiopathic pulmonary fibrosis
NSIP - nonspecific interstitial pneumonia
GM-CSF - granulocyte-macrophage colony-stimulating factor
NK - natural killer cell
TAM - tamoxifen
FA - filtered air
CS - cigarette smoke
qPCR - quantitative real-time PCR
BMDC - bone marrow derived DC

BCL-XL - B-cell lymphoma-extra large
BAL - bronchoalveolar lavage
BHD - Birt-Hogg-Dubé
LAM – lymphangioleiomyomatosis
PBMC - Peripheral blood mononuclear cell
PBS - phosphate-buffered saline
FMO - fluorescence minus one
SEM - standard errors of the mean
NKT - Nature Killer T cell
ULBP - UL-16 binding protein
NKG2D - killer cell lectin like receptor K1
Mult1 - UL16-binding protein-like transcript 1
Rae1 - retinoic acid–inducible early transcript

Chapter I

Introduction

1.1 Dendritic Cells

Dendritic cells (DCs) were first described by Ralph Steinman and Zanvil Cohn in 1973 as cells with branching, extended cellular processes that distinguish them from other adherent myeloid cells such as monocytes and macrophages (1). DCs are distributed throughout the body and are the "professional" antigen-presenting cells (APCs) of the immune system. Most notably, they are known to acquire antigen in tissues, migrate to draining lymph nodes (LNs), and initiate T cell-mediated immunity. Recently, our understanding of the origins, development, and effector functions of DCs has greatly expanded with the advent of DC-specific reagents and genetically engineered mice (2-8). Human DCs are notoriously difficult to isolate, maintain, and study. Therefore, most of our understanding of DC biology is derived from studies performed in mice.

DCs originate in the bone marrow, circulate in the blood and either enter the LNs via high endothelial venules (HEV) to give rise to lymphoid DCs or enter peripheral tissues to give rise to nonlymphoid DCs (9). Novel reporter mice reveal that DCs arise from monocyte-DC progenitors derived from hematopoietic stem cells (HSC). HSCs give rise to common myeloid progenitors (CMP), including a subset of FMS-related tyrosine kinase 3 (FLT3)- expressing cells, which

differentiate into more restricted macrophage and DC progenitors (MDP) in the bone marrow. The FLT3-expressing MDP are the direct precursors to common DC progenitors, which give rise to precursor DC (pre-DC) and plasmacytoid DC (pDC) (10, 11). Pre-DCs and pDCs leave the bone marrow and travel via the circulation to secondary lymphoid organs and non-lymphoid tissues. Pre-DCs terminally differentiate into conventional-DC (cDC) subsets in the periphery (12). Alternatively, MDP give rise to common monocyte progenitor (cMoP), which differentiate into circulating monocytes (13). Circulating Ly6C+ monocytes migrate into tissue or LNs via the HEV to either give rise to macrophages, if a niche is open, or differentiate into monocyte-derived DC (moDC) (14, 15). MoDCs are defined by their expression of MHC class II and CD11c and their DC functional properties include antigen presentation (16).

1.2 The lung and pulmonary DCs

Humans survive in a dangerous world that continuously faces the challenge of exogenous pathogens. Of all the organs, the lungs are at the frontier of this never-ending battle. To counter this threat, the lungs developed an intricate and complex defense system. The respiratory epithelium participates in this battle as a physical

barrier and by releasing antimicrobial compounds (17). However, if the innate processes of the respiratory epithelium is unable to clear such foreign pathogens, the body's next line of defense is an cellular and molecular immunological orchestra which is conducted by the professional antigen presenting cells – the dendritic cells (18).

In the lung, DCs are present throughout the epithelium and interstitium where they are ideally positioned to monitor the luminal microenvironment (19). DCs are comprised of a heterogeneous population of cells that possess unique sets of cell surface markers in different organs throughout the body. In the lung, DCs can be divided into three major subsets – plasmocytoid DCs (pDCs), conventional DCs (cDCs) and monocyte-derived DCs (moDCs). pDCs are important in maintaining self-tolerance and are responsible for the production of large amounts of type I IFN upon virus infection (20). moDCs are recruited to the lung in the inflammatory status and defined by their expression of major histocompatibility complex class II and CD11c, and their antigen presentation capacity (21). In mice, cDCs are divided into two subsets, CD103+ DCs and CD11b+ DCs, which are developmentally regulated by the transcription factors basic leucine zipper transcription factor ATF-like 3 (Batf3) and interferon regulatory factor 4 (Irf4), respectively. Compared with mouse DCs, there is no clear consensus regarding the classification of human pulmonary cDC subsets. Traditionally, the human cDCs

can be divided into CD1c+ DCs and CD141+ DCs (9). However, this classification is now challenged by a recent study that identified five different DC subsets in human lung based on differential expression of Langerin, CD1c, and CD14 (22). Clearly, it is important to obtain and collate additional transcriptional and functional data to definitively classify human pulmonary DCs and other mononuclear phagocytes. The surface phenotype and receptor expression of different subsets of mouse and human DCs are summarized in Table 1.

Table 1 Cell surface phenotype of human and mouse dendritic cells.

Species	Subpopulation	**Subsets**	**Cell Surface Marker**	**Residence in lung under steady state**	**Toll Like Receptors**	**Chemokine Receptors on Immature DC**	**Chemokine Receptors on Mature DC**
Mouse	**Conventional DC**	CD11b+ DC	CD11c+, CD8α–, CD11bhi, CD103–, MHC class II+, Langerin-	Yes	1,2,4,6,7,8,9,13	CCR1, CCR2, CCR4, CCR5, CXCR3, CXCR4	CCR 7, CXCR4
		CD103+ DC	CD11c+, CD8α–, CD11blo/–, CD103+, MHC class II+, Langerin+	Yes	2,3,4,6,9,11,12,13		
	Plasmacytoid DC	pDC	CD11cint, CD11blo/–, B220+, Ly6c+, MHC class II–/lo, SiglecH+	Yes	7,9,12		
	Monocyte-related DC	MoDC	CD11c+, CD64+, CD11bhi, CD103–, MHC class II+,Langerin-,Ly6C+	No	3,7,8		
Human	**Conventional DC**	CD1c+ DC	CD1c+, CD11b+, CD11c+, CD13+, HLA-DR+, BDCA-1+	Yes	1,2,3,4,5,6,8,10	CCR1, CCR2, CCR4, CCR5, CCR6, CXCR1, CXCR4	CCR 7, CXCR4
		CD141+ DC	CD141+, XCR1+, CLEC9A+, BDCA-3+	Yes	2,3,8		
	Plasmacytoid DC	pDC	CD11cdim, BDCA2+, BDCA4+, CD123+, L-selectin+, IL-3R+, HLA-DR–/lo	Yes	7,9		
	Monocyte-related DC	MoDC	CD14+, HLA-DR+, CD1c-, CD141-, DC-SIGN+, CD163+	No	3,7,8		

1.3 DC localization and migration

In mice, all DC subtypes are found in the lung under steady state conditions (23). However, subsets of lung DCs are differentially distributed. CD103+ DCs are closely associated with the respiratory epithelium and extend processes into the airway lumen, whereas CD11b+ DCs mainly reside beneath the airway basement membrane (Figure 2) (24-26). Under steady-state conditions, a limited number of DCs reside in lung tissue and patrol the environment, while circulating pre-DCs migrate into the lung at a constant rate to replenish the resident DC pool as it turns over every 10-14 days (12, 27, 28). In mice, DCs constitute up to 0.5-2% of total lung leukocytes at steady state (5). Following exposure to antigens, pathogens or pro-inflammatory cytokines, different subsets of lung DCs are rapidly recruited to the lung and comprise up to 5% of total lung leukocytes (18). However, the number of DCs in the lung is difficult to estimate given their relative short lifespan and their migratory behavior. For example, after DCs encounter antigens, they become activated, deploy innate immune defenses, and migrate to draining mediastinal LNs where they initiate adaptive immune responses and facilitate peripheral tolerance (29). Moreover, during inflammation, monocytes are rapidly recruited into the lung, differentiate into moDCs and participate in the

inflammatory response by secreting cytokines and chemokines, which in turn recruit and activate additional leukocytes (Figure 1) (30, 31).

DC migration is tightly regulated by specific chemokines and adhesion molecules under both physiological and inflammatory conditions (23). DC migration from the blood into the inflamed tissues is controlled by several chemokine receptors (CCR) including CCR1, CCR2, CCR5, and CCR6 (32-34). CCR6 on immature DCs and its ligand CCL20 is the most important chemokine axis for recruitment of DC to the lung from the circulation (23, 35). Lung epithelial cells express a basal level of CCL20 to maintain DC homeostasis. However, CCL20 expression is rapidly induced after encountering pathogenic and environmental stimuli (35). Lung DC recruitment is also mediated by additional chemokine receptors, such as CCR2, as well as other factors that facilitate DC migration including E- and P-selectins, adhesion molecule L1, and integrins CD11b/CD18 (36-39).

DC trafficking from the lung to the draining LNs rapidly increases during inflammation and infection (40, 41). Lymphatic channels provide important routes for cell migration and are critical for DC trafficking between peripheral tissues and LNs (42). In the lung, DCs first migrate to bronchopulmonary LNs through the lymphatics then drain into the mediastinal trunk (Figure 2) (43). Egress of DCs from lung to draining LNs is tightly regulated (23). Following pathogenic or environmental activation, DCs undergo maturation, decrease CCR6 expression and

increase CCR7 expression (23, 44). CCR7 is the chemokine receptor that drives DC migration along gradients toward higher concentrations of ligands CCL19 and CCL21 produced in the lymphatics and draining LNs (45, 46). CCL19 is primarily secreted by stromal cells and mature DCs in the T cell zone of LNs (47) while CCL21 is produced constitutively by stromal cells and endothelial cells of lymphatic vessels and of high endothelial venules (48). DC egress can also be influenced by other mediators such as prostaglandin E2 and sphingosine-1-phosphate (49, 50). Knowledge of how human antigen-laden DCs migrate from lung to peripheral LNs is limited. However, like mouse DCs, human DCs decrease CCR6 expression and increase CCR7 expression after maturation and to migrate towards CCR7 ligands (51).

1.4 DC's role in immunology

The past two decades are marked by significant progress toward understanding the role of DCs control of the immune system, arising from intensive work detailing the mechanisms of antigen processing and presentation, the organization of the DC-T cell immune synapse, the control of DC activation by Toll-like receptors (TLRs), the relevance of plasmacytoid DCs (pDCs) in antiviral responses, the role of DCs in polarizing T helper cell responses, the regulation of natural killer (NK) and B cell responses and the in vivo analysis of DC traffic and immune

interactions. These advances in knowledge, reagents, and techniques have equipped us with the tools to decipher the specific roles of DCs regulating the lung immunology in almost any disease.

It has been known that DC function is tissue, pathogen, and context specific. For example, during viral infection, DCs endocytose viral antigens and migrate to the mediastinal LNs, where they present the antigen and activate antigen-specific naive and memory T cells which finally initiate the cytotoxic effector T cells killing orchestrate (52). However, DCs respond differently in the context of Mycobacterium tuberculosis lung infections. During M. tuberculosis infection, DCs produce high levels of inflammatory cytokines, including IL-6, TNF-α, IL-12, IL-1α, and IL-1β which stimulate additional leukocytes and contribute to granuloma formation as a mechanism to control pathogen growth and distribution (53). In addition, the unique roles of DCs in asthma further exemplify the complex and plastic functional properties of DCs in lung diseases. In patients with asthma and mouse models of allergic asthma, multiple DC populations are increased in the lung that produce lymphocyte activating cytokines that resulting in an "over-excited" immune response towards the otherwise harmless antigens (54).

1.5 DC function in pulmonary disease

Much of our knowledge of DC function in pulmonary disease derives from the study of infectious diseases and common lung diseases. We know that DC function is tissue, pathogen, and context specific. For example, during viral infection, DCs endocytose viral antigens and migrate to the mediastinal LNs where they activate antigen-specific naïve and memory T cells (52). Mouse studies reveal that these T cells undergo multiple rounds of proliferation and migrate out of the LN into peripheral tissues where they interact with newly recruited DCs that present viral antigens within the infected tissue. In infected tissue, cytotoxic effector T cells orchestrate the direct killing of infected cells expressing viral antigens on the cell surface and contribute to the production of pro-inflammatory cytokines that help in the resolution of infection (55, 56). DCs respond differently in the context of Mycobacterium tuberculosis (Mtb) lung infections. During Mtb infection, DCs phagocytose the pathogen leading to the production of high levels of inflammatory cytokines including IL-6, TNF-α, IL-12, IL-1α, and IL-1β. These cytokines stimulate additional leukocytes which and contribute to granuloma formation as a mechanism to control pathogen growth and distribution (53). The unique roles of DCs in asthma further exemplify the complex and plastic functional properties of DCs in lung diseases. In asthma patients and mouse models of allergic asthma, multiple DC populations are increased in the lung that secrete lymphocyte

activating cytokines which are associated with disease severity (57, 58). In asthma, otherwise harmless antigens modify airway epithelial barrier function and activate epithelial cells in a manner that leads to DC activation and the initiation of an allergic T cell response. For example, house dust mite feces contains allergens with proteolytic activity that co-stimulate TLR receptors on resident lung cells. These events lead to production of epithelial chemokines, including CCL20, which recruit lung DCs. Further, the proteolytic activity of the allergens can promote the production of cytokines that drive immune responses in DCs (57, 59, 60).

1.6 DC function in rare lung disease

Pulmonary Langerhans cell histiocytosis (PLCH) is a rare interstitial lung disease characterized by the accumulation of Langerin-positive dendritic cells, bronchiolocentric nodule formation, and cystic remodeling of the lung (61). PLCH is usually a single-system disorder with pulmonary impairment ranging from asymptomatic disease to life-threatening respiratory failure (62). PLCH occurs almost exclusively in active and former smokers (61) with the crude prevalence estimated at 0.27 and 0.07 per 100,000 in males and females, respectively (62, 63). Historically, PLCH was considered an idiopathic reactive disease because of large numbers of inflammatory cells found around pulmonary lesions and the presence of

high levels of inflammatory cytokines (64). However, recent genetic analyses indicate that PLCH is more accurately defined as an inflammatory neoplastic disorder. This classification is based on studies that demonstrate more than 50% of PLCH patients have an acquired, activating mutation in the proto-oncogene BRAF within the DC lineage that results in constitutive activation of the mitogen-activated protein kinase (MAPK) pathway (65, 66). The most common mutation identified is BRAF V600E, but recent studies revealed mutations in other signaling proteins in the MAPK pathway (67, 68). Interestingly, the DCs in PLCH lesions express high levels of DC maturation markers, which may contribute to the local "cytokine storm" that drives nodule formation and/or cystic remodeling (69). As described, DCs exhibit decreased expression of CCR6 and increased CCR7 expression after maturation, homing receptors that promote DC migration towards draining LNs (23). However, Fleming et al. showed that DCs within lesions express both CCR6 and CCR7 in the pediatric form of systemic Langerhans cell histiocytosis (70). Therefore, it is possible that altered regulation of CCR6 and CCR7 contributes to the increased accumulation and activation of DCs in PLCH. Alternatively, the aberrant accumulation of DCs in the lung may be a consequence of enhanced DC proliferation or viability. Indeed, MAPK pathway activation, especially BRAF-V600E, has been known for promote increased cell proliferation or/and decrease cell apoptosis in melanoma and thyroid cancer (71, 72).

In addition to genetic mutations in the MAPK pathway, cigarette smoke is believed to be a key complementary factor in PLCH pathogenesis. Smoking is known to increase the expression of several pro-inflammatory mediators in the lung, such as TNF-α, granulocyte-macrophage colony-stimulating factor (GM-CSF), TGF-β and CCL20, which are involved in DC differentiation and function (73). The effects of smoking on DC function have been investigated in other smoking related diseases such as chronic obstructive pulmonary disease (COPD). Overall, the number and maturation state of pulmonary DCs is increased in COPD. However, regional lung differences in COPD patients are present, such as increased numbers of immature DCs in small airways and decreased total numbers of DCs in large airways (74-76). Cigarette smoke increases CCL20 and recruits DCs into the lung in COPD patients and lung cancer (77-79). In addition, DCs from COPD patients and mice exposed to cigarette smoke exhibit enhanced survival (80) and studies from smokers and mouse models indicate that multiple cytokines and chemokines that affect DC maturation, activation, and migration are elevated following smoking (81, 82). The fact that the majority of PLCH patients are current smokers, and that the disease sometimes regresses with smoking cessation, suggests the pulmonary microenvironment created by cigarette smoke is required for disease expression and persistence. However, the specific nature of the alterations in the pulmonary microenvironment responsible for recruiting and retaining DC are unknown.

Sarcoidosis is a systemic granulomatous disease of unknown etiology that causes inflammation and tissue damage in multiple organs, most commonly the lung. The prevalence of sarcoidosis in the United States is approximately 10.9 and 35.5 per 100,000 persons of European and African descent, respectively (83, 84). Although the etiology is unknown, increasing evidence suggests that sarcoidosis is an antigen-driven autoimmune disease (85, 86). It is characterized by T helper type 1 (Th1) T cell polarization and exaggerated immune responses against unknown causative antigens (87-89). Although most research has focused on alveolar macrophages as the primary pathogenic antigen presenting cells in sarcoidosis, more recent evidence indicates that DCs play a causative role. There is an increased number of DCs in the draining LNs of sarcoidosis patients and, unlike other inflammatory lung diseases, there is an increased number of immature DCs in the lung tissue, especially the alveolar space (88). Furthermore, there is a 2-fold increase in cDCs in bronchoalveolar lavage from sarcoidosis patients which express lower levels of the maturation marker CD83 and the co-stimulatory molecule CD86 (90). Pulmonary DCs from sarcoidosis patients demonstrate a reduced capacity to induce T cell proliferation ex vivo compared to DCs isolated from healthy lungs suggesting that the immature surface marker phenotype correlates with an observed reduction in DC function (91). Interferon-gamma

(IFN-γ) is one of the most important cytokines that induce DC maturation and cytokine production, including the major Th1 polarizing cytokine IL-12. Interestingly, IFN-γ and IL-12 levels are elevated in sarcoidosis bronchoalveolar lavage (BAL) fluid suggesting a defect in the process of IFN-γ dependent DC maturation (92, 93). Furthermore, moDCs isolated from sarcoidosis patients display normal maturation markers but have an enhanced ability to induce TNF-γ expression when co-cultured with allogeneic naïve CD4+ T cells (87). The role of TNF-α in sarcoidosis pathogenesis and prognosis has been well studied. Although the role of DCs remains to be defined, the high abundance of TNF-α receptor on DCs suggest that DCs may be important regulators of TNF-α mediated disease progression. Similar to another DC involved autoimmune disease, psoriasis, TNF-α inhibitors have been clinically tested in sarcoidosis patients with some promising preliminary outcomes in selected patient subsets (94, 95). Due to the undeveloped techniques and knowledge, most of earlier studies did not differentiate macrophages from DCs in BAL fluid, and additional studies are necessary to define distinct roles in sarcoidosis. Taken together, these data clearly demonstrate dysfunction within the DC population in sarcoidosis and the enrichment of DCs in the lung and draining LNs suggests that abnormal DC tracking contributes to pathogenesis. As increasing evidence emerges, it is possible that DC-targeted therapy may become a promising clinical option.

Hypersensitivity pneumonitis (HP) is an interstitial lung disease commonly characterized by granulomatous inflammation with prominent infiltration of lymphocytes, macrophages, and fibroblasts around indigestible antigens or particles. A large variety of antigen and/or particle exposures can result in HP. Based on the rate of progression, HP can be divided into acute, subacute and chronic forms, although clinical presentations may overlap (96). HP pathogenesis is complex but a consensus understanding of HP involves pre-existing genetic susceptibilities and/or environmental factors, followed by exposure to specific antigens. It has been suggested that acute HP is mediated by immune complex formation while enhanced Th1 responses are responsible for the subacute and chronic forms (96). Studies also implicate cytotoxic delayed hypersensitivity in the observed abundance of Th1/Th17 cytokines and mechanisms of tissue injury (97). Additionally, type III and type IV hypersensitivity have been noted to result in fewer granulomas but more extensive fibrotic remodeling in some patients (98). Given the importance of DCs in maintaining lung immune homeostasis, the development of granuloma formation and mediating hypersensitivity reactions, a causative role in the development and progression of HP is certain. Human data are limited although there is a 5-fold increase in the number of DCs in the lungs of chronic HP patients compared to healthy controls (99). Much of our current

understanding of HP pathogenesis is derived from animal models. An acute HP mouse model indicates that increased numbers of mature DCs persist in the lungs of Saccharopolyspora rectivirgula–challenged animals and that these DCs play a causative role in granuloma formation by via increased production of pro-inflammatory chemokines (100). Indeed, mice deficient in IFN do not develop granulomatous lesions after exposure to Saccharopolyspora rectivirgula (101). Further, depletion of CD34, a cell surface receptor involved in DC migration and activation, impairs DC migration from lung to peripheral LN and renders mice resistant to the development of acute HP (102). The DCs from CD34-deficient mice show impaired cytokine secretion and fail to appropriately deliver antigen to T cells in the acute HP model. Mouse studies also reveal that DCs are critical to the development of HP pathology, as depletion of the pathogen recognition receptor, TLR9, renders DCs unable to respond to antigens. The end result is restricted Th1 cytokine and chemokine release, and attenuated lung pathology (103). Similar to HP patients, there are increased numbers of mature DCs in the lungs of the acute HP mouse model (104). The apoptosis of granulocytes and non-hematopoietic cells are thought to contribute to HP pathogenesis by activating DCs to increase pro-inflammatory chemokine production (105). The local enrichment of these chemokines recruits other inflammatory cells to the lung, amplifying HP pathological changes. Together, the evidence suggests that DC maturation,

migration and interaction with other cells are critical to the pathogenesis of HP. Unfortunately, neither the human studies nor mouse models have identified specific populations of DCs involved in the pathogenesis of HP. Identifying these populations or other mechanistic details will facilitate future targeted approaches to reduce the immune-mediated components of HP pathology.

Idiopathic interstitial pneumonias (IIPs) are a cluster of diseases sharing similar clinical and radiologic presentations. Based on histological features, IIPs are further divided into 8 different subsets (106). The etiopathogenesis of all types of IIPs are poorly understood. In this introduction, we will focus idiopathic pulmonary fibrosis (IPF) and nonspecific interstitial pneumonia (NSIP), the most common members of this family of scarring lung diseases. NSIP is an important IIP with a clinical presentation that is similar to IPF but is associated with a better prognosis. NSIP is the second most common cause of IIP, and is commonly associated with autoimmune connective tissue diseases (107). Little is known about the pathogenesis of NSIP except that there is a robust accumulation of DCs in the lungs of NSIP patients which are in close proximity to CD8+ and CD4+ lymphocytes (108). In contrast, there are several lines of research that strongly implicate DC dysfunction in the pathogenesis of IPF which is one of the most lethal fibrotic lung diseases (109, 110). Lung biopsy of patients with IPF reveals

usual interstitial pneumonia, characterized by patchy, spatially and temporally heterogeneous areas of early and completed fibrosis in the lung periphery and lymphatic structures. The lungs of IPF patients are heavily infiltrated by immature DCs in areas of epithelial hyperplasia and fibrosis while mature DCs, characterized by the expression of maturation markers like CD40, CD86 and CD80, accumulate in well-organized lymph-node-like structures (111). This finding is supported by other studies demonstrating increased numbers of immature DCs in the lavage fluid of IPF patients (112). Moreover, fibroblasts and epithelial cells in IPF patients express high levels of CCL19 which can lead to increased DC recruitment DC from the circulation (113, 114). Along these lines, Freynet et al. have shown that co-culture of DCs with lung fibroblasts from IPF patients diminishes the expression of DC activation markers (115). Together, these findings suggest that pulmonary fibroblasts may influence IPF progression by maintaining populations of immature DCs, which are unable to suppress ongoing inflammation.

The most common mouse model for IPF involves the administration of bleomycin to induce acute or subacute fibrosis in the lung. In this model, there is a significant accumulation of DCs in the lung after bleomycin challenge. However, unlike human IPF, the mouse DCs express high levels of maturation markers including CD40, CD86 and CD83, and exist in close proximity to memory T cells (116).

These findings are consistent with observations in other pulmonary diseases, which have revealed that maturation of lung DCs is followed by a secondary activation of memory T cells that may perpetuate chronic inflammation. Interestingly, experiments using antibodies to block DC maturation or deplete mature DC chemokine receptors attenuate the pathological hallmarks of pulmonary fibrosis in this model (116, 117). Unfortunately, the discrepancy of DC phenotypes between mouse models and IPF patients suggest the bleomycin-induced model does not accurately reflect the immune alterations observed in human disease. Mouse models that more authentically recapitulate the immune dysfunction observed in IPF are needed to further our understanding of IPF pathogenesis and the possible involvement of DC dysfunction.

Figure 1 Distribution and migration of pulmonary DCs.

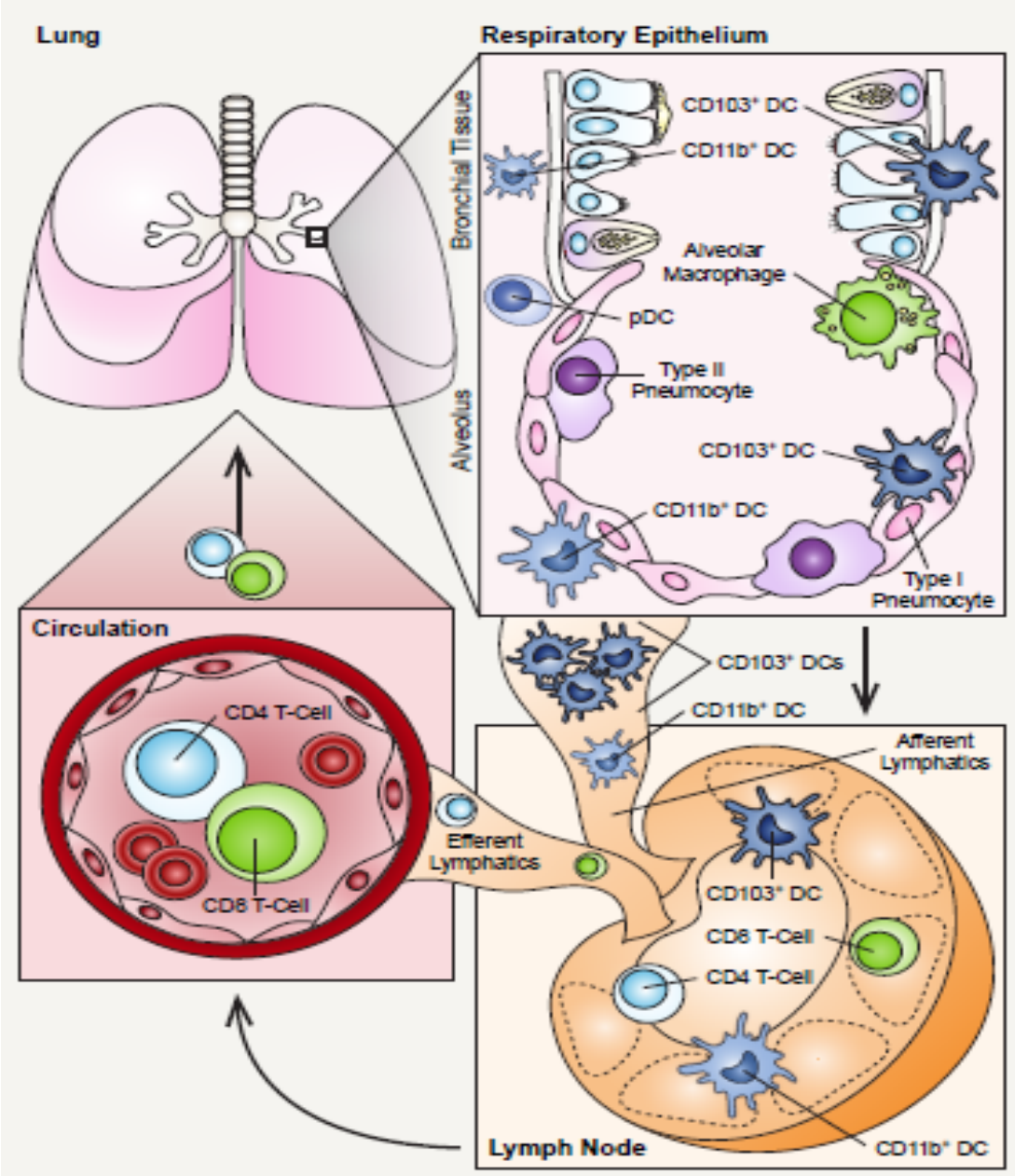

Figure 1. Subsets of DCs are widely distributed throughout the lung and segregate into unique niches that vary by lung compartment. In the upper respiratory tract, $CD103^+$ DCs mainly reside in the mucosal wall and extend processes into the airway lumen in between epithelial cells. $CD11b^+$ DCs and pDCs are mainly located underneath the basement membrane. After maturation, both $CD103^+$ DCs and $CD11b^+$ DCs can migrate to LNs via lymphatics and present antigens to T cells. $CD103^+$ DCs are the migratory subsets that populate LNs.

Chapter II

BRAF-V600E mutation regulates dendritic cell function and induces PLCH-like lesions in mice exposed to cigarette smoke

Huan Liu[1], Andrew R Osterburg[1], Jennifer Flury[1], Zulma Swank[1], Dennis McGraw[1,2], Gupta Nishant[1, 2], Kathryn Wikenheiser-Brokamp[1, 3], Ashish Kumar [4], Francis X McCormack[1, 2], Michael T Borchers[1,2]

1 Department of Internal Medicine, Division of Pulmonary, Critical Care and Sleep Medicine, University of Cincinnati, Cincinnati, OH 45267

2 Cincinnati Veteran's Affairs Medical Center, Cincinnati, OH 45267

3 Division of Pathology and Laboratory Medicine, and Perinatal Institute, Division of Pulmonary Biology, Cincinnati Children's Hospital Medical Center, Cincinnati, OH 45229

4 Division of Hematology, Cincinnati Children's Hospital, Cincinnati, OH 45229

2.1 Introduction

Epidemiology and current understanding of Pulmonary Langerhans cell Histiocytosis. Pulmonary Langerhans Cell Histiocytosis (PLCH) is a rare interstitial lung disease characterized by focal Langerin-positive dendritic cell accumulation, bronchiolocentric nodule formation, and cystic remodeling of the lung (118). PLCH is usually a single-system disorder with pulmonary impairment ranging from asymptomatic disease to life-threatening respiratory failure (119). PLCH in adults occurs almost exclusively in active smokers and no accurate epidemiological data is available. However, the crude prevalence of the disease is estimated at 0.27 and 0.07 per 100,000 population in males and females, respectively, and PLCH may account for up to 5% of all interstitial lung diseases (119, 120). Since first described, we have discovered little insight into the PLCH etiology. The discussion of whether the nature of PLCH is a neoplastic or reactive disease was recently settled when several mutually exclusive activating mutations within the mitogen-activated protein kinase (MAPK) pathway were found in more than 70% of PLCH patients (121, 122), indicating that PLCH is more accurately defined as an inflammatory neoplastic disorder (123, 124). The most common mutation identified is BRAF-V600E which is found the most often within the DC lineage (125). However, due to the rare nature of this disease and the lack of a

useful animal model, our understanding of PLCH pathogenesis is limited and mostly speculative. The current clinical management of PLCH is challenging and often ineffective (126). Therefore, it is both critical and urgent to identify mechanisms of pathogenesis so efficient treatment strategies can be tested and provided.

MAPK pathway mutation and PLCH. Braf kinase plays an essential role in mediating cellular differentiation, proliferation, senescence, and survival in response to extracellular cues by signaling through the MAPK pathway. It has been estimated that the RAS/BRAF/MEK/ERK pathway is mutated in an estimated 30% of all cancers, with mutations in the braf gene found in approximately 7% of cancers (127). The most common braf mutation is the V600E transversion. The conformational change of in the kinase domain allows the activation of the MAPK pathway in the absence of any extracellular stimuli (128). Several neoplasms harbor BRAF-V600E mutations and have uncontrolled proliferation and impaired migration in affected cells (129, 130). A recent study suggested that induction of the BRAF-V600E mutation in the CD11c DCs drives a systemic phenotype in mice (125). In addition to the BRAF-V600E mutation, it has been reported that MAP2K1, which is another component of MAPK pathway, mutated in 33% of the LCH patients who don't have a BRAF-V600E mutation (Figure 2). Similar to the

braf mutation, the MAP2K1 mutation results in continuous activation of the MAPK pathway (124). However, how this continuous activation of MAPK affect DC effector cell function and migration capacity is still unclear and will be the focus of this study.

The role of DC in PLCH pathogenesis. DCs are the most efficient antigen presentation cells and, therefore, have a pivotal role in the onset and regulation of innate and adaptive immune responses and the recruitment of a variety of leukocytes to the site of inflammation or injury (131). The dysregulation of DC function often results in a pathological immune response that likely contributes to disease pathogenesis in many pulmonary diseases (132). In PLCH, focal Langerin+ dendritic cell accumulation and the development and expansion of nodules in early disease are prominent features of PLCH despite variable clinical presentations (118). This common phenotype and DC lineage specific mutations strongly suggest the role of DCs in the pathogenesis of PLCH. As described previously, DC migration into and out of the lung is tightly regulated by multiple chemokines. It has been demonstrated that cigarette smoke (CS) affects DC numbers and maturity by increasing the expression of several pro-inflammatory mediators in the lung, such as TNF-α, GM-CSF, TGF-β and CCL20 in both smokers and mouse models of COPD (133-135). However, the effects of CS on DC function and the potential

contribution to the accumulation of DCs in PLCH is unknown (136). The fact that PLCH occurs predominantly in active smokers and the disease sometimes regresses with smoking cessation, it is fair to speculate that the CS related pulmonary microenvironment is required for the initiation and persistence of PLCH pathologies (119). However, due to the rare nature of the disease and the lack of animal models, the combined effects of BRAF mutations in the dendritic cell lineage along with a pulmonary microenvironment altered by exposure to CS is entirely speculative.

2.2 Knowledge Gaps

While the concept of BRAF-V600E mutation and the CS-induced microenvironment changes are well studied in other disease context, how they contribute to the pathogenesis of PLCH have not been examined. The lack of knowledge in the pathogenesis combined with the rare nature of the disease indicate an imperative demand for an animal model of PLCH. The next chapter describes the very first PLCH mouse model we established and how we are using it as a platform to decipher the contribution of BRAF-V600E mutation and CS-related changes to disease pathogenesis. In addition, there is no reliable biomarker for this orphan disease and the diagnosis is mainly based on the imaging which sometimes is easily confused with other interstitial lung diseases(118). Therefore, it is important to discover a biomarker that can facilitate the clinic diagnosis.

2.3 Aim of the current investigation

Under normal conditions, a limited number of DCs reside in tissue and patrol the environment. Once activated, DCs play a key role in the development of the innate immune response and migrate to draining lymph nodes to induce adaptive immune responses. In PLCH, however, mature DCs accumulate in small airways leading to nodular inflammatory lesions and eventually cystic lung destruction primarily in upper and middle lobes of the lung. Clinical data indicated that there may be either reactive or clonal expansions of DCs as a consequence of CS exposure but the cellular and molecular mechanisms controlling DC accumulation and effector functions in the development of PLCH are largely unknown. Exposure to CS leads to the elaboration of several mediators that may affect DC biology. Recent studies show that CS exposure increases expression of TNF-α, GM-CSF, TGF-β and CCL20 in lung which are involved in DC differentiation, migration and function. More recently, a causative link between a mutation in the BRAF gene in DC lineage cells and the development of DC neoplastic disease has been reported. A common, acquired mutation in BRAF (V600E) is found in more than half of PLCH patients. BRAF regulates the MAP kinase/ERK signaling pathway and the somatic BRAF V600E is an activating mutation in different neoplasms resulting in the constitutive activation of the MAPK/ERK pathway. These recent genetic data

along with the known effects of CS exposure on local pulmonary DC function lead us to hypothesize that: **the acquired BRAF-V600E mutation in DC lineage cells in combination with CS-induced DC activation and migration signals leads to the accumulation of pathogenic DCs into the lung which directs the development PLCH pathogenesis (Figure 3)**.

We have generated mouse models harboring the inducible BRAF V600E mutation in DC lineages. These mice will be used to investigate the effects of CS exposure on BRAF V600E mutant DC function and the combination of mutation and CS in the development of pulmonary pathologies in PLCH. Specifically, these models will be used to examine the effects of smoking and BRAF V600E mutation on DC proliferation, maturation, migration and effector functions in shaping innate and adaptive immune responses. We will test this hypothesis with the following Specific Aims:

Aim 1: Define the effects of CS exposure on Braf-V600E DC accumulation and proliferation in the lung. The accumulation of mature DCs in the lung is a prominent, defining event in PLCH pathogenesis. This aberrant accumulation may be a result of unrestrained proliferation, enhanced recruitment to the lung, or impaired circulation. Based on preliminary studies and relevant literature, we hypothesize that: 1) mutant DCs and progenitors from CS exposed mice have an

increased proliferation rate. 2) CS exposure generates a pulmonary microenvironment rich in growth/differentiation factors and activating cytokines that leads to the excessive recruitment and maturation of Braf V600E mutated DCs. CS-induced accumulation of DCs in WT and BRAF V600E mutant mice will be assessed in vivo by histological and flow cytometric methods. Proliferation will be studied both in vitro and in vivo using isolated and fluorescently labeled WT and BRAF DCs. DC recruitment and migration will be examined using adoptive transfer of isolated and labeled DC populations. The effects of CS exposure on migration capacity of DCs will be examined in vitro using lung dendritic cells and bone marrow DC progenitors by transwell microplate assays. DC chemokine receptor expression will be examined by flow cytometry. Completion of these studies will define the combined effects of BRAF mutations and CS exposure on BRAF V600E DC proliferation and migration, thus providing novel insight into the initiating event in the pathogenesis of PLCH.

Aim 2: Define the effects of CS exposure on Braf-V600E DC effector functions and lung pathogenesis. Many aspects of pulmonary immune functions are enhanced following CS exposure. DCs are mechanistically positioned to influence both innate and adaptive immune responses. We hypothesize CS exposure and Braf-V600E mutations results in overly reactive DCs that attract and activate other

immune cells to the lung resulting in the formation of nodular lesions and cyst formation. We will examine both direct and indirect DC effector functions using DCs isolated form filter air (FA) and CS exposed mice. Direct assays will measure the ability of DCs to respond to endogenous and exogenous signals. Indirect assays will measure the ability of DCs to influence other immune cell functions such as natural killer (NK) cells and T cells. The role of the CS and mutation in lung pathogenesis will be determined using multiple models of DC specific BRAF V600E mutant mice and various adoptive transfer strategies.

At the completion of these studies, we will define the mechanisms of DC accumulation and altered effector function in PLCH initiation and progression. Dissecting the mechanisms of PLCH pathogenesis will provide data to identify potential targets for treatment of PLCH patients. Finally, these studies will not only shed a light on dendritic cell function in other smoking-related diseases characterized by disrupted immune function, such as COPD, interstitial lung disease and lung cancer but also expand our knowledge of basic DC biology.

2.4. Result

2.4.1 BRAF-V600E expression in CD11c DC lineage drives PLCH-like pathologies in mice exposed to cigarette smoke. Recent genomic studies indicate that the BRAF-V600E mutation is mostly DC-lineage specific with a largely different frequency between patients (125, 137). The adult PLCH is normally only involved the lung and has a much fewer circulating BRAF-V600E positive cells than the systemic LCH (121, 138). A recent study suggested that continuous induction of the BRAF-V600E mutation in the CD11c DCs with high efficiency drives a systemic phenotype in mice (125). However, it has been speculated that the BRAF-V600E mutation in adult PLCH is acquired somatic mutation rather than a germline mutation. Thus, in order to generate a mouse model that recapitulate human situation, We generated a model of PLCH by crossing mice with a tamoxifen(TAM)-inducible CD11c promter driving Cre recombinase with transgenic mice harboring a floxed genomic cassette containing the BRAF-V600E mutation (referred to as $BRAF^{VE}$ hereafter). Placing the $BRAF^{VE}$ mice on TAM-containing chow at the age of 6 weeks old induced the recombination of the endogenous BRAF locus with the transgenic BRAF-V600E exon in CD11c-expresing cells. Following two weeks of TAM chow, mice were exposed to either filtered air (FA) or cigarette smoke (CS) as described in Methods

and tissues were harvested and analyzed at intervals up to 24 weeks (Figure 4A). The inducible CD11c promoter has an estimated excision rate of 4-8% (139) and the expression of BRAF-V600E following TAM administration in DCs was confirmed by quantitative real-time PCR (qPCR) (Figure 4B)

$BRAF^{VE}$ mice were viable and developed normally without prominent phenotypical alterations compare to WT littermates with a few exceptions which developed splenomegaly and hepatomegaly after five months. However, $BRAF^{VE}$ mice developed mild inflammatory infiltrates in lung at 14 weeks that were further exacerbated exposure CS (Figure 5A). Following 4 months of CS exposure, the $BRAF^{VE}$ mice exhibited characteristic human-like PLCH phenotypes including the presence of cellular nodules and cyst-like lung lesions. To identify and characterize the cell composition of the nodules in the lung, we conducted a series of IHC studies that showed that the nodules consist of centrally located histiocytes and peripherally distributed lymphocytes (Figure 5B). These findings are similar to those observed in PLCH (121). MicroCT images further demonstrate that presence of multiple identifiable nodules in the lung of $BRAF^{VE}$ mice (Figure 5C). These findings demonstrate that we have established a mouse model that recapitulate the hallmark characteristics of human PLCH. More importantly, our data demonstrate that CS is not only a demographic identifier of

PLCH patients but also a catalyst for the disease pathogenesis in the context of BRAF-V600E mutations.

2.4.2 BRAF^{VE} mice exhibit pulmonary inflammation and disrupted DC homeostasis in the lung following CS exposure. To examine the populations and phenotypes of cells accumulated in the lung of BRAF^{VE} mice exposed to CS, we examined single cell suspensions obtained by enzymatic digestion by flow cytometric analysis. There was a significant increase in DCs and T cells but not macrophages in the lung of BRAF^{VE} mice exposed to CS (Figure 6A). The histiocytes marker CD68 is expressed on DCs and macrophages in murine lung (140). The fact that the number of macrophages did not change between BRAF^{VE} mice and WT mice suggests the CD68 positive histiocytes accumulated in granulomas (Figure 5B) may have a DC origin. In human PLCH patients, the accumulating DCs are CD1a positive and often co-express Langerin (141, 142). Similarly, to their human counterparts, mice pulmonary DCs can also be divided into conventional and plasmacytoid DCs (19). Our data shows that the DCs accumulated in BRAF^{VE} mice were primarily CD103^{+} DCs (Figure 6B). CD103+ DCs in the mouse lung are thought to be the counterparts of lymphoid CD8^{+}DCs and can be replenished by LY-6C^{high} CCR2^{high} circulating monocytes (143). DCs accumulated in PLCH patients express high level of maturation markers and are

important for the local excessive cytokine microenvironment (144). In our mouse model, we observe an increase of CD86+ matured DCs existing in the lung of $BRAF^{VE}$ mice that further increased after exposed to CS (Figure 6C). Next, we assessed the functional effects of the BRAF-V600E mutation and CS exposure by activating the pulmonary DCs *ex vivo* using TLR ligands. Our data showed that the pulmonary DCs isolated from $BRAF^{VE}$ mice secreted more IL-6 and IL-12 upon activation which further increased in mice also exposed to CS (Figure 6D-E). These data indicate that aberrant DC function in PLCH is a consequence of both the BRAF-V600E mutation and CS exposure.

2.4.3 BRAF-V600E mutation in DCs increases cell viability and expression of anti-apoptotic factor BCL-XL. One possibility that may explain the accumulation of DCs in the lungs of PLCH is an increased activation and proliferation of DCs due to the BRAF-V600E mutation. To further examine the effects of BRAF-V600E mutation in DCs and their potential contribution to the pathogenesis of PLCH, we utilized an *in vitro* model of bone marrow derived DCs (BMDCs) to examine cellular activation, proliferation and apoptosis. BMDCs from BRAF-V600E transgenic mice were transfected with adenovirus contains Cre recombinase and generated a population of mutant DCs of ~65% (Figure 7A and 7B). The result of transfection was confirmed by RT-PCR using

mRNA isolated from transfected $BRAF^{VE}$ BMDC (Figure 7C). Similar to melanoma cells with a BRAF-V600E mutation and DCs isolated from LCH patients (123, 145), the BRAF-V600E mutation enhanced ERK phosphorylation indicating a constitutive activation of the MAPK pathway (Figure 7D). The p-ERK expression in the BRAF-V600E BMDCs was specific to the recombinant mutation demonstrated by the complete inhibition with the BRAF-V600E-specific inhibitor PLX4720 (Figure 7D). Constitutive activation of the MAPK pathway by BRAF-V600E is associated with increased cell proliferation and disrupted cell apoptosis (146, 147). To investigate if BRAF-V600E mutation affects DC proliferation, we enumerated the number of BMDC each day after transfection and observed no difference between WT and BRAF-V600E BMDCs (Figure 7E). We also examined *in situ* proliferation in lesions of our mouse model. Consistent with our *in vitro* results, we observed no Ki67 expression in lung histiocytes in $BRAF^{VE}$ mice (data not shown). Alternatively, it has been shown that MAPK signaling is important in regulating apoptosis under different physiological and neoplastic conditions (148, 149). We next examined whether the BRAF-V600E mutation affects DC viability in BMDCs. Transfected WT and BRAF-V600E BMDCs were collected at day 7 and cultured with/without the DC survival dependent growth factor GM-CSF for 24 hours. Flow cytometric analysis showed that the healthy non-apoptotic population (Pi-, Annexin V-) of

BRAF-V600E BMDCs was increased compared to WT BMDCs (Figure 7F). To further investigate the mechanism of enhanced BRAF-V600E DC viability, we measured the anti-apoptotic protein BCL-XL expression level in the BMDCs. Consistent with the observed reduction in apoptosis, the expression of BCL-XL in BRAF-V600E BMDCs was increased compared to WT (Figure 7G).

2.4.4 Increased CCL20 expression and CCR6 responsiveness is associated with increased BRAF-V600E DC accumulation in the lung. Along with increased cell viability, an alternative or complementary mechanism for pulmonary DC accumulation is the increased recruitment from the periphery. The lung resident DC pool is replenished by circulating DCs and pre-DCs at a constant rate under steady-state conditions. This can be rapidly increased during inflammation and infection, and follows a gradient concentration of CCL20 (150-152). We measured CCL20 levels in BAL fluid was collected from WT and $BRAF^{VE}$ mice exposed to FA and CS. CCL20 levels were increased in $BRAF^{VE}$ mice compared to WT and further increased in $BRAF^{VE}$ mice that were exposed to CS (Figure 8A). In order to identify the source of the CCL20 production, WT and $BRAF^{VE}$ BMDCs were treated with/without LPS plus IFN-gamma and CCL20 quantities measured in culture supernatants by ELISA. The

$BRAF^{VE}$ BMDCs secreted more CCL20 compared to WT BMDCs which was further increased after activation (Figure 8B).

We next examined whether BRAF-V600E mutation affects BMDC responsiveness to CCL20. The receptor for CCL20, CCR6 is a Gi coupled receptor that inhibits intracellular cAMP following receptor activation (153). Therefore, we assessed CCR6 responsiveness on $BRAF^{VE}$ BMDCs by measuring cellular cAMP levels following CCL20 exposure. Our data showed that the reduction of cAMP level was greater in BRAF-V600E BMDCs compared to WT indicative of increased CCR6 responsiveness (Figure 8C). CCR7 responsiveness assessed by CCL19 and CCL21 stimulation was not different between WT and BRAF-V600E BMDC (Figure 9A). Consistent with this finding, we also observed enhanced functional responses to CCL20 as measured by increased migration of BRAF-V600E BMDCs compare to WT BMDCs towards CCL20 (but not CCR7 chemokines CCL19 or CCL21, Figure 9B) using a transwell migration assay (Figure 8D).

We hypothesize that the altered lung microenvironment is a key factor in the recruitment, accumulation and activation of BRAF-V600E DC's in PLCH. To examine the effects of CS exposure on DC accumulation in the lung, we assessed the migration capacity of BRAF-V600E BMDCs by adoptive transfer. Donor WT or BRAF-V600E BMDCs on a CD45.2 background were injected

into the tail vein of CD45.1 recipient mice that were pre-exposed to FA or CS. Lungs and mLN were collected from recipient mice 2 days post-injection and the retention of donor BMDCs in these organs was analyzed by flow cytometry. These data show that BRAF-V600E BMDC accumulation in the lung was higher than WT BMDCs and was further increased in the CS-exposed recipients (Figure 8E). The migration to the mLN was not changed between WT and BRAF-V600E BMDCs.

Together, these studies showed that the accumulation of DCs in the lung of our $BRAF^{VE}$ mice was likely due to the combination of enhanced cell viability, and increased recruitment due to the combined effects of the BRAF mutation and CS exposure. The idea that both the BRAF-V600E mutation and CS exposure are both requirements for the development of increased DC accumulation is further supported by the fact that the CS-conditioned lung had increased $BRAF^{VE}$ BMDC accumulation compared to WT BMDCs (Figure 8E).

2.4.5 CCL7 chemokine expression is increased $BRAF^{VE}$ mice and is induced by BRAF-V600E mutation in DCs. The characteristic inflammatory lesions and nodules in PLCH and $BRAF^{VE}$ mice consist primarily of macrophages, T cells and eosinophils besides DCs (121) (Figure 1D). This indicates that

although the mutant DCs precipitate the inflammation and nodules, the recruitment of other cells to the site of DC retention in a BRAF-V600E-dependent manner is a critical component of PLCH pathology. Using multiplex ELISA, we measured the expression of several chemokines and cytokines in serum that are expressed by DCs. This analysis demonstrated that CCL7 showed a unique expression pattern in that it is expressed at very low levels in WT mice exposed to FA or CS but was increased in $BRAF^{VE}$ mice exposed to either FA or CS (Figure 10A). CCL7 (MCP3) is a pluripotent chemokine that can bind to multiple receptors including CCR1, CCR2, CCR3 and CCR5 expressed on inflammatory cells such as T cells, monocytes, eosinophils, and NK cells (154, 155). In order to identify the source of this increased level of CCL7 in the $BRAF^{VE}$ mice, we isolated pulmonary DCs from mice and measured the CCL7 secretion following stimulation. Our data indicates that the pulmonary DCs isolated from $BRAF^{VE}$ mice produced CCL7 at baseline compared to negligible amounts in WT. Additionally, CCL7 levels were further increased following activation (Figure 10B). In addition, we show that CCL7 secretion is dependent on the BRAF-V600E mutation as the BRAF-V600E specific inhibitor PLX 4720 decreased CCL7 expression in these cells (Figure 10B). The association between BRAF-V600E mutation and enhanced CCL 7 secretion was confirmed in BRAF-V600E BMDC by immunofluorescence staining for CCL7 (Figure (10C).

Analysis of BRAF-V600E BMDCs show that mutant DCs produced CCL7 at baseline which is upregulated following DC stimulation and almost completely inhibited following BRAF-V600E inhibition (Figure 10D). Examination of CCL2 levels (another pluripotent cytokine that can bind similar receptors as CCL7) demonstrate a significant amount of chemokine at baseline which is also increased by DC activation (Figure 10E). However, there is no difference between WT and mutant DCs and there is no effect of BRAF inhibition of CCL2 secretion demonstrating specificity for the BRAF-V600E mutation and CCL7 production. Identical patterns of CCL7 and CCL2 expression was confirmed at the level of mRNA by RT-PCR (Figure 10F). These results suggest that the recruitment of other inflammatory cells into the lung is a secondary event to the accumulation of BRAF-V600E DCs and driven by the CCL7 secreted from the mutated pathogenic DCs.

2.4.6 CS and Tamoxifen cessation ameliorate the PLCH phenotype in the BRAF^{VE} mice. We have shown that both the CS-conditioned local pulmonary environment and BRAF-V600E mutation are important for the pathogenesis of PLCH. Therefore, both smoking cessation and BRAF inhibition provide potential therapeutic targets. To investigate the efficacy of this treatment strategy, we discontinued the CS exposure and Tamoxifen (stop generating new

BRAF-V600E DCs) treatment for the $BRAF^{VE}$ mice that had been exposed to CS for 4 months (Figure 11A). Micro-CT images were captured before and after 1 month of cessation from the same mice. The images indicate that nodules noticeable in the $BRAF^{VE}$ mice disappeared after cessation (Figure 11B). In addition, CCL7 and CCL20 levels in BAL fluid decreased after cessation and there was no difference between WT and $BRAF^{VE}$ mice (Figure 11C). Furthermore, the number of total cells, $CD103^{+}$ DCs and T cells in the lung of $BRAF^{VE}$ mice was decreased after the cessation and returned to baseline (Figure 11D). The lung lesion in $BRAF^{VE}$ mice also decreased after cessation (Figure 12). More studies in the future are needed to address the specific roles and mechanisms of these two treatment arms. However, here we showed that this combination treatment, which consisted with discontinuing the exposure to CS and generation of new $BRAF^{VE}$ DCs, was capable of mitigating lung pathology in $BRAF^{VE}$ mice.

2.4.7 BRAF-V600E PLCH patients express increased levels of CCL7 and CCL20. We further examined CCL7 and CCL20 levels in PLCH patient samples. We obtained plasma from 8 PLCH patients with 3 having a known BRAF-V600E mutation. CCL7 levels in PLCH was not was not significantly different compared to healthy control and smokers, or other cystic lung diseases

including Birt-Hogg-Dubé (BHD) or lymphangioleiomyomatosis (LAM) (Figure 13A). Next we isolated Peripheral blood mononuclear cell (PBMCs) from three BRAF-V600E positive PLCH patients and examined CCL7 production. Among these PLCH patients, PBMC isolated from two of the three demonstrated increased secretion of CCL7 compared to healthy controls after activation (Figure 13B). A detailed flow cytometry analysis showed that there was a prominent cell population in PLCH patient 1 and 3 producing CCL7 following stimulation activation (Figure 13C). Additionally, we examined CCL20 expression in lung biopsies of healthy controls, PLCH patients and smokers. Immunostaining of lung tissue showed increased CCL20 staining in smokers compared to controls and high levels of CCL20 expression in the PLCH patients including intense localization to cells within the inflammatory nodules (Figure 13D).

2.5 Discussion

PLCH is an orphan lung disease with no established animal models. The incomplete understanding of pathogenesis of PLCH is a major obstacle to develop effective and safe clinical therapies. This study aims to establish the first mouse model that resemble human PLCH phenotype and using it to study the mechanisms how BRAF-V600E mutation and CS contribute to the disease pathogenesis. Our experiments show that after 4 months of CS exposure, $BRAF^{VE}$ mice developed PLCH-like lesions in the lung. We demonstrate that CS exposure is important in recruiting inflammatory cells, especially CD103 DCs into the lung and the accumulation of DCs is the result of BRAF-V600E related increased viability and migration capacity. Moreover, we observed increased CCL20 and CCL7 secretion from $BRAF^{VE}$ DCs that was inhibited by BRAF-V600E inhibitor PLX 4720. Finally, we show that the PLCH phenotype in $BRAF^{VE}$ mice was ameliorated after the cessation of CS exposure and Tamoxifen treatment. Collectively, these data demonstrate both BRAF-V600E mutation and CS exposure are important to the pathogenesis of PLCH and provide a new therapeutic strategy.

Even though the majority of PLCH patients are identified as active smokers, there was no evidence suggest the CS is required for the onset of disease (118).

However, our data shows that the PLCH-like phenotype only occurred in $BRAF^{VE}$ mice that were exposed to CS and the lesions progressed with increasing exposure time (Figure 5A). Moreover, in consistence with the clinical experiences of PLCH patients, the phenotype in CS-exposed $BRAF^{VE}$ mice were ameliorated after the smoking cessation (Figure 11-12). This observation suggests that CS generates a conditioned lung that favors the accumulation of pathogenic cells, especially $BRAF^{VE}$ DCs. Our data suggests the CCL20 level in the BAL fluid of CS-exposed $BRAF^{VE}$ mice was increased compare to FA-exposed mice and may contributed to the increased recruitment of $BRAF^{VE}$ DC.

PLCH is characterized by the nodule formation in the early stage and cystic lesions in the advanced stage (119). Thus it is important to understand the mechanism of abnormal cell accumulation so the disease progression can be stopped at the early stage. Previous studies shows that the CD1a+ DCs in the LCH lesions exhibit a low proliferation activity (156). Consistently, our data suggests the BRAF-V600E mutation is not associated with increased proliferative index in the DCs (Figure 7E). However, we found BRAF-V600E is associated with increased expression of anti-apoptotic protein BCL-XL and enhanced DCs viability (Figure 7F, G).

An alternative mechanism of the DC accumulation is through the chemotaxis. DCs migrate through the lung utilizing different chemokines (19).

BRAF-V600E has been known to promote thyroid cancer cell migration and invasion by affects extracellular matrix composition (157). Our data suggest BRAF-V600E mutation directly effects CCL20 secretion (Figure 8B) and migration capacity (Figure 8E) of DCs that both may can contribute to the increased recruitment from circulation to the lung. Interestingly, even though the $BRAF^{VE}$ DCs recruited to the CS-conditioned lung more efficiently than the WT DCs in the in-vivo transplant assay, the number of donor cells in the mLN showed no difference between $BRAF^{VE}$ DCs and WT DCs (Figure 8E). In consistence with this observation, in-vitro cell functional assays showed no difference in migration capacity between $BRAF^{VE}$ DCs and WT DCs (Figure 9) suggests that the BRAF-V600E is irrelevant of CCR 7-CCL 19/21 axis. Collectively, we demonstrate that the accumulation of DCs in the lung of $BRAF^{VE}$ mice is the result of the combination of increased viability and recruitment.

The MAPK pathway is important in regulating DCs maturation and effector cell functions (158, 159). Here, we show the $BRAF^{VE}$ DCs secreted large amount of cytokines both in the immature and mature conditions (Figure 6D, E). This increased cytokines secretion from DCs suggests that the pathogenic DCs in the PLCH may not only play the role as a conductor of the local immune responses but also a main contributor for the excessive cytokine secretion that

often seen in patients (160). The increased level of cytokines like IL-12 can skew the immune balance towards Th-1 response and may play a role in inducing the local tissue damage. The mechanism of how increased cytokines related to the local lesions will be further studied in the future.

The nodules in the PLCH patients consist of different kinds of immune cells which gave this disease an arguable nature as a reactive immune disorder in the past. Similar to DCs, other immune cells like monocytes, macrophages and T cells can be recruited into the lung following chemotaxis (161). CCL7 is a powerful chemokine that binds to different receptors including CCR1, CCR2, CCR3 and CCR5, which can be identified on different types of inflammatory cells (155, 162). Our data suggests that the BRAF-V600E mutation induces the secretion of CCL 7 in DCs that results in an elevated level of CCL 7 in the serum and BAL fluid of $BRAF^{VE}$ mice (Figure 10 A, B). In addition, the mRNA level and protein level of CCL7 in the lung of $BRAF^{VE}$ mice was increased compared to WT mice and continue to increase as the CS exposure prolonged (Figure 10A). As the CCL7 level increases, the inflammatory cell continue to be recruited to the lung. This correlation suggests a plausible mechanism that the cells participate in the nodule formation are recruited to the lung following a CCL7 gradient that secreted by $BRAF^{VE}$ DCs.

The clinical management of PLCH has been empirical and lack of consensus (126). We have shown that both the BRAF-V600E mutation and CS exposure are important to the pathogenesis of PLCH. Our data suggests that the PLCH-like phenotype in $BRAF^{VE}$ mice ameliorated after the cessation of CS exposure and Tamoxifen treatment (Figure 11 B). The amelioration of phenotype was associated with a decrease of DC related cytokine and chemokine levels in the BAL fluid that further confirmed the culprit role of $BRAF^{VE}$ DCs. Since the discovery of mutation in MAPK pathway, multiple studies showed that the PLCH and LCH patients treated with BRAF inhibitors resulted a favorable outcome (163, 164). However, the inhibition of BRAF protein can cause an alternative activation in the MAPK pathway that carry significant risks from a board spectrum such as cutaneous side effect including cutaneous squamous cell carcinomas and keratoacanthomas (165). Miriam and her group recently developed a nanoparticle based MAPK inhibitor drug delivery strategy that successfully decreased the tumor burden in their LCH mouse model with reduced side effects (166). Due to the similarity of LCH and PLCH, this innovative drug delivery system will be tested in our PLCH mouse model in the future.

In summary, we have established the first mouse model for PLCH and provided a novel insight into the underlying mechanism of PLCH pathogenesis.

Here we show that the $BRAF^{VE}$ DCs are recruited into the lung following CS induced CCL20 secretion. Then the locally accumulated $BRAF^{VE}$ DCs secrete CCL7 that further recruited other inflammatory cells to the lung and contribute to the nodule formation. The discovery of this mechanism encourages the development of new treatment strategies that targeting these chemokines. In addition, our data suggests that the BRAF-V600E inhibitor is sufficient to rescue the mutation-related effector cell functions in DCs and justify the rationale using BRAF-V600E inhibitors in the advanced stage of PLCH.

To examine whether our working hypothesis relates to human PLCH, we measured CCL7 and CCL20 expression in PLCH patients (Figure 13A, D). Lung tissues IHC showed diffuse CCL20 staining in the lesions of PLCH patients compared to healthy controls as well as intense staining of histiocyte-like cells within the inflammatory nodules suggest a specific cellular origin of the excessive CCL20 secretion. Future studies are needed to phenotype and examine these CCL20 secreting cells. However, unlike in our mouse model, we did not observe a consistent elevation of CCL7 in the plasma of PLCH patients. We observed only 1 patient of 3 expressing CCL7 levels above baseline detection and 2 of 3 patients showed increased production of CCL7 in stimulated PBMCs. Nevertheless, flow cytometry reveals significant population of CCL7-producing CD11c+ cells following activation. It is likely that the number of circulating

BRAF-V600E-mutant cells is very low in these patients. A recent study examining BRAF-V600E mutations in pediatric LCH revealed that the portion of DCs or monocytes carrying the mutations varied between 0.02% and 25.0% with the majority being less than 1% (125). Given that pediatric LCH manifests as a severe, systemic, multi-focal disease with a spectrum of mutations in the myeloid/monocyte lineages that are very similar or identical to those of PLCH, it is possible that even lower mutation frequencies exist in the milder, highly restricted organ involvement patterns observed in adult PLCH patients. In addition, the point in the DC lineage where the mutation occurs determines the progression and severity of LCH (125). Even though it is very likely PLCH shares this pattern, there are no studies describe such correlation. Future studies targeting the frequency and scope of mutations in a large PLCH patient cohort are required to answer these important questions. Furthermore, there were studies show that virus infection is associated with disease aggression in LCH (167, 168). Our model suggests that the stimulus like virus infection and cigarette smoke may serve as a role to activate the $BRAF^{VE}$ DC and increase the secretion of CCL7 which then recruit other inflammatory cells to the site and initiate the disease pathogenesis.

Overall, these studies also identify new roles for MAPK pathways in regulating general DC biology, including migration, survival and effector cell

responses. The discovery of this association will not only help decipher the pathogenesis of PLCH, but also provide insights into other DC-related diseases.

2.6 Material and methods

Mice. C57BL/6J, CD45.1, CD45.2 wild type mice and BRAF-V600Eflox/flox mice were obtained from Jackson Laboratories (Bar Harbor, ME). CD11c-CreERT mice were a kind gift from Dr. Maries van den Broek and have been previously described (139). Inducible CD11c-BRAF-V600E mice were generated by crossing BRAF-V600Eflox/flox mice with CD11c-CreERT mice. All experimental groups used mice with one BRAF-V600Eflox allele and one CD11c-CreERT allele. Littermates that are negative for the Cre recombinase transgene construct were used as controls. Induction of the BRAF-V600E allele was accomplished with a diet containing tamoxifen (80 mg/kg, Envigo) two weeks after weaning. Both male and female mice were included in the study. All mice were housed in the University of Cincinnati animal care facilities. All experimental procedures were performed in accordance with the University of Cincinnati Institutional Animal Care and Use Committee (06-04-07-01).

Cigarette smoke exposure. Mice were exposed to either filtered room air (FA) or cigarette smoke (CS) generated from 3R4F Kentucky Reference Cigarettes (University of Kentucky, Lexington, KY) as previously described (169). Whole body exposure were performed 4h/day, 5d/wk for up to 4 months with a TE-10z smoking machine attached to an exposure chamber (Teague Enterprises,

Woodland, CA). The concentration of the smoke/air mixture was maintained at 150 ± 15 mg/m3 total suspended particulates.

Cell isolation. Purification of DCs from lung and mediastinal lymph nodes (mLN) were performed as previously described (170). Single cell suspensions of mLNs were obtained by passing the nodes through a 100-μm nylon mesh. To obtain lung DCs, the lung vasculature was perfused with 10 ml phosphate-buffered saline (PBS) containing 0.6 mM EDTA, via the right atrium. Lung single cell suspensions were obtained by using a gentle-MACS Dissociator (Miltenyi Biotec Inc, Auburn, CA) after incubating harvested lung tissues with 100 mg/mL collagenase type IV and 20,000 U/mL DNases (Millipore-Sigma, St Louis, MO) as described (171). After ammonium chloride red blood cell lysis, CD11c+ cells were isolated by positive selection using CD11c magnetic MicroBeads beads following the manufacturer's protocol (Miltenyi Biotec Inc, Auburn, CA).

Generation and transfection of bone marrow derived DCs . Bone marrow DCs (BMDC) were derived from bone marrow as previously described (172). Briefly, bone marrow was collected from both femurs. Red blood cells were

lysed and the remaining cells passed through a 100 μm cell strainer to remove small pieces of bone and debris. Cells were then washed twice with Ca/Mg free PBS and seeded on 10 cm petri dishes at 5 × 105 cells/ml with complete DC medium (RPMI 1640 containing 10% FBS, 2 mM L-glutamine, 1mM sodium pyruvate, 0.1 mM nonessential amino acids, 50 μM β-mercaptoethanol, 1000 U/mL Pen/Strep and 20 ng/ml GM-CSF). At day 3, cell culture media was replaced with fresh complete DC media. At day 5, non-adherent and loosely-adherent cells were collected and re-seeded in a 6-well plate at the 5 × 105 cells/ml with fresh complete DC media. Cre Recombinase Adenovirus mCherry (Ad-Cre) and control null virus (SignaGen, Gaithersburg, MD) was added to the culture at a multiplicity of infection (MOI) of 150. At day 7, non-adherent and loosely-adherent cells were collected and used to perform experiments.

Lung lavage, fixation, and pathology. Bronchoalveolar lavage (BAL) fluid for cytokine analysis and cell enumeration was collected by instilling the lungs once with 1.0 mL (5 mM EDTA, Ca/Mg free PBS) followed by fluid withdraw via a tracheal cannula. For pathology, mouse lungs were inflation-fixed with buffered formalin and embedded in paraffin for histological analysis as previously described (173). Processing and staining of tissue sections was performed at

Cincinnati Children's Hospital Research Pathology Core. Three non-contiguous tissue sections were stained with hematoxylin and eosin (HE), CCL20 (1:50; R&D Systems), CD68 (1:25; Abcam), B220 (1:1000; Abcam) and CD3 (RTU; Roche). Healthy human controls and PLCH lung tissue obtained by biopsy was preserved in formalin and embedded in paraffin. Human lung tissue was obtained from the Department of Pathology and Laboratory Medicine at the University of Cincinnati Medical Center.

MicroCT. Lung MicroCT was performed using a Siemens Inveon PET/SPECT/CT scanner (Siemens Medical Solutions, Malvern, PA, USA). Parameters were as follows: 220° rotation, 440 projections, 500 ms exposure time, 2 frames summing, 80 kV voltage, 500 μA current, and effective pixel size 35.90 μm. Acquisitions were reconstructed with the Feldkamp algorithm, matrix size 1024 × 1024 × 1408, using manufacturer-provided software. Briefly, mice were anesthetized with isoflurane and connected to cardio-respiratory gating during image acquisition to minimize breathing motion artifacts. The Inveon Research Workplace (Siemens) general analysis and ImageJ (US National Institutes of Health) software were used for image review and analysis.

Flow cytometry. For cell surface marker analysis, cells were blocked with anti-CD16/CD32 (ThermoFisher Scientific) for 30 minutes followed by incubation with specific monoclonal antibodies at 4°C for 30 min in Flow Buffer (FB) (1X Ca/Mg free PBS, 0.5% bovine serum albumin (BSA), 0.1% sodium azide). Cells were washed twice with FB and immediately analyzed by flow cytometry (Attune, Thermofisher). All antibodies were obtained from ThermoFisher-ebioscience; (PE-cyanine 7 anti-mouse CD11c (N418), APC-efluor 780 anti-mouse CD11b (M1/70), APC anti-mouse CD86 (GL1), PE anti-mouse PDCA-1 (ebio129c), anti-pERK (T202/Y204 Clone MILAN8R)); BD Biosciences (PerCP-Cy 5.5 anti-mouse CD103 (M290); and anti-Bcl-xL (54H6, Cell Signaling). For p-ERK and Bcl-xL staining, bone marrow derived DCs (BMDC) were fixed with 4% PFA for 30 min at room temperature followed by fixation/permeabilization with ice cold methanol (90% final concentration) for 30 min. Cells were then washed 2X with FB and stained with anti-pERK and anti-Bcl-xL. Data was analyzed using Flowjo software (v10) (Flowjo, LLC) and/or FCS Express V5 (De Novo Software). Cells were first gated on lymphocytes and doublets were excluded by gating on single cells (FSC-A vs FSC-W). CD11c+ cells were then gated, and macrophages were discriminated from DCs based on high cellular autofluorescence. DCs were gated as CD11c+, MHCII+ and autofluorescence mid/low cells. Subsets of DC and CD86

expression were then further gated from CD11c+, MHCII+ and autofluorescence mid/low DC populations. The compensation matrix was determined by using UltraComp eBeads (ThermoFisher/eBioscience). Appropriate fluorescence minus one (FMO) and negative controls were used to set gates for the above populations.

Immunofluorescence staining. Immunofluorescence staining was performed on cytospin preparations by double indirect immunofluorescence method as previously descripted (174). Briefly, slides were blocked with goat serum and then incubated overnight at 4°C with rabbit anti-mouse CCL7 (1:200; Biorbyt (Polyclonal)). Secondary labelling was performed with a 24 hour incubation with goat anti-rabbit (1:500; ThermoFisher). Nuclei were counterstained with DAPI (Sigma-Aldrich; 1:2,000). Images were captured using a Zeiss LSM710 inverted confocal microscope at the Live Microscopy Core, Department of Molecular and Cellular Physiology, University of Cincinnati. Negative controls (unstained and secondary only) were included in each experiment.

Adoptive transfers. BMDCs (> 90% purity) were derived from CD45.2 wild type and BRAF-V600E bone marrow as described above. BMDCs were

transfected with Ad-Cre at day 5. At day 7, a total of 2 x 106 BMDCs in 50 µl PBS were injected into recipient CD45.1 transgenic mice via tail vein. Two days after injection, the lung and mLN were collected and digested from the recipient mice as described. The donor BMDCs in lungs and mLN were determined by the surface expression of CD45.2 by flow cytometry.

DC stimulation. Freshly isolated pulmonary DCs and BMDCs were maintained in complete DC medium. Toll-like receptor (TLR) ligand activation was assessed using 1 x 105 freshly isolated DC seeded in 100 uL of DC media in 96-well round bottom plates. DCs were rested for 1 hour followed by a pre-incubation with 20 ng/ml IFN–γ (PeproTech) for 2 hours. DCs were then treated for 16 hrs with 1 µg/ml poly IC (InvivoGen), 1 µg/ml LPS (Sigma Aldrich). IL-12 p40 and IL-6 in supernatant were then measured by ELISA (ThermoFisher).

Cyclic AMP assay. cAMP levels were measured using the AlphaScreen cAMP assay kit (PerkinElmer) per manufacture's protocol in 384 well plates (PerkinElmer). Briefly, 5 µl of cells at 1x106/ml and 5 µl of acceptor bead solution was added to each well in triplicate. Cells were stimulated with 5 µl of Forskolin (1x10-5 M) was added and the plate was incubated at 37 ºC for 15

min. Chemokines (5 µl) were then added to a final concentration of 300 ng/ml. After a further 30 minute incubation at 37 ºC, 15 µl of donor beads was added all wells. After 1 hour of incubation, cAMP levels were measured using a florescence plate reader at excitation 680/30 and emission 570/100 (Synergy HTX, Biotek).

Chemotaxis assays. Migration assays were performed using 24-well Transwell cell culture chambers with 5.0 µm pore size (Corning Glass) as previously described (175). Briefly, 3x105 day 7 BMDCs were placed in the upper chamber and allowed to migrate towards the lower chambers containing either recombinant mouse CCL19 (300 ng/ml), CCL20 (300 ng/ml), or CCL21 (300 ng/ml) in complete medium at 37°C. After 3 hours, the number of cells in the lower chamber were determined by flow cytometry.

RNA extraction and Real-Time Quantitative PCR. Total RNA was extracted using TRIzol Reagent (Invitrogen) and RNeasy MinElute kit (Qiagen). Reverse transcription was performed using the Quantitect Reverse Transcription kit (Qiagen), per manufacturer's instructions. Quantitative PCR with chemokine genes was conducted with the Power SYBR Green Master Mix (ThermoFisher)

with the following primers from Integrated DNA Technologies, Inc: CCL2 (Mm.PT.58.42151692), CCL5 (Mm.PT.58.43548565), and CCL7 (Mm.PT.58.17719534). The RPL32 (F: 5'-gaagttcctggtccacaacg-3' R:5'-gcgatctcggcacagtaag-3') was used as a house keeping gene for normalization. The quantitative PCR with mutation-specific BRAF primers was conducted using the iTaq™ Universal Supermix (Bio-Rad) as previously described (125). Briefly, the reaction was performed with 500 nM of the mutation specific BRAF-V600E mRNA primer: (F: 5'-TAGGTGACTTTGGTCTAGCCACGGA-3'

R: 5'-GTAGCTGGCCGGTCATCAGTTCG-3') and 250 nM of the FAM-labeled hybridization probe (6-FAM-TCAGACGTGTATGCGTTTGGGATTG-MGB-NFQ) at an annealing temperature of 68°C for 45 cycles. Experiments were performed in triplicate and relative fold change was determined by the delta delta Ct method.

Statistics. 4-8 mice were used in each group with at least 3 independent experiments. Ex vivo experiments were performed in duplicate on at least three separate occasions. Unless otherwise indicated, data are expressed as mean ± standard errors of the means (SEMs). Student's t tests and ANOVA were used for statistical analyses. $P < 0.05$ was considered statistically significant.

2.7 Study limitations.

The efficiency of the Cre-ERT mediated BRAF-V600E recombination in the DC lineage varied between mice and resulted in inconsistent disease penetrance. Due to the limitation of an assay to define excision efficiency , the correlation of the disease severity with the mutation frequency was beyond the scope of this study. In addition, we observed that the CD11c promotor in the Cre-ERT mice seemed leak to the type 2 alveoli epithelium cells and resulted in type 2 cell hyper-proliferation in some mice. However, we observed no prominent phenotypical and physiological alterations compare to littermates that did not develop the type 2 cell hyper-proliferation. Another limitation of our PLCH mouse model is that the lung tissue destructions in the mice were not surrounded by a fibrotic wall and did not represent the characteristic cystic lesion observed in human patients. Finally, we showed that the PBMCs isolated from PLCH secrete more CCL7 upon activation. However, due to the limitation of sample size and the variance between samples, we were not sufficiently powered to determine if CCL7 can be used as a potential biomarker for PLCH.

2.8 Future direction

We have established the first PLCH mouse model and suggested a chemotaxis-based pathogenesis. Future studies should focus on examining the mechanism of lung tissue destruction. Granzymes and matrix metalloproteinases (MMPs), particularly MMP2 and MMP9, can be produced by DCs and other infiltrating monocytoid cells in inflammatory nodules and may contribute to the airway remodeling in various cystic lung diseases including PLCH. To explore this idea, lung histology, immunohistochemical (IHC) for MMPs in PLCH patient biopsies and PLCH mouse lungs should be assessed for increased expression and activation. Both WT and mutant DCs can be isolated from FA or CS exposed mice and the secretion of MMPs can be measured by zymography, enzymatic activity and western blots. Furthermore, it will be important to study the mechanism of how the BRAF-V600E mutation controls the increased responsiveness of DC towards TLR ligands and CCL20 and how this mutation increases DCs secretion of CCL20 and CCL7. Currently, the diagnosis of PLCH relay heavily on HRCT and pathology. In order to identify a potential biomarker, and more importantly, correlate the circulating mutant cells with disease progression, efforts are already underway to collect more PLCH patient samples

through local recruiting and international collaborations to test the potential of CCL7 to answer these important questions.

2.9 Figure

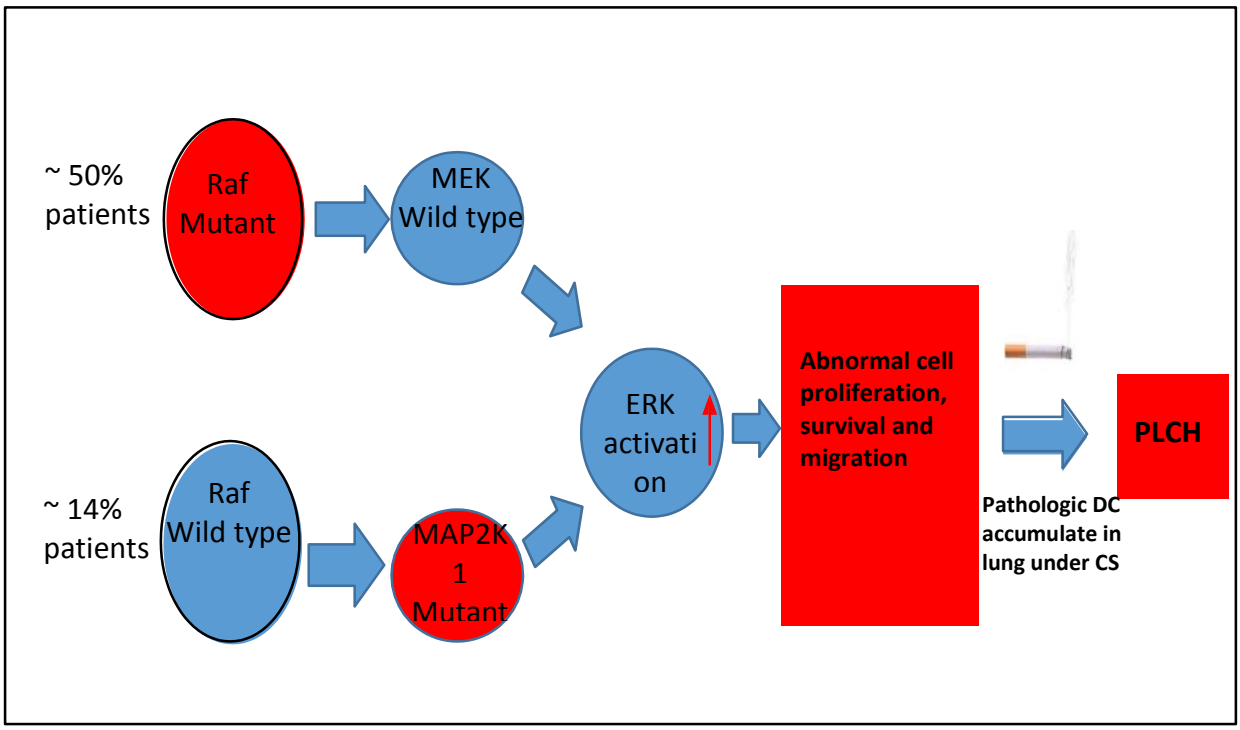

Figure 2. Schematic illustration of the MAPK pathway mutations in PLCH.

The RAS-RAF-MEK-ERK pathway represents a driver in the pathogenesis of LCH while offering the potential explanation of pathogenesis and targeted therapeutic approaches for PLCH. Around 50% of LCH and PLCH patients carry mutated form BRAF (V600E) capable of constitutive phosphorylation of the downstream effectors MEK that ultimately drive ERK activity. Up to 33%BRAF-V600E–negative cases (14% total) harbor a mutation in MAP2K1 that leads to constitutive MEK1 and consequent ERK activation, promoting downstream proliferation and survival networks which may drive LCH pathogenesis.

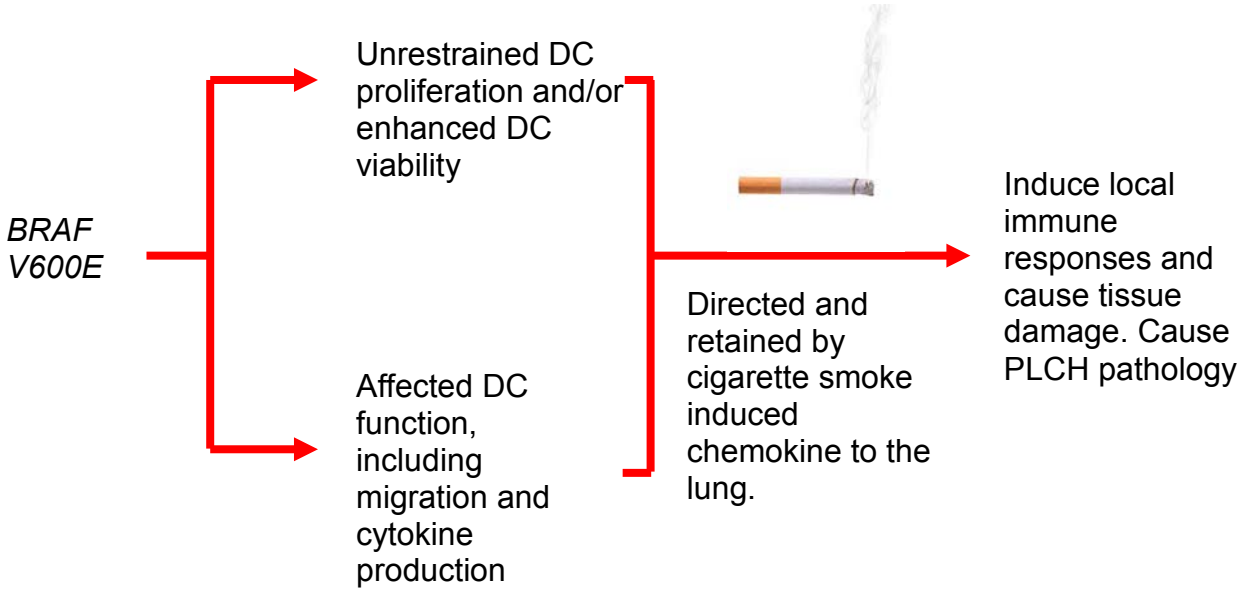

Figure 3. Schematic illustration of the central hypothesis.

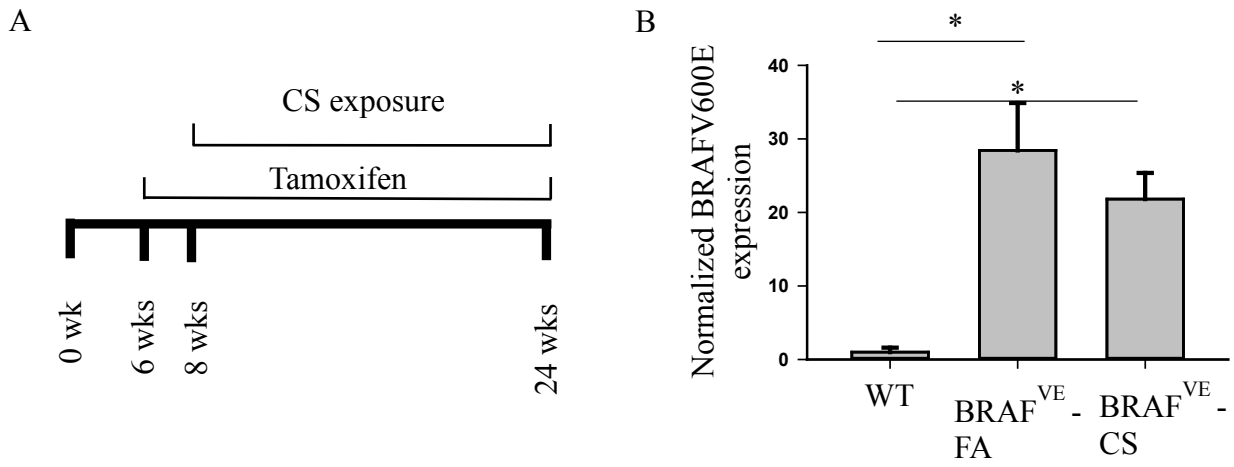

Figure 4. Generate of BRAF^{VE} mice that harbors BRAF-V600E mutation in CD11c lineage. (A). Scheme of how to generate PLCH mouse model. CD11c-ERT- BRAF^{VE} mice were treated with Tomaxifen and exposed to CS at indicated time. (B) The expression of BRAF-V600E mRNA in lung of WT mice and BRAF^{VE} mice that exposed to FA or CS was measured by RT-PCR. Data are shown as the mean ± SEM of at least 3 independent experiments. *$p < .05$ (unpaired student t test).

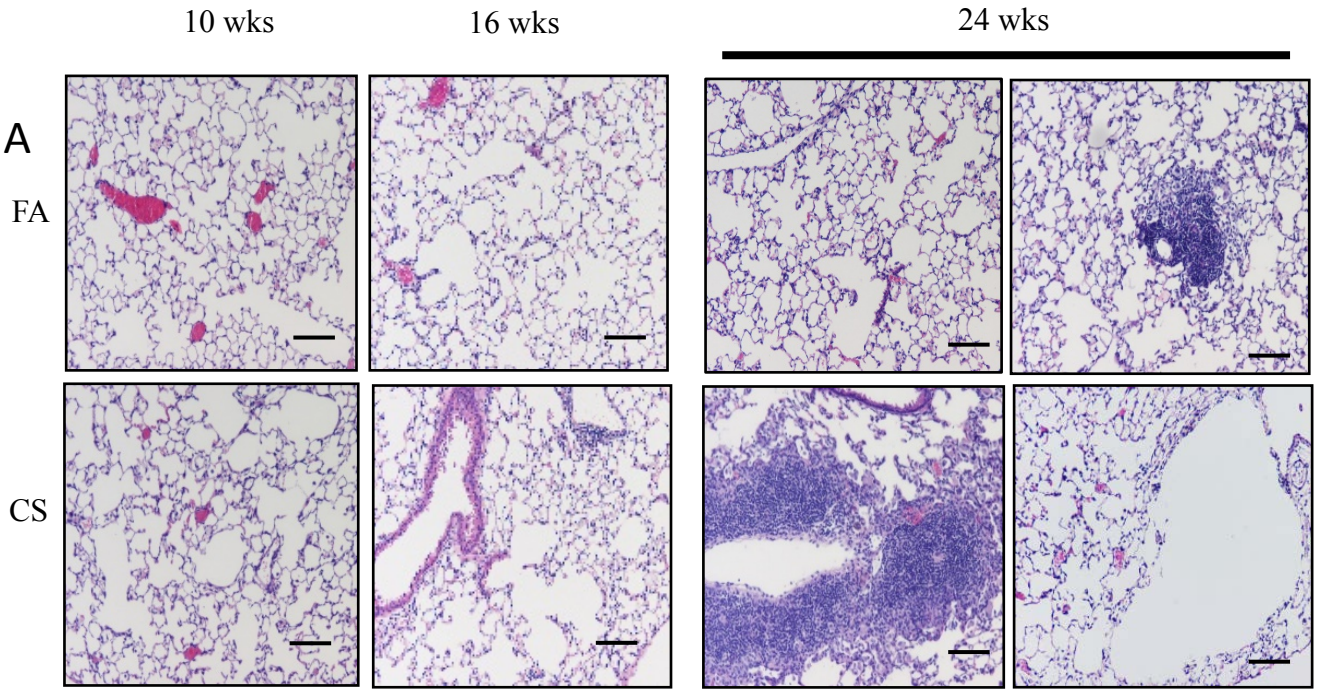
10 wks
16 wks
24 wks
A
FA
CS

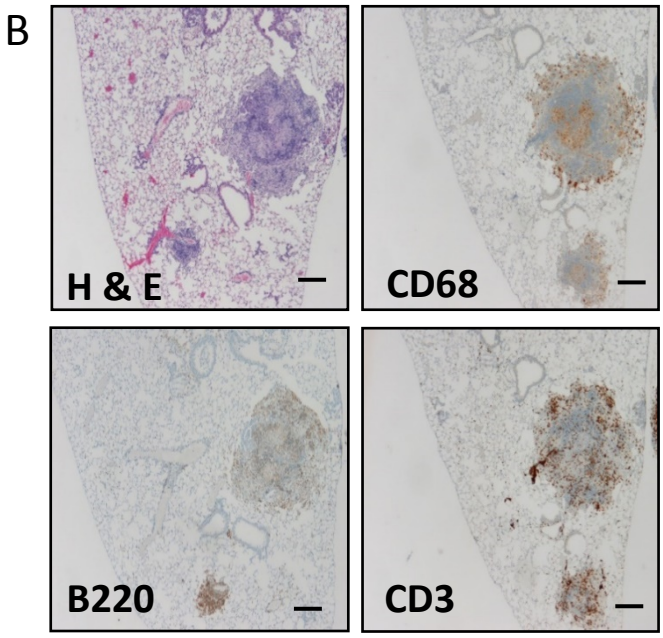
B
H & E
CD68
B220
CD3

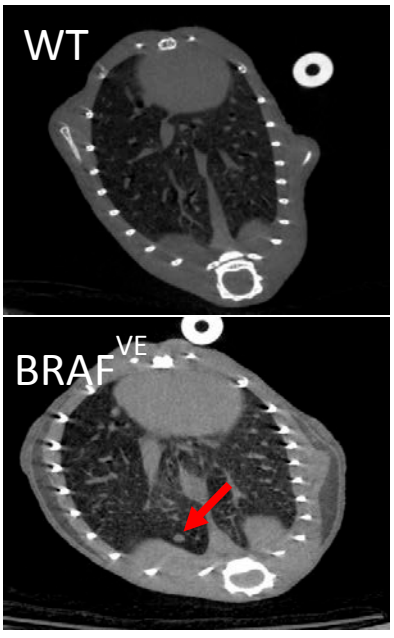
C
WT
BRAF VE

Figure 5. BRAF-V600E expression in CD11c DC lineage drives PLCH-like lesion in mice exposed to CS. (A) Representative H&E lung histology from $BRAF^{VE}$ mice that exposed to FA or CS at indicated time. Scale bar, 100 μm, n=6. (B) Representative H&E and IHC staining of lung granuloma lesion in $BRAF^{VE}$ mice that exposed to CS for 4 months. Scale bar, 250 μm, n=6. (C) Representative Micro-CT images of WT mice and $BRAF^{VE}$ mice that exposed to CS for 4 months. n=4.

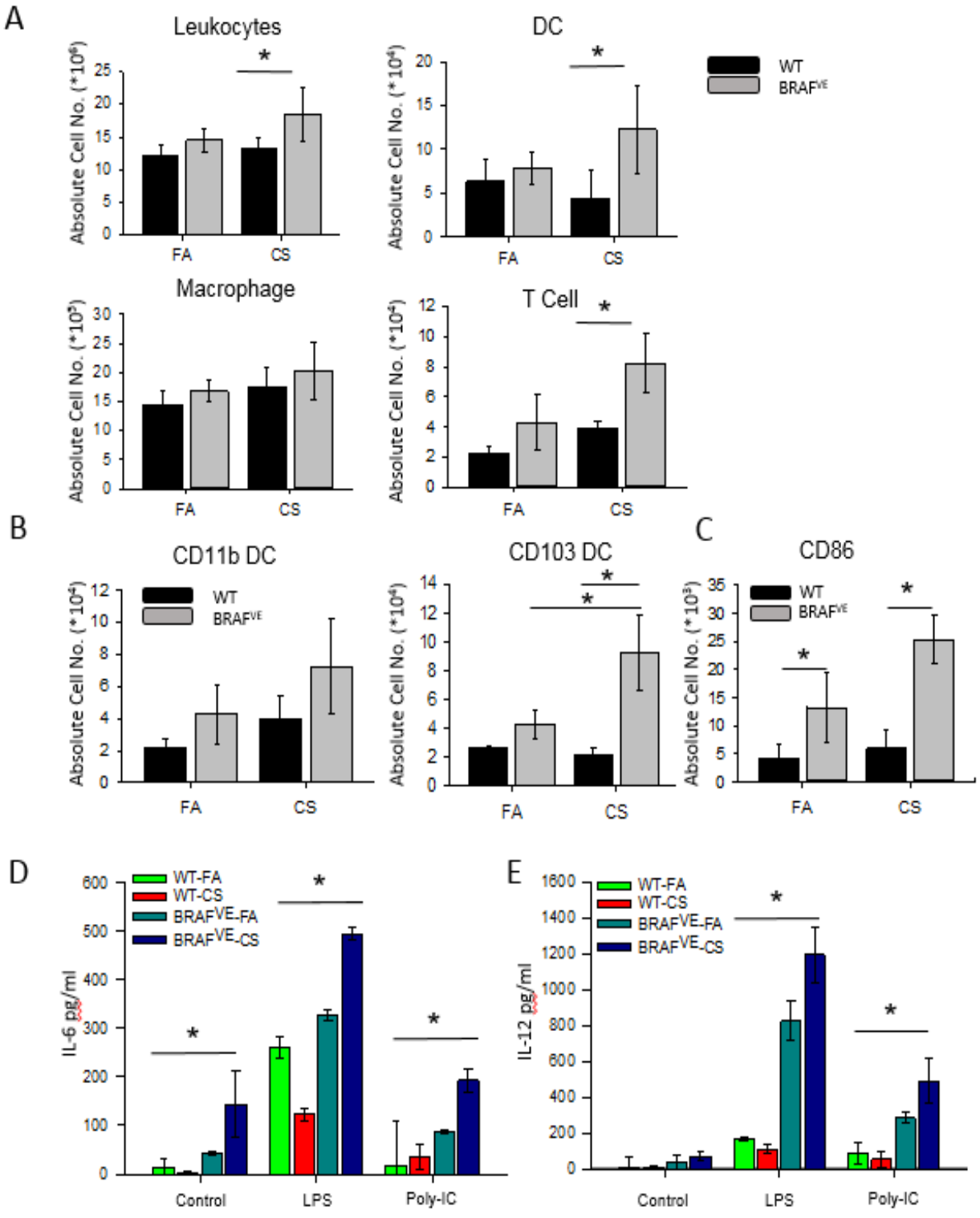
A
Leukocytes
Absolute Cell No. (*10⁶)
FA
CS
DC
Absolute Cell No. (*10⁴)
WT
BRAFVE
Macrophage
Absolute Cell No. (*10³)
T Cell
Absolute Cell No. (*10⁴)
B
CD11b DC
CD103 DC
C
CD86
Absolute Cell No. (*10³)
D
WT-FA
WT-CS
BRAFVE-FA
BRAFVE-CS
IL-6 pg/ml
Control
LPS
Poly-IC
E
IL-12 pg/ml

Figure 6. Increased inflammatory cells and disrupted DC homeostasis in the lung of $BRAF^{VE}$ mice. (A) Absolute cell number of leukocytes, DCs, macrophages and T cells were determined by flow cytometry. Leukocytes were gated as $CD45^+$, DCs were gated as $CD11c^+$, $MHCII^+$ and autofluorescence $^{mid/low}$ cells, macropages were gated as $CD11c^+$and autofluorescence ^{high} cells, T cells were gated as $CD11c^-$ and $CD3^+$cells. (B) The absolute number of CD11b DCs and CD103 DCs were determined by flow cytometry. Both subsets were gated from DCs population. CD11b DCs were gated as $CD11b^-$ and $CD103^+$ cells and CD103 DCs were gated as $CD11b^-$ and $CD103^+$ cells. (C) The number of DCs expressed maturation marker CD86 was determined by flow cytometry. (D, E) DCs were isolated from lung and treated with or without 20ng/ml IFN-gamma for 2 hours before treated with 1 μg/ml Poly IC, 1 μg/ml LPS for 16 hrs. The supernatant was collected and the IL-6 and IL-12 p40 was measured by ELISA. Data are shown as the mean ± SEM of at least 4 independent experiments. *$p < .05$ (unpaired student t test).

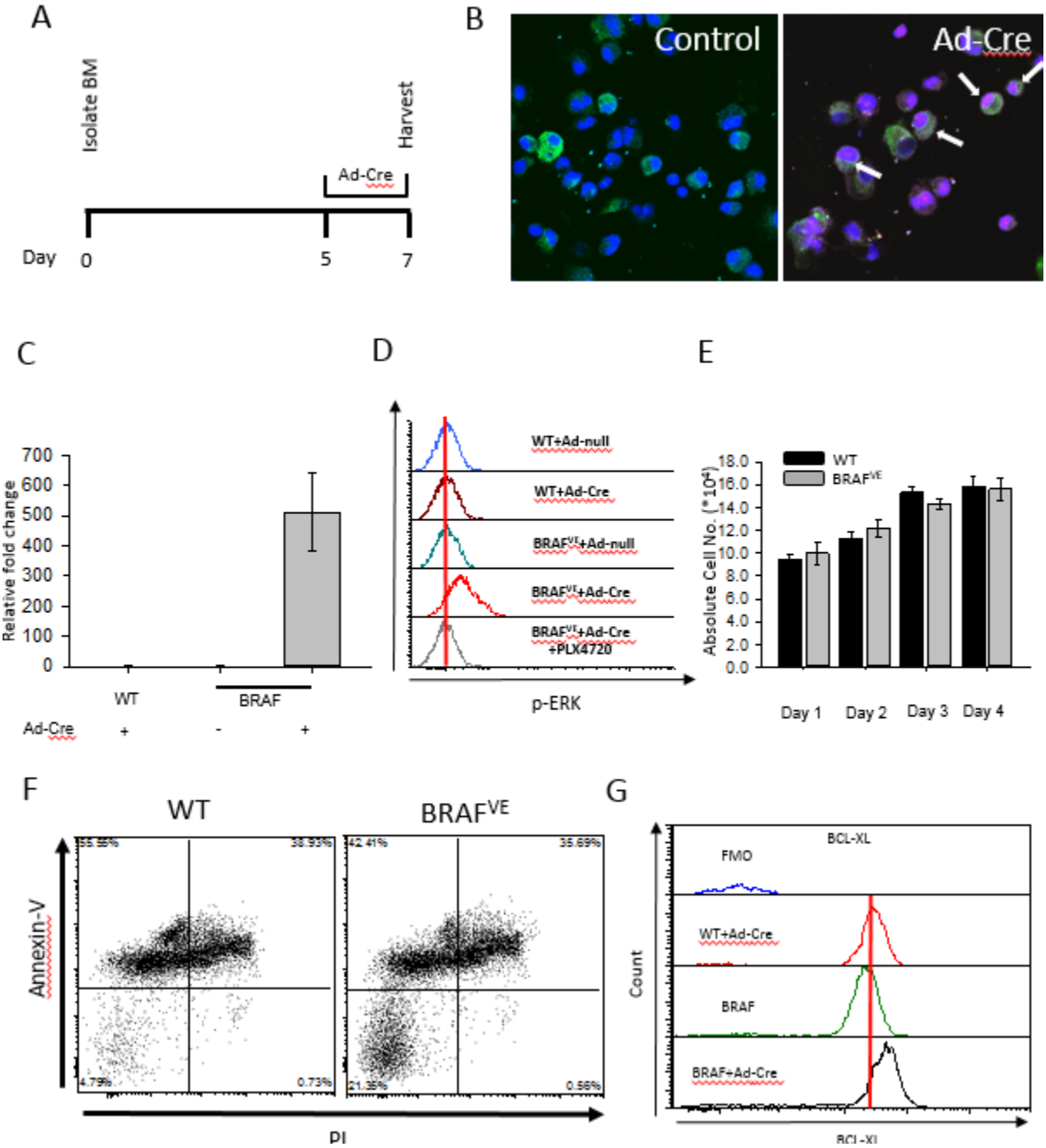
A
Isolate BM
Harvest
Ad-Cre
Day
0
5
7
B
Control
Ad-Cre
C
Relative fold change
700
600
500
400
300
200
100
0
WT
BRAF
Ad-Cre
+
-
+
D
WT+Ad-null
WT+Ad-Cre
BRAFVE+Ad-null
BRAFVE+Ad-Cre
BRAFVE+Ad-Cre +PLX4720
p-ERK
E
Absolute Cell No. (*10⁴)
18.0
16.0
14.0
12.0
10.0
8.0
6.0
4.0
2.0
0.0
WT
BRAFVE
Day 1
Day 2
Day 3
Day 4
F
WT
BRAFVE
Annexin-V
55.58%
38.93%
4.79%
0.73%
42.41%
35.69%
21.35%
0.56%
PI
G
BCL-XL
FMO
WT+Ad-Cre
BRAF
BRAF+Ad-Cre
Count
BCL-XL

Figure 7. BRAF-V600E mutation is associated with increased cell viability by increasing expression of BCL-XL. (A) Scheme of how to generate $BRAF^{VE}$ BMDC. Ad-Cre that carried a mCherry reporter was added to the culture of BMDC at the indicated time and the cells were harvested and used for assays two days later. (B) Representative IF staining of the BMDCs generated from CD11c-ERT- $BRAF^{VE}$ mice that were transfected with or without Ad-Cre for 2 days. Arrows point cells that positive for CD11c and mCherry staining (Blue – DAPI, Green – CD11c, Red – mCherry). n=4 (C) The expression of BRAF-V600E mRNA in WT BMDCs and $BRAF^{VE}$ BMDCs with or without the Ad-Cre transfection was measured by RT-PCR. $*p < .05$ (D) The p-ERK expression level in BMDCs were determined by flow cytometry. At indicated group, PLX-4720 was added to the culture at day 6 at the concentration of 1 μM. (E) Absolute number of BMDCs were determined by flow cytometry at the indicated time. Data are shown as the mean ± SEM of at least 4 independent experiments. $*p < .05$ (F) GM-CSF was deprived from the culture medium at day 7 and after 16 hours the apoptotic status of BMDCs was measured by flow cytometry. Data show representative flow cytometry analysis of four independent experiments. (G) The expression of BCL-XL in BMDCs was measured by flow cytometry. Data show representative flow cytometry analysis of four independent experiments.

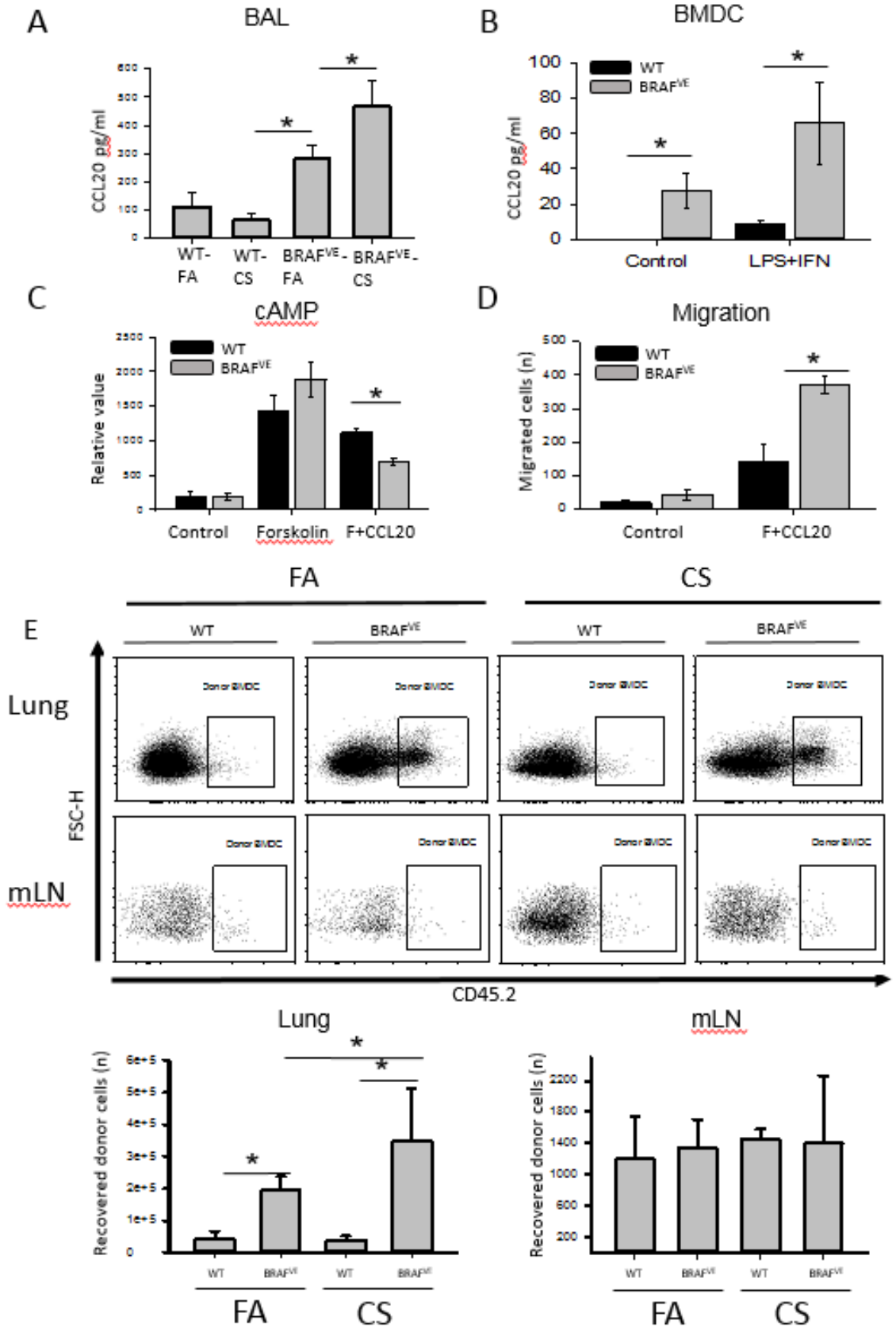
A
BAL
CCL20 pg/ml
WT-FA
WT-CS
BRAFVE-FA
BRAFVE-CS
B
BMDC
WT
BRAFVE
CCL20 pg/ml
Control
LPS+IFN
C
cAMP
Relative value
Control
Forskolin
F+CCL20
D
Migration
Migrated cells (n)
Control
F+CCL20
E
FA
CS
WT
BRAFVE
Lung
mLN
FSC-H
CD45.2
Lung
mLN
Recovered donor cells (n)
FA
CS

Figure 8. BRAF-V600E mutation increases the recruitment of DCs to the lung. (A) CCL-20 level in the BAL of mice that were exposed to FA/CS for 4 months was measured by ELISA. Data are shown as the mean ± SEM of 5 independent experiments. *p < .05 (unpaired student t test). (B) CCL-20 secretion of BMDCs that were treated with/without LPS+IFN-gamma for overnight was measured by ELISA. Data are shown as the mean ± SEM of 5 independent experiments. *p < .05 (unpaired student t test). (C) The cellular cAMP level was measured by florescence plate reader at excitation 680/30 and emission 570/100. Data are shown as the mean ± SEM of 3 independent experiments. *p < .05 (unpaired student t test). (D) The number of cells migrated into the lower chamber of the transwell plate was determined by flow cytometry after 3 hours incubation. Data are shown as the mean ± SEM of 3 independent experiments. *p < .05 (unpaired student t test). (E) 2 million of WT/ $BRAF^{VE}$ donor BMDCs were injected into the recipient CD45.1 mice that were exposed to FA/CS for 6 months. The number of donor cells in the lung and mLN of the recipient mice were determined by gating on the CD45.2 expression after 2 days of transplantation. Data are shown as the mean ± SEM of 3 independent experiments. *p < .05 (unpaired student t test).

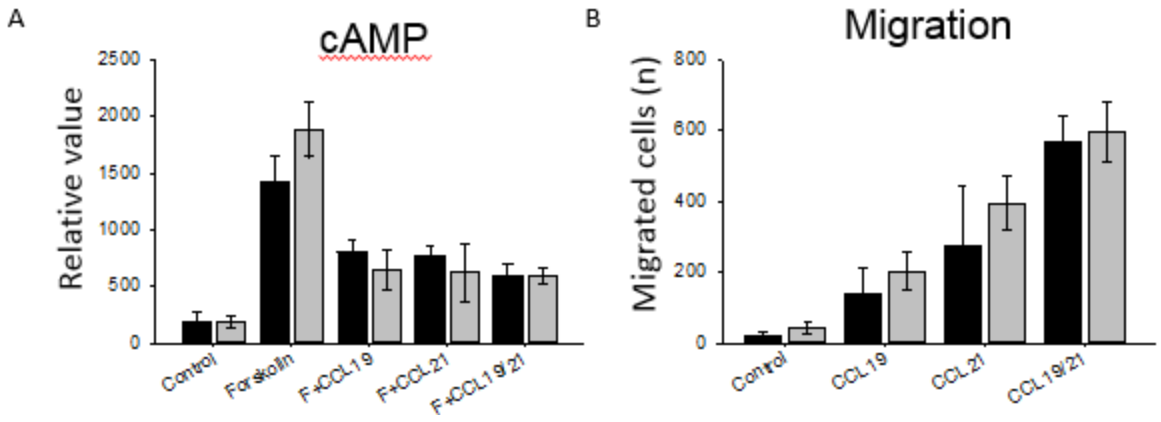

Figure 9. BRAF-V600E mutation does not alter CCR 7-CCL19/21 migration capacity. (A) The cellular cAMP level was measured by florescence plate reader at excitation 680/30 and emission 570/100. Data are shown as the mean ± SEM of 3 independent experiments. *p < .05 (unpaired student t test). (B) The number of cells migrated into the lower chamber of the transwell plate was determined by flow cytometry after 3 hours incubation. Data are shown as the mean ± SEM of 3 independent experiments. *p < .05 (unpaired student t test).

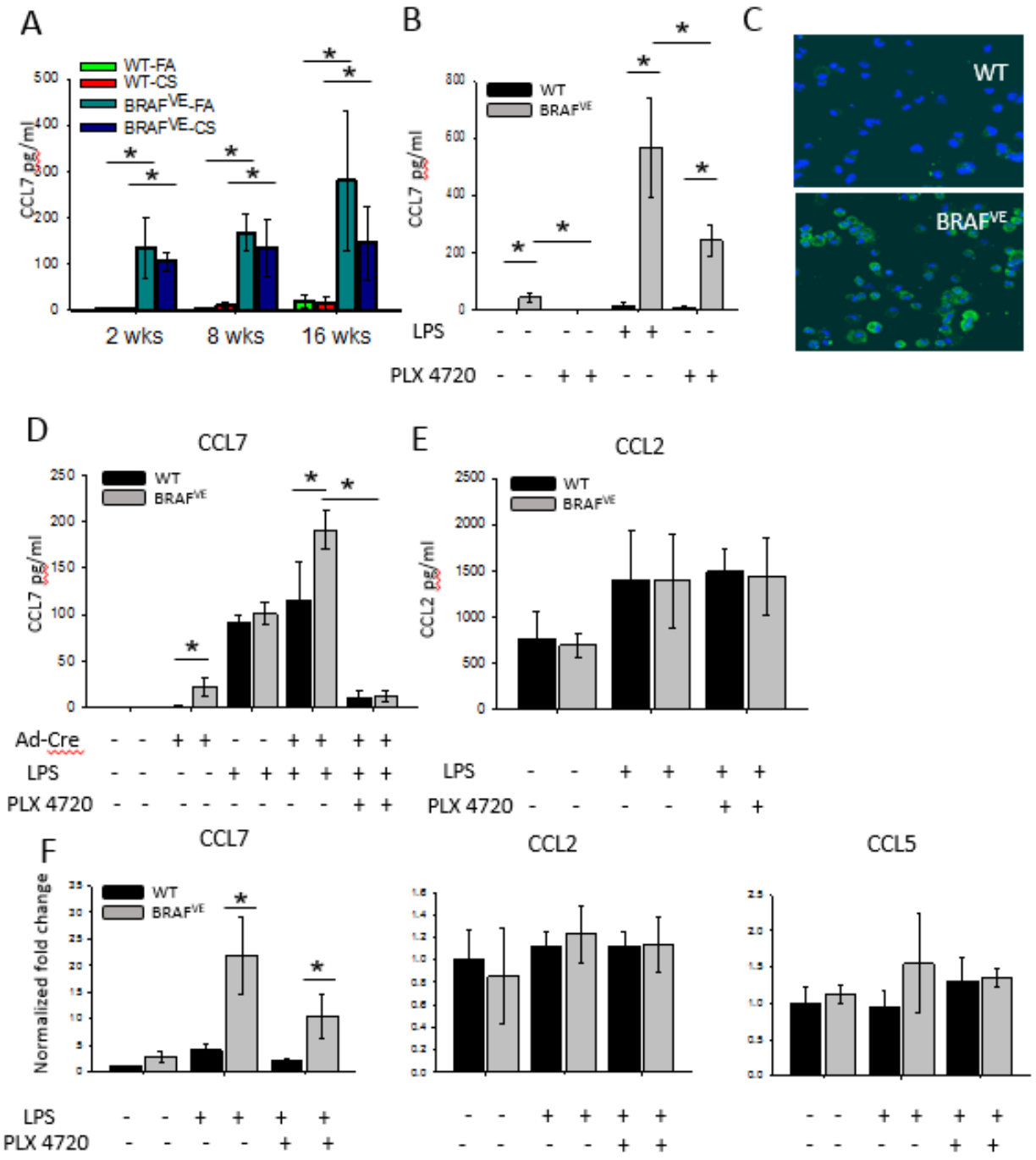
A
WT-FA
WT-CS
BRAFVE-FA
BRAFVE-CS
CCL7 pg/ml
2 wks
8 wks
16 wks
B
WT
BRAFVE
CCL7 pg/ml
LPS
PLX 4720
C
WT
BRAFVE
D
CCL7
WT
BRAFVE
CCL7 pg/ml
Ad-Cre
LPS
PLX 4720
E
CCL2
WT
BRAFVE
CCL2 pg/ml
LPS
PLX 4720
F
CCL7
CCL2
CCL5
WT
BRAFVE
Normalized fold change
LPS
PLX 4720

Figure 10. BRAF-V600E mutation induces DCs secretion of CCL 7. (A) Peripheral blood was collected from mice that exposed to FA/CS for indicated period and the CCL 7 level in the serum was measured by ELISA. Data are shown as the mean ± SEM of 5 independent experiments. *p < .05 (unpaired student t test). (B) The secretion of CCL 7 from WT/ $BRAF^{VE}$ pulmonary DCs treated with/without 1 ug/ml LPS and 1 μM PLX-4720 was determined by ELISA. Data are shown as the mean ± SEM of 5 independent experiments. *p < .05 (unpaired student t test). (C) Representative IF staining of the BMDCs that were treated with 1 ug/ml LPS for overnight. (Blue – DAPI, Green – CCL 7). Data are shown as the mean ± SEM of 3 independent experiments. *p < .05 (unpaired student t test). (D, E) The secretion of CCL 7 and CCL 2 from WT/ $BRAF^{VE}$ BMDCs treated with/without 150 MOI Ad-Cre, 1 ug/ml LPS and 1 μM PLX-4720 was determined by ELISA. Data are shown as the mean ± SEM of 5 independent experiments. *p < .05 (unpaired student t test). (F) The CCL 2, CCL 5 and CCL 7 mRNA expression level in BMDCs treated with/without 1 ug/ml LPS and 1 μM PLX-4720 was determined by RT-PCR. Data are shown as the mean ± SEM of 3 independent experiments. *p < .05 (unpaired student t test).

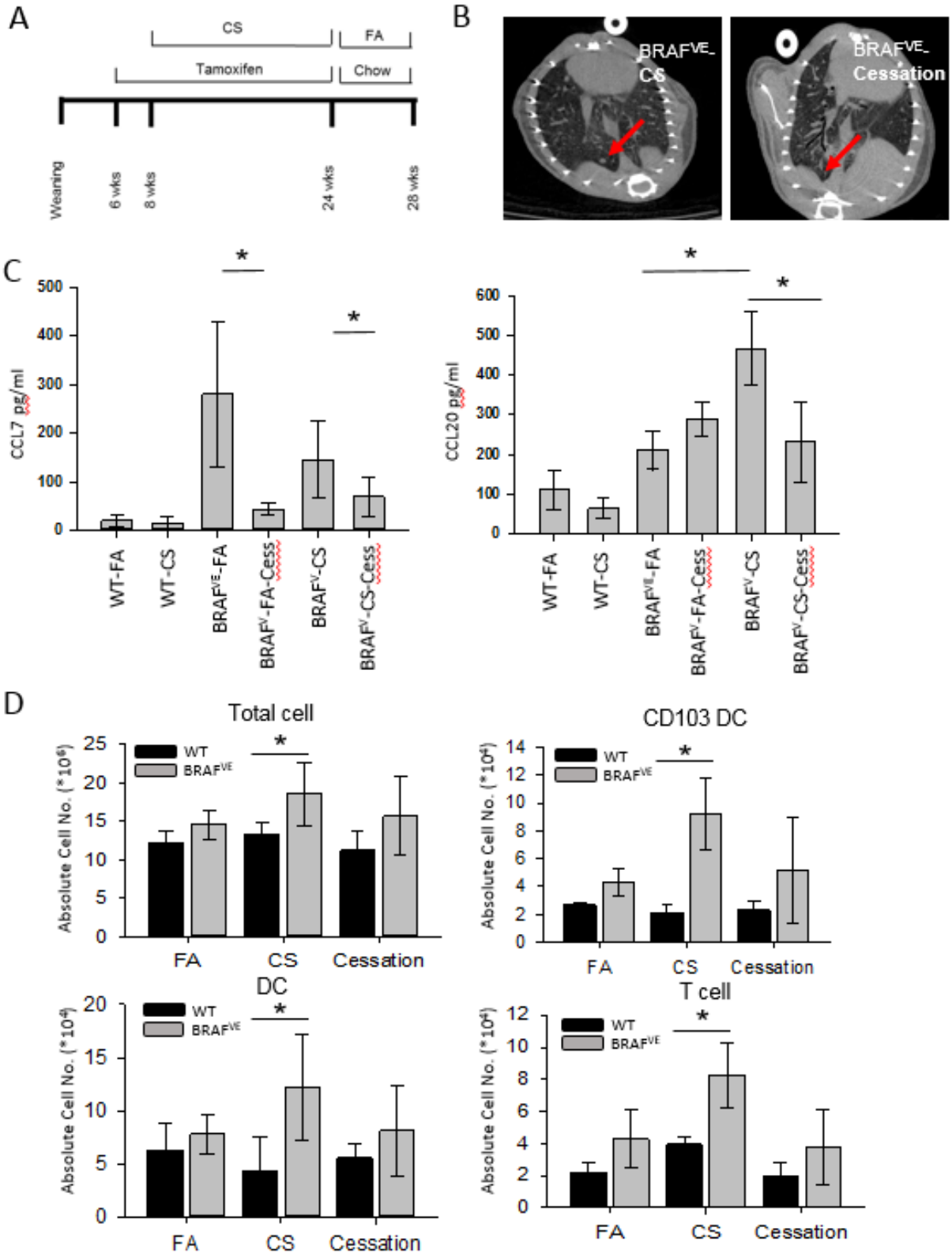
A
CS
FA
Tamoxifen
Chow
Weaning
6 wks
8 wks
24 wks
28 wks
B
BRAFVE-CS
BRAFVE-Cessation
C
CCL7 pg/ml
CCL20 pg/ml
WT-FA
WT-CS
BRAFVE-FA
BRAFV-FA-Cess
BRAFV-CS
BRAFV-CS-Cess
D
Total cell
CD103 DC
DC
T cell
Absolute Cell No. (*10⁶)
Absolute Cell No. (*10⁴)
WT
BRAFVE
FA
CS
Cessation

Figure 11. CS and Tamoxifen cessation ameliorated the PLCH phenotype in the BRAF^{VE} mice. (A) Scheme of cessation experiments. Mice were treated with Tamaxifen chow and exposed to CS and then switched to normal chow and FA at indicated time. (B) Representative Micro-CT images of mice that were pre-exposed to CS for 4 months and treated with cessation for 1 month. Pictures show the pre-and after- cessation images of the same mouse. n=4. (C) The CCL 7 level in the serum and CCL 20 level in the BAL of mice exposed to FA/CS for month with/without 1 month of cessation was measured by ELISA. Data are shown as the mean ± SEM of 4 independent experiments. *$p < .05$ (unpaired student t test). (D) The absolute number of inflammatory cells in the mice was determined by flow cytometry with gating strategy explained in Figure 2A. Data are shown as the mean ± SEM of 4 independent experiments.

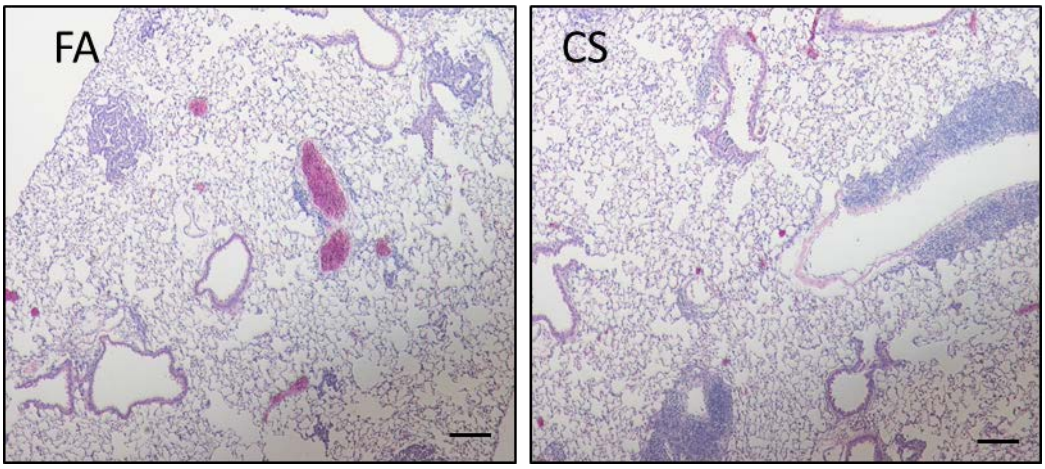

Figure 12. CS and Tamoxifen cessation ameliorated the lung lesions in the BRAF^{VE} mice. Representative H&E lung histology from BRAF^{VE} mice that exposed to FA or CS at indicated time. Scale bar, 100 μm, n=6.

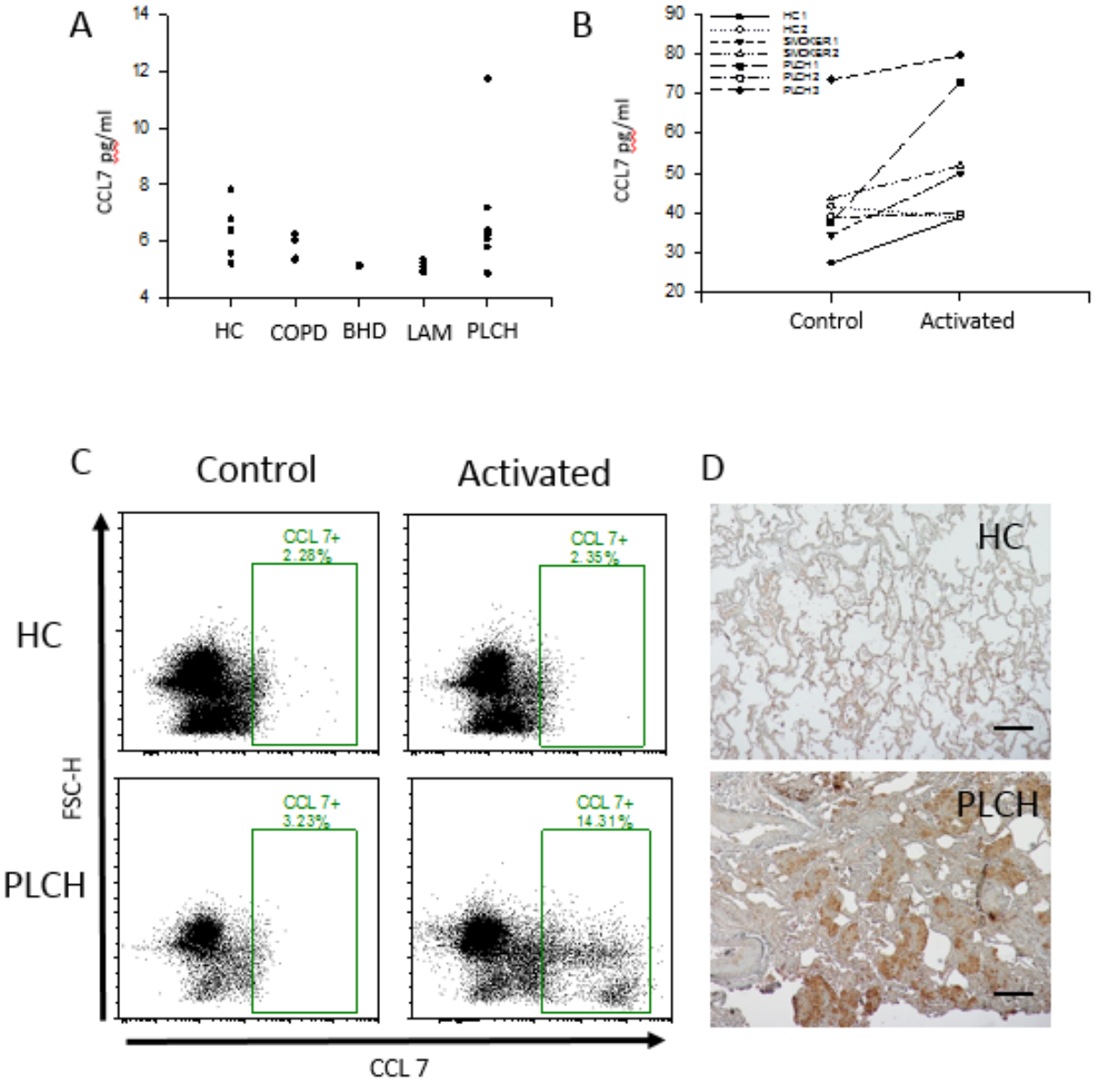
A
CCL7 pg/ml
14
12
10
8
6
4
HC
COPD
BHD
LAM
PLCH
B
CCL7 pg/ml
90
80
70
60
50
40
30
20
HC 1
HC 2
SMOKER 1
SMOKER 2
PLCH 1
PLCH 2
PLCH 3
Control
Activated
C
Control
Activated
HC
PLCH
FSC-H
CCL 7
CCL 7+
2.28%
CCL 7+
2.35%
CCL 7+
3.23%
CCL 7+
14.31%
D
HC
PLCH

Figure 13. PLCH patients were associated with increasing level of CCL 7 and CCL 20. (A) The CCL 7 level in the plasma of patients was measured by ELISA. Data are shown as the mean ± SEM of 3 independent experiments. (B) PBMCs were isolated from patients and treated with/without LPS+IFN-gamma overnight. The CCL 7 in the supernatant was determined by ELISA. Data are shown as the mean ± SEM of 3 independent experiments. *$p < .05$ (unpaired student t test). (C) Representative flow cytometry analysis of CCL 7 positive cells in PBMCs that were treated with/without LPS+IFN-gamma. n=4. (D) Representative CCL 20 staining on healthy controls' and PLCH patients' lung biopsy. Scale bar, 100 μm, n=5.

Chapter III

NKG2D is required for regulation of lung pathology and DC function following RSV infection

Huan Liu[1], Andrew R Osterburg[1], Jennifer Flury[1], Shuo Huang[1], Francis X McCormack[1, 3], Stephania A Cormier[2], Michael T Borchers[1,3]

[1]Department of Internal Medicine, Division of Pulmonary, Critical Care and Sleep Medicine, University of Cincinnati, Cincinnati, OH 45267

[2] Departments of Pediatrics, Infectious Disease, University of Tennessee, Memphis, TN 38163

[3] Cincinnati Veteran's Affairs Medical Center, Cincinnati, OH 45267

3.1 Introduction

The importance of proper DC function maintaining the normal Lung immune response against virus infection

As the most efficient antigen presentation cells, DC play a pivotal role in the onset and regulation of innate and adaptive immune responses against virus infection. On the one hand, DC has highly efficient mechanisms that allow them to detect, capture, process and present antigens, and to activate and guide the differentiation of T cells into effector and memory cells present virus antigen and coordinate other inflammatory cells in the lung that initiate and participate the anti-viral immune response (176). On the other hand, some virus like HIV using DC like transinfection vehicle that avoid the proper immune surveillance and assistance in disease spreading (177). During virus infection, the homeostasis of lung microenvironment is disturbed in aspects such as the TLR expression on epithelial cells, DCs and macrophages; local cytokine milieu and cell-cell interactions (178).

Current understanding of RSV infection

Respiratory syncytial virus (RSV) is a common cause of respiratory tract infection in young, elderly, and immunocompromised patients. It is estimated that there are 33.8 million new cases and 199,000 RSV related deaths worldwide each year (179). In susceptible populations the RSV infection can spread to the lower respiratory tract, causing bronchiolitis and pneumonia associated with airway epithelial cell destruction and sloughing, mucus secretion, and pulmonary immune cell infiltration (180, 181). Currently, there are no safe and effective RSV vaccines and therapeutic options are limited. The incomplete understanding of RSV infection related pathogenesis, combined with the urgent need to identify safe and effective therapeutic targets, underscore the need to investigate the host response during RSV infection.

The association of NKG2D and RSV infection

Natural killer (NK) cells are important effector cells in controlling RSV infection although the mechanisms are not fully understood (182, 183). NKG2D (KLRK1, killer cell lectin like receptor K1, CD314) is a well characterized activating

receptor expressed on virtually all NK cells (184), most Nature Killer T cells (NKT) cells and subpopulations of γδ T cells (185). Additionally, all human CD8+ αβ T cells express NKG2D, whereas mice express NKG2D only on activated and memory type αβ CD8+ T cells (186). Effector cells of both the innate and adaptive immune system utilize NKG2D in the surveillance of inflammation and cancers as well as in some autoimmune processes and transplantation reactions. NKG2D recognizes multiple ligands including MICA, MICB, and the UL-16 binding proteins in humans (ULBP1-6) and the mouse UL16-binding protein-like transcript 1 (Mult1), retinoic acid–inducible early transcripts (Rae1), and H60 in mice (187) . NKG2D ligands exhibit little or no surface expression under homeostatic conditions but are induced under conditions of stress including cellular transformation, DNA damage, infection, and other cellular stresses on several cell types (188).

The cross talk between NK cells and DCs and its role in RSV infection

As the most efficient antigen presentation cells, dendritic cells (DC) play a pivotal role in the onset and regulation of innate and adaptive immune responses (19); with NK and DC cross-talk being a critical mechanism for effective

antiviral immunity (189). Multiple studies have shown the importance of DC and NK cells in RSV infection (182, 190). Human DCs express NKG2D ligands after in vitro stimulation with viral mimetics and RSV (183). However, the interactions between NK cells and DCs and their roles in lung pathogenesis in response to RSV infection are not well defined. Therefore, we sought to examine the role of NKG2D and DCs in the response to RSV infection in our mouse model.

3.2 Knowledge Gap

Proper DC function is important in maintaining local lung hemostasis and orchestrating the immune response following viral infection. Specifically, the cooperation between DCs and other inflammatory cells play an important role in lung local immunity (191). It is understood that DCs maintain and promote NK cell and T cell proliferation and effector functions in the lung (192, 193). However, how NK cells reciprocally affect DC function has not been well studied. NKG2D is an important activating receptors expressed on NK cells and NKT cells and play important role in regulating immune response during RSV. In this study, we will examine how this pathway affects DC function to regulate the pathogenesis of RSV infection.

3.3 Aim of the current investigation

Respiratory syncytial virus (RSV) is a common cause of respiratory tract infection in vulnerable populations. Natural killer (NK) cells and dendritic cells (DC) are important for the effector functions of both cell types following infection. In this study, we will use RSV infected Wild type and NKG2D deficient mice to study the role of NKG2D in regulating DC function and RSV infection. Lung pathology, was assessed by histology. DC function and phenotype was evaluated by ELISA and flow cytometry. The expression of NKG2D ligands on lung and lymph node DCs was measured by immunostaining and flow cytometry. Adoptive transfer experiments were performed to assess the importance of NKG2D dependent DC function in RSV infection. In the study, we observed that NKG2D deficient mice exhibited greater lung pathology, marked by the accumulation of DCs following RSV infection. DCs isolated from NKG2D deficient mice had impaired responses towards TLR ligands. DCs expressed NKG2D ligands on their surface, which was further increased in NKG2D deficient mice and during RSV infection. Adoptive transfer of DCs isolated from WT mice into the airways of NKG2D deficient mice ameliorated the enhanced inflammation in NKG2D deficient mice after RSV infection. In summary, our study indicate that NKG2D-dependent interactions with DCs

control the phenotype and function of DCs and play a critical role in pulmonary host defenses against RSV infection.

3.4 Results

3.4.1 Increased severity of RSV-induced lung pathology in NKG2D-deficient mice. We first examined lung inflammation, weight loss, and viral clearance in NKG2D- deficient and wild type (WT) mice following RSV infection. The B6 mice are semi-permissive to RSV strain A2 and the infection induced only mild lung pathology (194, 195). However, we found that bronchiolitis and alveolitis induced by A2 in B6 NKG2D-deficient mice was severe compared to the B6 control mice (Fig. 14A). There was also increased inflammatory cell infiltration (Fig. 14B) and weight loss in the infected NKG2D-deficient mice compared to WT mice (Fig. 14C). The inter- mouse strain difference in RSV titer in lung homogenates was not different after 5 days of incubation but there was a trend toward higher titer in NKG2D-deficient mice (Fig. 14D). These data suggest that NKG2D performs a critical function in the immune response to RSV infection.

3.4.2 Altered DC phenotype in NKG2D-deficient mice following RSV infection. DCs play a critical role in RSV infection as they impart specific

effector functions to cells mediating both the innate and adaptive immune response. Following intranasal RSV infection, NKG2D-deficient mice exhibited increased whole lung DC accumulation and BAL DC accumulation (Fig. 15B) compared to WT mice with a peak difference at day 2 post-infection (Fig. 15A). A more detailed examination of the DC populations revealed that there is a larger subpopulation of mature DCs in the BAL and lung of NKG2D deficient mice (Fig. 15C). The lung leukocyte phenotypic analysis revealed that the increased number of DCs in NKG2D-deicient mice are mainly comprised by plasmacytoid DCs (pDC) (PDCA-1+ CD11c+ CD11b- CD103-) and CD103 DCs (CD11c+ CD103+ CD11b-) (Fig. 15D). The discrepancy of DC composition and increased number of DCs in NKG2D-deficient mice we observed demonstrates that the NKG2D receptor also plays an important role in regulating DC biology during RSV infection.

3.4.3 NKG2D ligand expression in lymph node and pulmonary DCs. Multiple reports have demonstrated the presence of NKG2D ligands on human DCs in naïve or inflammatory states (183, 196). However, mouse DC expression of NKG2D ligands has not been reported. We isolated mediastinal lymph node

(mLN) from naïve and RSV infected mice and measured the NKG2D ligands Rae1 and Mult-1 on DCs by flow cytometry. We found two populations of DCs that express either Rae1 or Mult-1 in mLN and the percentages of these subpopulations increased following RSV infection (Fig. 16A, B). The NKG2D ligand expressing DC subpopulations appear to be distinct based on the lack of co-expression of either assayed NKG2D ligands. The percentages of these subpopulations of DCs were significantly higher in both naïve and RSV-infected NKG2D-deficient mice compared to WT (Fig. 16A, B). Lung DCs exhibited the same expression patterns of NKG2D ligands. The number of DCs expressing Rae1 or Mult-1 increased in NKG2D KO mice compared to WT and further increased following RSV infection (Fig. 16C, D). The expression of NKG2D ligands is independent of DC maturity as further gating strategies showed Rae1 and Mult-1 expression can be found on both mature and immature DCs.

3.4.4 DCs from NKG2D-deficient mice are hyporesponsive to toll-like receptor (TLR) activation. The difference in surface expression of NKG2D ligands on DCs prompted us to examine their potential functional implications by assessing TLR ligand stimulation and antigen presentation capabilities. IL-12 is a critical pro-inflammatory cytokine secreted by DCs and is also important in activating NK cells (197). Therefore, we assessed IL-12 secretion as an indicator

of DC responsiveness. Interestingly, the responses to TLR3 and TLR4 ligands were significantly lower in DCs isolated from the lungs of NKG2D-defcient mice compared to WT mice. In, contrast, there were no detectable differences in lung DC responsiveness to TLR7 and TLR9 ligands (Fig. 17A). Impaired responsiveness towards TLR3 and TLR4 ligands was not observed in splenic DCs or bone marrow derived DCs (Fig. 17A) isolated from NKG2D deficient mice suggesting a unique role for the pulmonary microenvironment in modulating DC phenotype. To confirm that the IL-12 p40 was produced by DCs but not pulmonary macrophages that may be contaminating the DC isolates, we measured intracellular IL-12 expression level and found that, indeed, most of the IL-12 was produced by DCs (Fig 17B).

We next assessed the capacity of DCs to induce T cell proliferation given their critical role as antigen presenting cells. We explored antigen presentation using a model of ex vivo antigen presentation that utilizes fluorescently labeled CD8+ T cells (OT-1) isolated from transgenic mice engineered to over-express T cell receptors specific for an ovalbumin peptide. OT-1 T cells were then co-cultured with DCs pulsed with the specific ovalbumin peptide. Following 5 days of co-culture, the proliferation index of the T cells was calculated by the dilution of the CSFE fluorescent label by flow cytometry. These data demonstrate that

the capacity of DCs to internalize and present antigen to T cells was unaffected in DCs from NKG2D-deficient mice compared to WT mice (Fig. 17C).

3.4.5 Adoptive transfer of WT DCs ameliorates enhanced RSV-induced pathology in NKG2D-deficient mice. We performed adoptive transfer experiments to directly test whether WT DCs can modulate enhanced lung inflammation in NKG2D-deficient mice. Specifically, we transferred freshly isolated pulmonary DCs from WT or NKG2D-deficient mice into WT or KO recipient mice followed by RSV challenge and examined lung pathology 5 days post-infection. These studies demonstrate that adoptive transfer of neither WT DCs nor KO DCs into WT recipient mice altered the disease course and lung pathology (Fig. 18A). However, transfer of WT DCs into KO recipient alleviated the lung pathology and partially rescued the phenotype displayed in NKG2D-deficient mice (Fig. 18B). Furthermore, elaboration of the NK cell pro-inflammatory mediator IFN-gamma was significantly lower in NKG2D-deficient recipient mice that received WT DCs (Fig. 18C). The amelioration of lung inflammation after adoptive transfer indicates that NKG2D depend DC editing is important in regulating immune response during RSV infection.

3.5 Discussion

The incomplete understanding of immunologic pathogenesis of RSV infection is a major obstacle to the development of effective and safe clinical therapies. This study aims to examine NKG2D-dependent DCs functions in murine RSV infection, with an emphasis on the host immune response. Our experiments show that RSV infection induced pulmonary inflammation is enhanced in NKG2D deficient mice. We demonstrate that the NKG2D receptor is important in regulating DC accumulation, especially CD103 DCs, during RSV infection. Moreover, we observed subpopulations of DC expressing NKG2D ligands that increase in number in a NKG2D deficient environment and during RSV infection. Furthermore, DCs isolated from NKG2D deficient environments have impaired responses towards TLR3 and 4 ligands. Finally, lung inflammation in NKG2D deficient mice after RSV infection was ameliorated after adoptive transfer of WT DCs prior to infection. Collectively, these data demonstrate a role for NKG2D in DC regulation that is important in the immune response to RSV infection.

The NKG2D receptor is a well characterized activating receptor. Despite its well-known function in regulating the pathogenesis of other virus infections like influenza (198) and human cytomegalovirus infection (199), the importance of the NKG2D receptor in regulating RSV infection has received little attention.

Data shows that NK cells increased expression of NKG2D in response to RSV infection and secret IFN-gamma that results in acute lung injury (182). Our data suggests that there is no difference in viral titer in wild type and NKG2D deficient mice 5 days after RSV challenge, indicating that RSV clearance is independent of the NKG2D receptor-ligand effects on DCs and suggests that the exaggerated lung pathology and weight loss induced by RSV infection is likely due to an impaired DC related host immune response. In addition to DCs, other cells in the lung (such as epithelial cells and alveolar macrophages) may express NKG2D ligands during RSV infection and contribute to the response to and resolution of RSV infection. Future studies will examine the role of non-DC alveolar cells in the recruitment of and modulation of DC phenotype and function.

DCs play important role in regulating immune response against RSV infection and the impaired antigen uptake and processing of neonatal DCs may explain some of the vulnerability of neonates to RSV (200, 201). Previous studies indicate lung DCs can be infected with RSV directly (202). After encounter with RSV, both CD103 DCs and CD11b DCs migrate to mLN where they present the antigens to T cells and induce adaptive immune responses (202). Different subsets of DCs play different roles in RSV infection with myeloid DCs (mDC) and plasmacytoid DCs modulating the innate immune response (202-

204). The presence of large number of mDC often indicates an adverse response to infection. The abnormal accumulation of mDC in lung impairs efficient pDC induced Th-1 based antiviral responses, tipping the immune balance in favor of a Th-2 based response (205). We observed enhanced RSV induced lung inflammation in the NKG2D-deficient mice accompanied by abnormal mDC accumulation. Interestingly, the accumulated mDCs in the NKG2D-deficient mice are composed primarily of CD103+ DCs as opposed to the CD11b DC predominant inflammation found in WT mice. Whether these two subsets of mDC play different roles in RSV infection has not been well studied. In other infectious diseases, CD103 DCs elicit stronger Th1 and Th17 responses and can induce T cells to secrete large quantities of IFN compared to CD11b DCs (206).

DC effector functions are precisely coordinated during infection (207). We are the first to show murine pulmonary DCs express NKG2D ligands that are further induced in NKG2D-deficient mice and in response to RSV infection. Previous in vitro studies have shown that human DCs express NKG2D ligands after infection with RSV (183) and that NK cells enhance DC responses to Toxoplasma gondii through an NKG2D-dependent mechanism (208). Transwell experiments demonstrate direct cell-cell contact is required for this regulation and blocking the NKG2D receptor decreases IL-12 secretion from activated DCs when coculturing with NK cells (208). It has been demonstrated that RSV-

induced lung inflammation is increased in IL-12-deficient mice compared to wild type mice (209). In our study, we found that DCs isolated from NKG2D deficient mice have impaired IL-12 secretion when activated with TLR ligands 3 and 4 but not 7 and 9. Interestingly, this impaired in vitro responsiveness towards TLR ligands by pulmonary DCs isolated from NKG2D deficient mice was not observed in bone marrow derived DCs or DCs isolated from spleens suggesting that unique NKG2D-dependent DCs functional subsets reside in the lung. Thus, our data suggests that NKG2D is not only important in mediating DC function during RSV infection but also has an important role in maintaining pulmonary DC homeostasis. Future studies will be required to identify the NKG2D receptor carrying cells (e.g., NK cells, T cells, NK T cells) that modify DC phenotype and function in lung by either direct (editing) or indirect mechanisms.

Adoptive transfer of DCs isolated from wild type mice into the NKG2D-deficient mice before the RSV infection ameliorated viral induced inflammation. The decreased IFNγ secretion and pathology score demonstrate the protective role of the transplanted "normal" DCs. This rescue of phenotype demonstrates the importance of NKG2D receptor ligand interactions with DCs during an RSV infection. However, it is important to point out the pathology in the recipient mice is still more severe compare to wild type, emphasizing the possibility that

there are likely other cells affected by the absence of NKG2D receptors and contribute to the pathology. It is interesting to point out the transfer of DCs isolated from NKG2D-deficient mice into wild type mice does not alter the phenotype which indicates that host DCs have a survival advantage over DCs isolated from NKG2D deficient mice. Alternatively, there may be enough remaining host DCs to maintain the normal immune response against RSV.

Taken together, our data demonstrate that NKG2D is necessary for the normal control of RSV infection. We speculate that the NKG2D expressing cells are important in eliminating "unhealthy" DCs that express NKG2D ligands in lung. In the absence of this surveillance mechanism, DCs accumulate during RSV infection. Thus even some pulmonary DCs have impaired response towards TLR ligands individually, the huge influx of DCs in lung still produce increased levels of pro-inflammatory cytokines in the NKG2D deficient mice (data not shown) that impair the host immune response and result in enhanced pathology, such as augmented weight loss and lung inflammation. This newly described DC-NK cell pathway has novel implications for the regulation of DC function and provides insight into developing new potential targets aimed at resolving RSV-induced inflammation.

3.6 Material and methods

Mice. C57BL/6J mice and OT-1 mice (female, 8 to 10 wks old) were purchased from The Jackson Laboratory (Bar Harbor, ME). NKG2D-deficient (Klrk1−/−) mice were generated and maintained as described (210). Both male and female mice (6-8 weeks old) are included in the study. All mice were housed in the University of Cincinnati, animal care facilities and experimental procedures were performed in accordance with the Institutional Animal Care and Use Committee at the University of Cincinnati Medical Center.

Respiratory syncytial virus and infection. RSV strain A2 was passaged in Vero cells (ATCC; Manassas, VA) cultured in serum-free-media (SFM4MegaVir; Hyclone, Logan, UT). Mice were infected intranasally with 1 x 106 PFU or control vehicle in 50 µl PBS. Mice were monitored and body weight changes were recorded daily after infection. Viral load was determined by RT-PCR of lung as described (211).

Cell isolation. Purification of DCs from lung and mediastinal lymph nodes (mLN) were performed as previously described (198). Briefly, mice were

euthanized with an i.p. injection of sodium pentobarbital. Lung vasculature was perfused with 10 ml phosphate-buffered saline (PBS) containing 0.6 mM EDTA, via the right atrium. Single cell suspensions of mLNs were obtained by passing the nodes through a 100-μm nylon mesh. Lung single cell suspensions were obtained by using a gentle MACS Dissociator (Miltenyi Biotec Ltd, Woking, United Kingdom) after incubating harvested lung tissues with 100 mg/mL collagenase type IV and 20,000 U/mL DNases (Sigma Aldrich Company Ltd, Gillingham, United Kingdom) as described (171). After red blood cell lysis, CD11c+ cells were isolated by positive selection using CD11c magnetic MicroBeads beads following manufacturer's protocol (Miltenyi Biotec GmbH, Germany). T cells from OT-I mice were isolated from spleens following the manufacturer's protocol using the EasySep Mouse T Cell isolation kit (Stemcell).

Lung lavage, fixation, and pathology. Bronchoalveolar lavage (BAL) fluid for cytokine analysis was collected by instilling the lungs once with 1.0 mL (5 mM EDTA, calcium and magnesium free PBS) via a tracheal cannula. In separate mice, lungs were lavaged three times to obtain BAL for cell enumeration. Centrifuge the BAL fluid and resuspend the cells at 5 x 105 cell/ml. The cells were then directly used for flow cytometry and cytospin staining. Cytospin cell

preparations were obtained with 300 µl of BAL cells centrifuged at 300 × g for 5 min on cytospin slides (Newcomer Supply, Middleton, WI). Mouse lungs were inflation-fixed with buffered formalin and embedded in paraffin for histological analysis as previously described (173). Three non-contiguous tissue sections were stained with hematoxylin and eosin (HE), and the number of infiltrated inflammatory cells were assessed by light microscopy. The pathology scoring was similar to previously described (212). Specifically, "1" represented within normal range; "2" represented mild immune cell infiltration and accumulation; "3" represented moderate, multifocal aggregation; "4" represented to high cellularity and aggregation.

Flow cytometry. DCs were incubated with anti-CD16/CD32 for 30 minutes followed by incubation with specific monoclonal antibodies at 4°C for 30 min in PBS containing 1% bovine serum albumin (BSA). Cells were washed twice with PBS containing 0.1% sodium azide and 0.5% BSA and immediately analyzed by flow cytometry (Attune, Thermofisher). All antibodies were obtained from Ebioscience; (PE-cyanine 7 Anti-mouse CD11c (N418), APC-efluor 780 Anti-mouse CD11b (M1/70), APC Anti-mouse CD86 (GL1)); BD Bioscience (PerCP-Cy 5.5 Anti-mouse CD103 (M290)); and R&D systems (APC Anti-mouse Rae1 pan specific (186109), PE Anti-mouse Mult-1 (237104)). Data was analyzed

using Flowjo software (v10) (Flowjo, LLC) and FCS Express V5 (De Novo Software). Cells were first gated on lymphocytes and doublets were excluded by gating on single cells. CD11c cells were then gated, and macrophages were discriminated from DCs based on cellular autofluorescence. DCs were gated as CD11c+, MHCII+ and autofluorescence mid/low cells. Subsets of DC and CD86 expression were then further gated from DC populations. The compensation matrix was determined by using UltraComp eBeads (eBioscience). Appropriate fluorescence minus one and negative controls were used to set gates for the above populations.

Immunohistochemistry. Immunofluorescent staining was performed on cytospin preparations by double indirect immunofluorescence method as previously descripted (213). Briefly, slides were blocked with serum and then incubated overnight at 4°C with biotin anti-mouse CD11c (1:500; eBioscience (N418) and either APC Anti-mouse pan-specific Rae1 (1:500) (R&D Clone 186107) or Anti-mouse Mult-1 (1:500) (R&D Clone 237104). Binding was detected following 24 hr incubation with streptavidin 488 (1:500; Vector Labs). Nuclei were counterstained with DAPI (Sigma-Aldrich; 1:2,000). Images were captured using a Zeiss LSM710 inverted confocal microscope at the Live

Microscopy Core, Department of Molecular and Cellular Physiology, University of Cincinnati. negative controls were included in each experiment.

Adoptive transfers. DCs (> 90% purity) from wild type and Klrk1−/− mice were isolated from lung as described above. A total of 1.5 x 106 DCs in 50 µl PBS or vehicle only were transferred intranasally to recipient mice 16 hours before the RSV challenge. \

DC Stimulation. Freshly isolated DCs were maintained in complete medium (RPMI containing 10% FBS, 2 mM L-glutamine, 1mM sodium pyruvate, 0.1 mM nonessential amino acids, 50 µM β-mercaptoethanol and 1000 U/mL Pen/Strep). TLR ligand activation was assessed using 1 x 105 freshly isolated DC seeded in 100 uL of DC media in 96-well round bottom plates. DCs were rested for 1 hour followed by a pre-incubation with 20 ng/ml IFN-gamma (PeproTech) for 2 hours. The DCs were then treated for 16 hrs with 1 µg/ml poly IC (InvivoGen), 1 µg/ml LPS (Sigma Aldrich), 100 ng/ml ssRNA40 (InvivoGen) or 50 ng/ml CpG ODN 1826 (InvivoGen). IL-12 p40 was measured by ELISA (ThermoFisher). To assess antigen presentation capacity, freshly isolated DCs were pulsed with 100 ng/ml ovalbumin (OVA) peptide SIINFEKL

(InvivoGen) or irrelevant peptide for one hour then cultured with CFSE-labeled OT-1 T cells at 1:5 ratio for 5 days. OT-1 T cell proliferation index was then measured by flow cytometry (214).

Statistics. 4-8 mice were used in each group with at least 3 independent experiments. Unless otherwise indicated, data are expressed as mean ± standard errors of the means (SEMs). Student's t tests and ANOVA were used for statistical analyses. $P < 0.05$ was considered statistically significant.

3.7 Study limitations.

Even though we have shown that the NKG2D dependent pathway is important in regulating DC function in both steady state and RSV infection, we did not show which specific cell type was executing this modification and where this editing occurred. NK cells are a major cell type that expresses NKG2D receptors and the mechanisms of NKG2D effector functions are well studied (215). However, in this study, we found no difference of NK cell dependent cell apoptosis in DCs by incubating DCs with WT and NKG2D-deficient NK cells (data not shown). Besides NK cells, some mouse T cells also express NKG2D receptors on the surface. The effect of these T cell on DC function in the context of NKG2D-deficiency was not examined in this study. We have shown only pulmonary DCs' function is altered in the NKG2D-deficient mice under steady state but not BMDCs and splenic DCs which suggested a tissue-specific influence. Another limitation of the current study is that we did not examine the DC development state this NKG2D-dependent modulation occurred.

3.8 Future directions.

In the current study, we have shown that the NKG2D-dependent DC function is not only important in regulating RSV infection, but also plays an important role in regulating DC biology under steady state. We speculate that the NKG2D expressing cells are important in eliminating "unhealthy" DCs that express NKG2D ligands in lung. In the absence of this surveillance mechanism, DCs accumulate during RSV infection. Thus, although some pulmonary DCs have impaired response towards TLR ligands individually, the influx of DCs in lung still produce increased levels of pro-inflammatory cytokines in the NKG2D deficient mice. In the future, mechanistic study focusing on how and where this regulating occurs during DC maturation should be conducted. A better understanding of this mechanism may not only help illustrate the importance of this pathway during RSV infection, but also shed light upon other DC related diseases and applications.

3.9 Figure

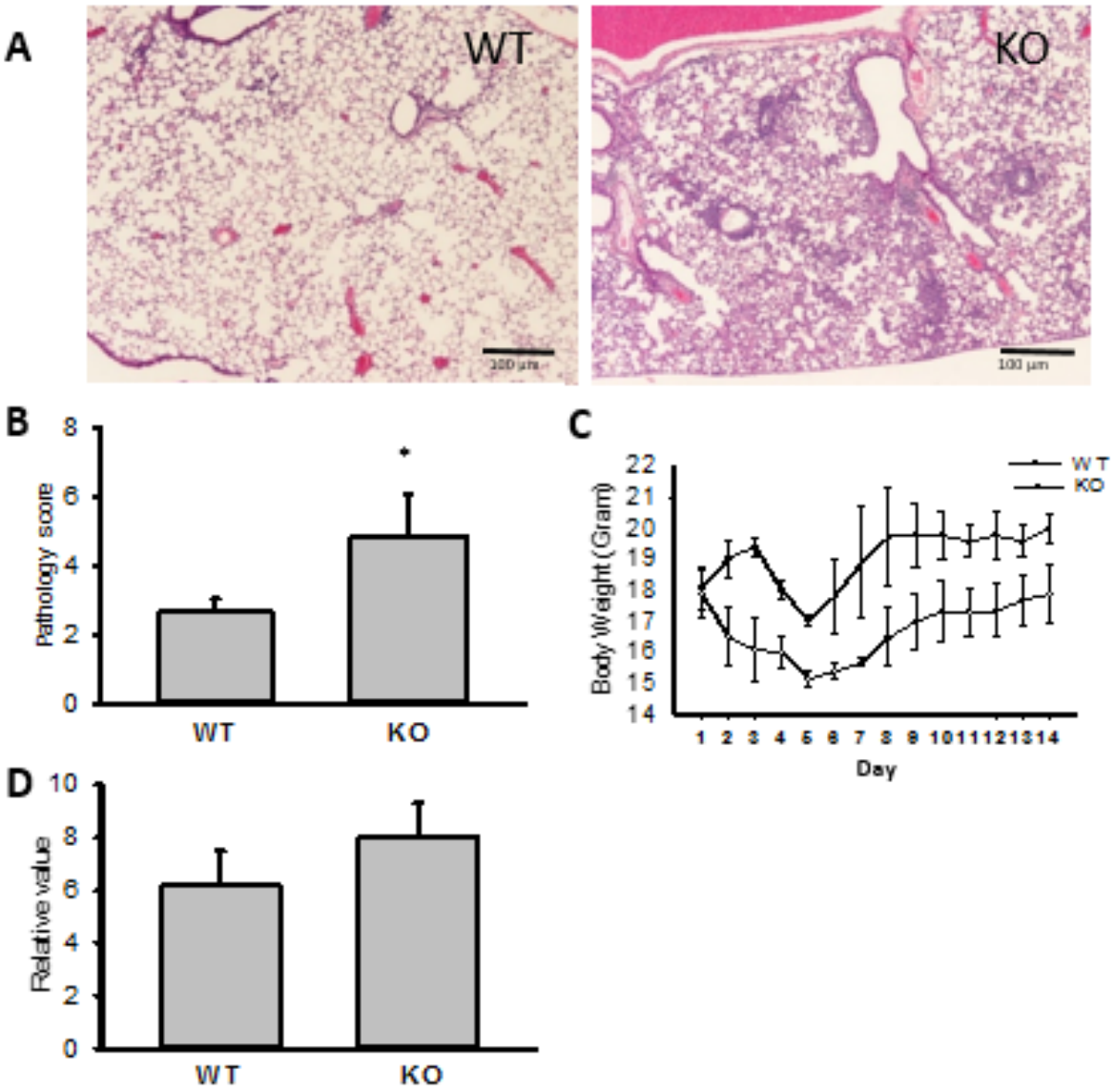
A
WT
KO
B
Pathology score
0
2
4
6
8
WT
KO
C
Body Weight (Gram)
14
15
16
17
18
19
20
21
22
1 2 3 4 5 6 7 8 9 10 11 12 13 14
Day
WT
KO
D
Relative value
0
2
4
6
8
10
WT
KO

Figure 14. NKG2D deficiency augments RSV-induced lung pathology. Mice were challenged intranasally with saline or RSV. (A) Representative H&E lung histology from WT and NKG2D-deficient mice 5 days post-RSV infection (dpi). Scale bar, 100 μm, n=6. (B) Mouse lungs were harvested for pulmonary histopathology examination 5 dpi. The pathology features were scored as described in the Materials and Methods. Data are shown as the mean ± SEM from at least 5 independent experiments. *p < .05, (C) Daily weight changes of control and RSV-infected mice were measured individually post infection. Data are means ± SEM, n=3 for each group. (D) Relative RSV titer in lung was measured by PCR 5-days post infection. n=8, *p < .05

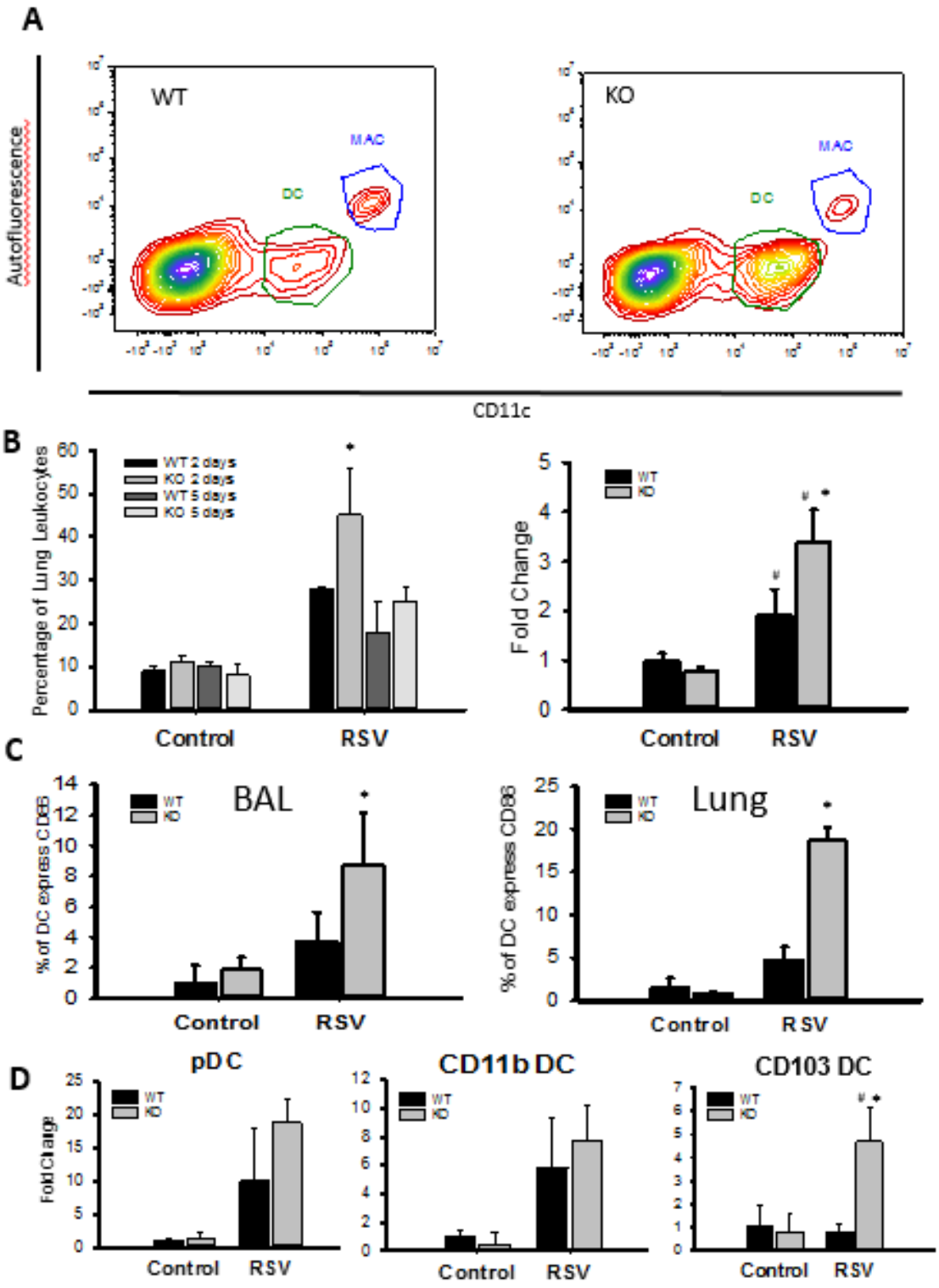
A
WT
KO
MAC
DC
Autofluorescence
CD11c
B
Percentage of Lung Leukocytes
WT 2 days
KO 2 days
WT 5 days
KO 5 days
Control
RSV
Fold Change
WT
KO
C
BAL
Lung
% of DC express CD86
D
pDC
CD11b DC
CD103 DC
Fold Change

Figure 15. Altered pulmonary DC phenotype after RSV infection in NKG2D deficient mice. Mice were challenged intranasally with saline or RSV. Pulmonary DCs were isolated from lung tissue. (A) Representative flow cytometry plot for DC population in lung after RSV challenge 2 dpi. DCs were gated as $CD11c^{high}$ autofluorescence ^{low}. Alveolar macrophage (AM) were gated as $F4/80^{+}$, $CD11c^{high}$ $autofluorescence^{high}$. (B) Percentage of DCs in lung single cell homogenate of early infection (2 dpi) and late infection (5 dpi) and the fold change of DC number compare to WT control mice was assessed in BAL fluid of 2 dpi mice by flow cytometry. Data are shown as the mean ± SEM of at least 5 independent experiments. *$p < .05$ (C) CD86 expression on DC populations in BAL and lung were measured by flow cytometry. Data are shown as the mean ± SEM of at least 3 independent experiments. *$p < .05$ (D) DC subpopulations in BAL measured by flow cytometry. pDCs are gated as $CD11c^{+}$, $PDCA1^{+}$, $CD11b^{-}$, $CD103^{-}$; CD11b DC as $CD11c^{+}$, $CD11b^{+}$ and $CD103^{-}$; CD103 DC as $CD11C^{+}$, $CD103^{+}$ AND $CD11b^{-}$. Data are shown as the mean ± SEM of at least 3 independent experiments. Each experiments consist at least 4 mice. *$p < .05$

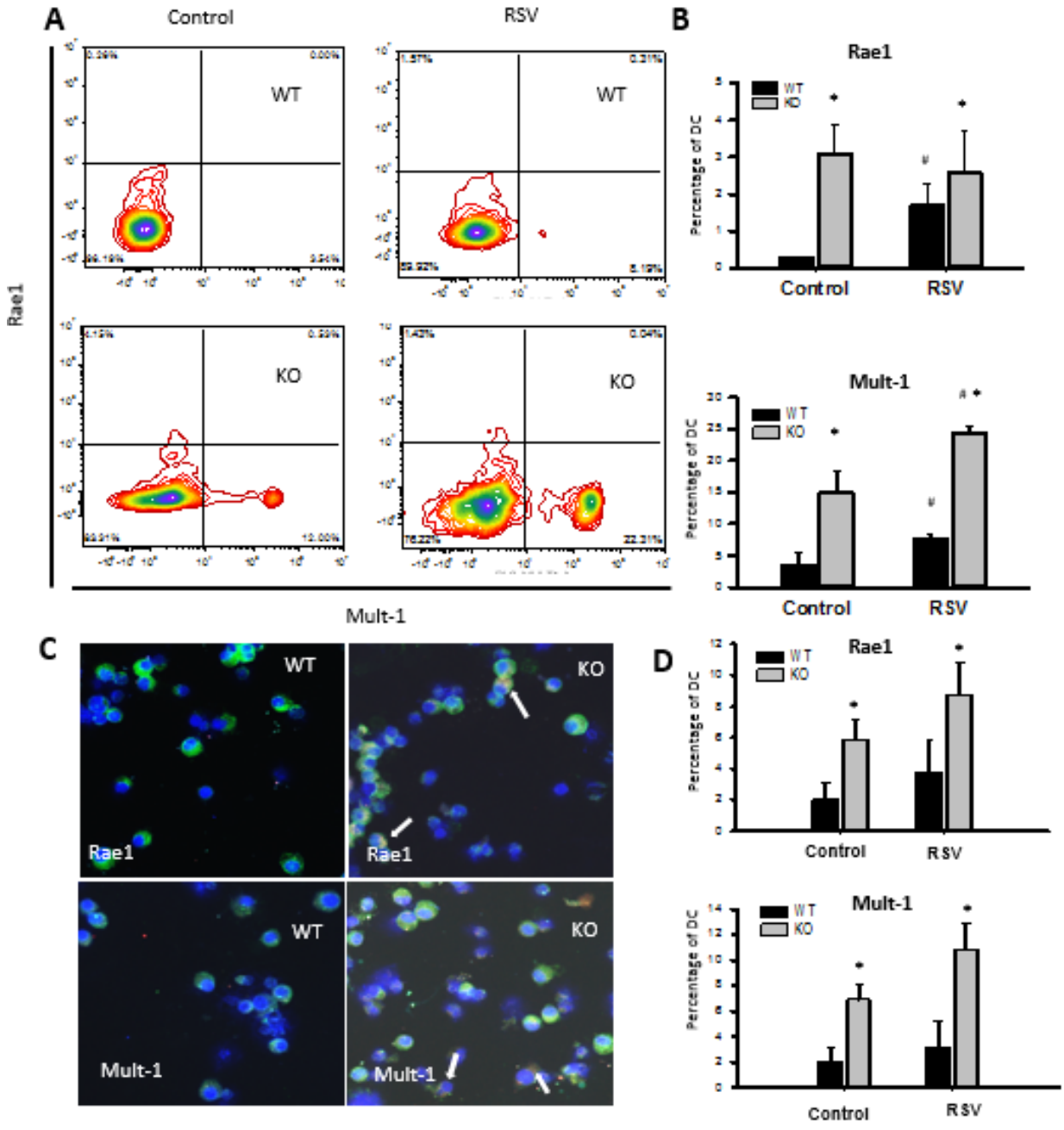
A
Control
RSV
WT
KO
Rae1
Mult-1
B
Rae1
Mult-1
Percentage of DC
WT
KO
Control
RSV
C
WT
KO
Rae1
Mult-1
D
Rae1
Mult-1
Percentage of DC
Control
RSV

Figure 16. Increased expression of NKG2D ligands on DCs in NKG2D-deficient mice that is enhanced during RSV infection. (A, B) Rae1 and Mult-1 expression on mediastinal lymph node (mLN) DCs were measured by flow cytometry 2 dpi of RSV infection. Single lung cell suspension was prepared from mice at 2 dpi of RSV infection and stained with Rae1 and Mult-1 (C,D) Arrows point cells that positive for CD11c and Rae1 or Mult-1 staining (Blue – DAPI, Green – CD11c, Red – Rae 1 / Mult-1). Data is representative of 4 independent experiments with n= 6-8 mice. *$p < .05$.

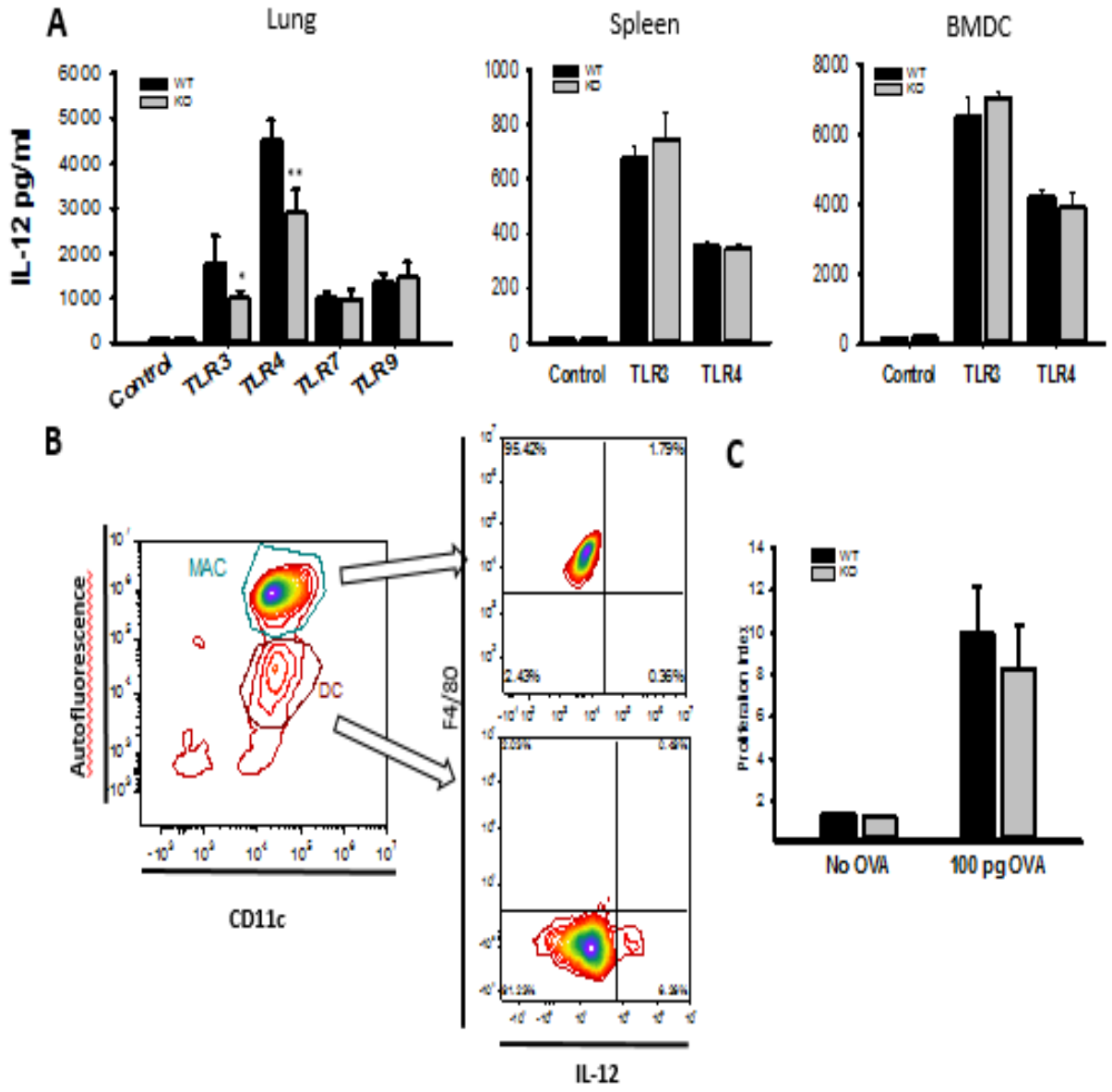
A
Lung
Spleen
BMDC
IL-12 pg/ml
WT
KO
Control
TLR3
TLR4
TLR7
TLR9
B
MAC
DC
Autofluorescence
CD11c
F4/80
IL-12
95.42%
1.79%
2.43%
0.36%
C
Proliferation Index
No OVA
100 pg OVA

Figure 17. DCs from NKG2D-deficient mice have impaired responsiveness to TLR ligands. DCs were isolated from lung, spleen and derived from bone marrow and treated with 20ng/ml IFN-gamma for 2 hours before treated with 1 μg/ml Poly IC (TLR 3), 1 μg/ml LPS (TLR 4), 100 ng/ml SSRNA40 (TLR 7) and 50 ng/ml CpG ODN 1826 (TLR 9) for 16 hrs. The supernatant was collected and IL-12 p40 was measured by ELISA (A). Data are shown as the mean ± SEM of at least 5 independent experiments. *$p < .05$, ** $p<.01$. (B) Schematic flow cytometry plot of intracellular staining of IL-12 p40 after LPS treatment. Macrophages were gated as $CD11c^{+}$ $autofluorescence^{high}$ and DCs were gated as $CD11c^{+}$, $autofluorescence^{low}$. (C) Freshly isolated DCs were pulsed with 100 ng/ml OVA peptide for one hour then cultured with CFSE-labeled OT-1 T cell at 2:10 ratio. OT-1 T cell proliferation index was measured after 5 days. Data is shown as average proliferative index ± SEM from 4 independent experiments.

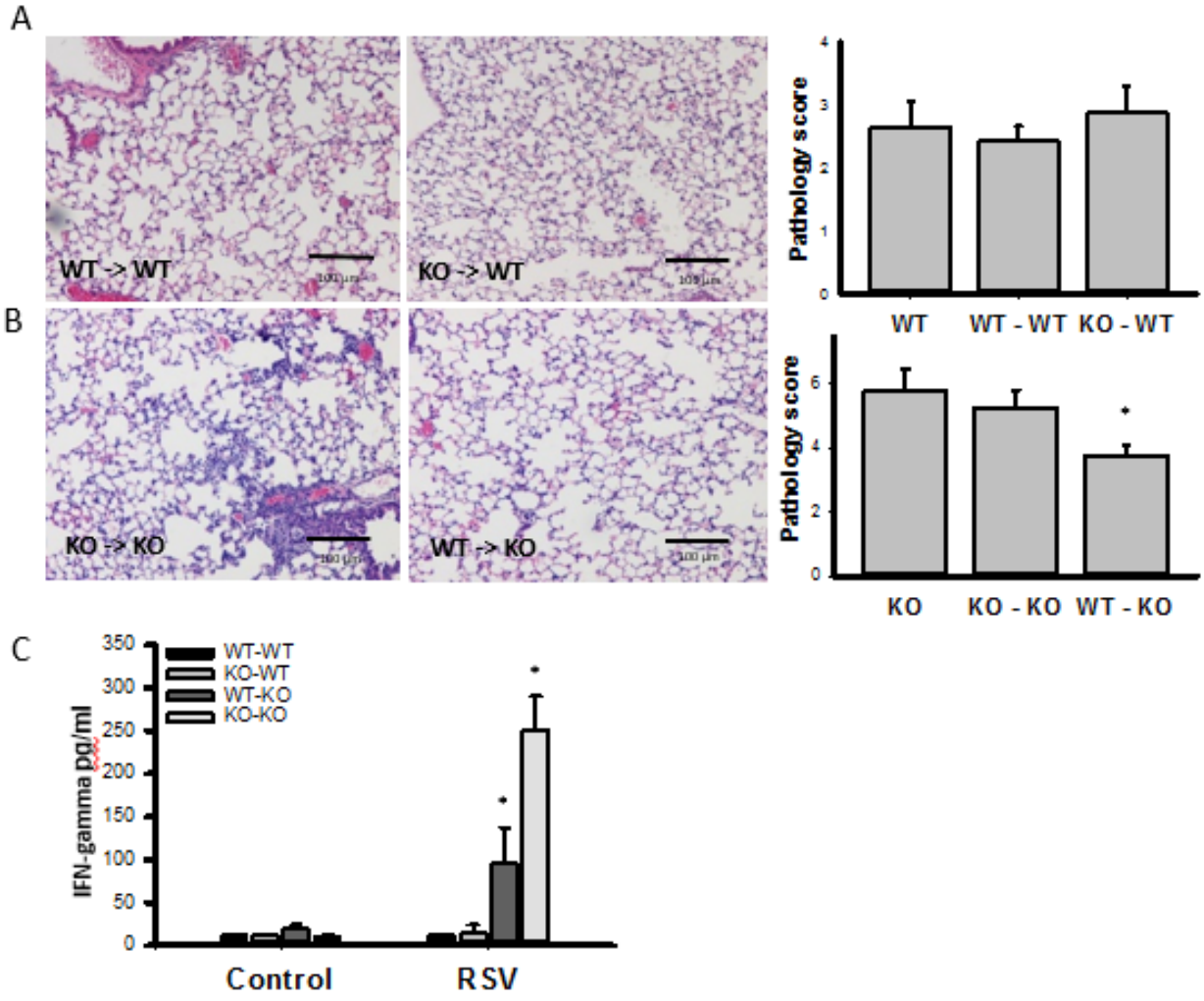
A
WT -> WT
KO -> WT
Pathology score
WT
WT - WT
KO - WT
B
KO -> KO
WT -> KO
Pathology score
KO
KO - KO
WT - KO
C
WT-WT
KO-WT
WT-KO
KO-KO
IFN-gamma pg/ml
Control
RSV

Figure 18. Adoptive transfer of WT DC into NKG2D-deficient mice alleviates the RSV-induced pathology. DCs were isolated from lung of wild type and NKG2D-deficient mice as described in Materials and Methods. Recipient mice received 2 million freshly isolated DCs intranasally in 50 µl of PBS 24 hours before RSV challenge via the same route. Representative H&E lung histology from WT (A) and NKG2D deficient (B) recipient mice who received DCs isolated from WT/KO mice, 5 dpi. Scale bar, 100 µm. Lung pathology scores from WT/KO recipient mice were calculated as described (A, B). Data are shown as the mean ± SEM of at least 5 independent experiments. *P < .05 (C) IFN-gamma level is measured in BAL of recipient mice by ELISA 5 days post infection. n=5, *P < .05

Chapter IV

Thesis summary and conclusion

4.1 Summary of section-II

Pulmonary Langerhans cell histiocytosis (PLCH) is a rare interstitial lung disease characterized by focal dendritic cell (DC) accumulation, bronchiolocentric nodule formation, and cystic remodeling of the lung and occurs predominantly in active smokers. Approximately 50% of PLCH patients harbor somatic BRAF-V600E mutations identified mainly within the DC lineage. However, the rare nature of the disease and lack of animal models impedes the study of the pathogenic mechanisms of PLCH. We have established the first mouse model that recapitulates the hallmark characteristics of PLCH. In addition, we show that the BRAF-V600E mutation is associated with increased DC responsiveness towards multiple stimuli including the DC-chemokine CCL20. We provide evidence that DC accumulation in the lung is due to both increased viability and enhanced recruitment. Further evidence indicates that the accumulation of other inflammatory cells in PLCH is a secondary event driven by CCL7 secreted from DCs in a BRAF-V600E-dependent manner. Moreover, we demonstrate that PLCH-like phenotype in the mouse model can be attenuated following smoking cessation and removal of BRAF-V600E DCs. Furthermore, we show PBMCs isolated from PLCH patients harboring the BRAF-V600E mutation produce

CCL7. Collectively, our studies provide the first mechanistic insights into the role of DC BRAF-V600E mutation and CS exposure that mediate PLCH pathogenesis.

4.2 Summary of section-III

Respiratory syncytial virus (RSV) is a common cause of respiratory tract infection in vulnerable populations. Natural killer (NK) cells and dendritic cells (DC) are important for the effector functions of both cell types following infection. To investigate the importance of NKG2D pathway in regulating RSV infection, Wild type and NKG2D deficient mice were infected with RSV. Lung pathology was assessed by histology and DC function and phenotype was evaluated by ELISA and flow cytometry. The expression of NKG2D ligands on lung and lymph node DCs was measured by immunostaining and flow cytometry. Adoptive transfer experiments were performed to assess the importance of NKG2D dependent DC function in RSV infection. We found that NKG2D deficient mice exhibited greater lung pathology, marked by the accumulation of DCs following RSV infection. DCs isolated from NKG2D deficient mice had impaired responses towards TLR ligands. DCs expressed NKG2D ligands on their surface, which was further increased in NKG2D deficient mice and during RSV infection. Adoptive transfer of DCs isolated from WT mice into the airways of NKG2D deficient mice ameliorated the enhanced inflammation in NKG2D deficient mice after RSV infection. In summary, we discovered that the NKG2D-dependent interactions

with DCs control the phenotype and function of DCs and play a critical role in pulmonary host defenses against RSV infection.

4.3 Thesis summary and conclusion

An increasing volume of research on DCs in recent years show that pulmonary DCs occupy a pivotal role in regulating lung immune responses. Through the relentless sampling of inhaled antigen and in response to cues from the surrounding environment, DCs uphold the delicate homeostasis between initiating immune reaction to pathogens and tolerance to harmless substances. Any breach of this immunological equilibrium may lead to pathologic states. In this study, we have tested this theory from two different aspects using two different disease models.

Collectively, these results support the concept that the balance of DC-mediated lung equilibrium can be affected by both innate defects and the tissue-specific environment. Specifically, in section II, we showed that an intrinsic defect (BRAF-V600E mutation) of DCs can result an altered cellular function and results in a PLCH-like phenotype in mice exposed to CS. Our findings not only provide insights into the pathogenesis of PLCH but also offer a potential alternative therapeutic strategy in clinic. Moreover, we showed that the BRAF-V600E mutation increases DC's responsiveness against different ligands and enhance secretion of chemokines which indicated the importance of examining an under-studied area that links the MAPK pathway and DC biology in the future. In

section III, we demonstrated that without a proper NKG2D-dependent editing and selection from the surrounding micro-environment, DCs accumulate in the lung and result in severe RSV infection. In this study, we discovered a NKG2D-dependent DC-NK cell pathway that provides insight not only into developing new potential targets aimed at resolving RSV-induced inflammation but also other DC-related diseases.

4.4 Future directions

In chapter 2, we shown that we have established the first PLCH mouse model that recapitulate human pathology in many different aspects. Moreover, we reported the direct association of excessive CCL7 and CCL20 secretion, improved viability by increasing BCL-XL expression, increased response when activated with TLR ligands and CCL20 and enhanced migration capacity with BRAF-V600E mutation. In addition, we have shown that the PLCH-like phenotype was ameliorated after CS and tamoxifen cessation. We believe by using this mouse model, we can answer important questions regarding the PLCH pathogenesis therefore develop and test new clinic treatment strategies. However, some questions were raised when conducting the experiments that need to be answered in the future.

(1) **To examine the mechanism of enhanced migration capacity in BRAF-V600E DCs**. We have shown that the migration capacity was increased in BRAF-V600E DCs. However, if this enhancement was directly induced by the mutation and the related mechanism was not examined in this study. To investigate this, another experiment group that treated with BRAF-V600E inhibitor will need to be added in the migration assays. One possible

mechanism of how BRAF-V600E mutation enhance DC's response towards CCL20 is by increasing the expression of CCL20 receptor -- CCR6. Future studies examining the CCR6 expression level on mutant DCs will help to elucidate this hypothesis. In addition, using techniques like RNAseq can help to discover genes that expressed differently in mutant DCs and may provide evidences that can connect the CCR6-CCL20 axis and MAPK pathway. Finally, the importance of the CCR6-CCL20 axis in the PLCH pathogenesis should be tested in the CCR6 knock-out mice that harbors BRAF-V600E mutations in CD11c cells or alternatively, using CCL20 neutralizing antibody on the existing animal model. Because of limited antibody availability and application, we could not obtain reliable and specific CCL20 staining on our mouse tissue. It will be interesting to study the source and distribution pattern of local secretion of CCL20 in the lung of the PLCH model using newer antibodies and techniques. Meanwhile, the cells that expressed high levels of CCL20 in the human tissue can be phenotyped by IHC and RT-PCR following laser captured microdissection. The successful identification of the cellular source of CCL20 may help to develop new clinical strategies.

(2) **To examine the association of BRAF-V600E mutation and DC differentiation.** One prominent feature of PLCH is the accumulation of a specific DC subset -- $CD1a^+$ DC in human and $CD103^+$ DC in our mouse model. In mice, cDCs are divided into two subsets that each consist of 50% of the cDC population, CD103+ DCs and CD11b+ DCs, which are developmentally regulated by the transcription factors basic leucine zipper transcription factor Batf3 and Irf4, respectively. In human, the cDCs can be divided based on the surface expression markers and consists of similar percentage of the cDCs. The accumulation of the specific DC subset in PLCH brings up the question of whether this accumulation is due to a targeted recruitment or altered differentiation. Recent studies indicate that MAPK signaling is involved in regulating different aspects of phenotypic maturation, cytokine production, and functional maturation of DCs. However, how a hyper-activating MAPK pathway induced by BRAF-V600E affects DC differentiation has not been studied. To investigate this question, future studies are needed that focus on examining the differentiation of BRAF-V600E mutant BMDCs and the expression of DC differentiation dependent transcription factors Batf3 and Irf4 in the mutant BMDCs.

(3) **To examine the potential of using CCL7 as a biomarker.** We observed a consistent increase of CCL7 in the serum and BAL of our mouse model that may be secreted by BRAF-V600E mutant DCs. However, the CCL7 level was not consistent in the serum of PLCH patients. The CC7 level in the serum was very high in one patient while the rest were at base line. As we suggested in our experiments, the increased CCL7 in the serum was secreted by BRAF-V600E mutant DCs. We did not examine if there is a correlation between CCL7 level and the number of circulating BRAF-V600E mutant DCs in the peripheral blood. However, we observed a large increase of CCL7 in the serum of a LCH patient who has high frequency of BRAF-V600E mutant DCs in the blood which suggests such a correlation. It is known that in LCH patients, the frequency of BRAF-V600E mutant DCs in PBMCs has a wide range from 0.03% to 20%. Given the fact that PLCH often only affects a single organ, it is expected that PLCH patients have fewer circulating mutant DCs compare to LCH patients, thus making it difficult to accumulate enough mutant DCs in the blood of PLCH patients that secrete significant levels of CCL7. In PLCH, most BRAF-V600E mutant DCs accumulate in the lung and surround airspace. Thus it is important to measure the CCL7 level in the BAL and examine the potential of using it as a marker to identify PLCH. In

addition, future studies that aim at measuring the frequency of BRAF-V600E mutant DCs in the PBMC of PLCH patients and the PLCH mouse model will help to examine if there is a correlation between BRAF-V600E mutant DC frequency and CCL7 level.

In chapter 3, we have shown that the NKG2D-dependent effects on DC function is not only important in regulating RSV infection, but also plays an important role in regulating DC biology under steady state. We speculate that the NKG2D expressing cells are important in eliminating "unhealthy" DCs that express NKG2D ligands in lung. In the absence of this surveillance mechanism, DCs accumulate during RSV infection. Thus, even some pulmonary DCs have impaired response towards TLR ligands individually, the huge influx of DCs in lung still produce increased levels of pro-inflammatory cytokines in the NKG2D-deficient mice. However, these experiments raised some questions that need to be answered in the future. The impaired DC function was only observed in pulmonary DCs but not shared with splenic DC and BMDC which suggests that this NKG2D-dependent regulation is specific to lung. Although in most cases the function of DCs are similar in different organs, there are several precedents for phenotypic differences among DCs in different microenvironment. For instance, Langerhans cells are present only in the skin, and $CD103^{+}$

$CD11b^+$ double-positive cells are found in large numbers in the lamina propria of the gut but are rare in the lung (216). And study showed that the regulations of pulmonary DC from different developmental lineage are also different (217). Thus, mechanistic studies focusing on how and where this regulation occurs during DC maturation are needed to better understand this pathway. Furthermore, the identification of NKG2D receptor-expressing cells responsible for the modification such as decreased response towards TLR ligands and how it is regulated is needed to be examined in the future. In addition, it will be important to investigate the importance of this NKG2D dependent mechanism in other diseases.

References

1. Steinman RM, Cohn ZA. 1973. Identification of a novel cell type in peripheral lymphoid organs of mice. *Journal of Experimental Medicine* 137: 1142-62

2. Misharin AV, Morales-Nebreda L, Mutlu GM, Budinger GR, Perlman H. 2013. Flow cytometric analysis of macrophages and dendritic cell subsets in the mouse lung. *Am J Respir Cell Mol Biol* 49: 503-10
3. Kim HS, Woo J, Lee JH, Joo HJ, Choi Y, Kim H, Moon WK, Kim SJ. 2015. In vivo Tracking of Dendritic Cell using MRI Reporter Gene, Ferritin. *PLOS ONE* 10: e0125291
4. Lee HW, Yoon SY, Singh TD, Choi YJ, Lee HJ, Park JY, Jeong SY, Lee S-W, Ha J-H, Ahn B-C. 2015. Tracking of dendritic cell migration into lymph nodes using molecular imaging with sodium iodide symporter and enhanced firefly luciferase genes. *Scientific reports* 5: 9865
5. Lancelin W, Guerrero-Plata A. 2011. Isolation of mouse lung dendritic cells. *J Vis Exp*: e3563-e
6. Rocha-Martins M, Cavalheiro GR, Matos-Rodrigues GE, Martins RA. 2015. From Gene Targeting to Genome Editing: Transgenic animals applications and beyond. *An Acad Bras Cienc* 87: 1323-48
7. Patel VI, Booth JL, Duggan ES, Cate S, White VL, Hutchings D, Kovats S, Burian DM, Dozmorov M, Metcalf JP. 2017. Transcriptional Classification and Functional Characterization of Human Airway Macrophage and Dendritic Cell Subsets. *J Immunol* 198: 1183-201
8. Breton G, Zheng S, Valieris R, da Silva IT, Satija R, Nussenzweig MC. 2016. Human dendritic cells (DCs) are derived from distinct circulating precursors that are precommitted to become CD1c+ or CD141+ DCs. *Journal of Experimental Medicine* 213: 2861-70
9. Collin M, McGovern N, Haniffa M. 2013. Human dendritic cell subsets. *Immunology* 140: 22-30
10. Liu K, Nussenzweig MC. 2010. Origin and development of dendritic cells. *Immunol Rev* 234: 45-54
11. Belz GT, Nutt SL. 2012. Transcriptional programming of the dendritic cell network. *Nat Rev Immunol* 12: 101-13
12. Liu K, Victora GD, Schwickert TA, Guermonprez P, Meredith MM, Yao K, Chu FF, Randolph GJ, Rudensky AY, Nussenzweig M. 2009. In vivo analysis of dendritic cell development and homeostasis. *Science* 324: 392-7
13. Hettinger J, Richards DM, Hansson J, Barra MM, Joschko AC, Krijgsveld J, Feuerer M. 2013. Origin of monocytes and macrophages in a committed progenitor. *Nat Immunol* 14: 821-30
14. Helft J, Ginhoux F, Bogunovic M, Merad M. 2010. Origin and functional heterogeneity of non-lymphoid tissue dendritic cells in mice. *Immunol Rev* 234: 55-75
15. Jakubzick C, Gautier EL, Gibbings SL, Sojka DK, Schlitzer A, Johnson TE, Ivanov S, Duan Q, Bala S, Condon T, van Rooijen N, Grainger JR, Belkaid Y, Ma'ayan A, Riches DW, Yokoyama WM, Ginhoux F, Henson PM, Randolph GJ. 2013. Minimal differentiation of classical monocytes as they survey steady-state tissues and transport antigen to lymph nodes. *Immunity* 39: 599-610
16. Larson SR, Atif SM, Gibbings SL, Thomas SM, Prabagar MG, Danhorn T, Leach SM, Henson PM, Jakubzick CV. 2016. Ly6C(+) monocyte efferocytosis and cross-presentation of cell-associated antigens. *Cell Death Differ* 23: 997-1003
17. Whitsett JA, Alenghat T. 2015. Respiratory epithelial cells orchestrate pulmonary innate immunity. *Nature immunology* 16: 27
18. Condon TV, Sawyer RT, Fenton MJ, Riches DW. 2011. Lung dendritic cells at the innate-adaptive immune interface. *Journal of leukocyte biology* 90: 883-95
19. Liu H, Jakubzick C, Osterburg AR, Nelson RL, Gupta N, McCormack FX, Borchers MT. 2017. Dendritic Cell Trafficking and Function in Rare Lung Diseases. *American journal of respiratory cell and molecular biology* 57: 393-402
20. Colonna M, Trinchieri G, Liu Y-J. 2004. Plasmacytoid dendritic cells in immunity. *Nature immunology* 5: 1219

21. Kim TH, Lee HK. 2014. Differential roles of lung dendritic cell subsets against respiratory virus infection. *Immune network* 14: 128-37
22. Patel VI, Booth JL, Duggan ES, Cate S, White VL, Hutchings D, Kovats S, Burian DM, Dozmorov M, Metcalf JP. 2017. Transcriptional classification and functional characterization of human airway macrophage and dendritic cell subsets. *The Journal of Immunology* 198: 1183-201
23. Hammad H, Lambrecht BN. 2007. Lung Dendritic Cell Migration. 93: 265-78
24. Kim TH, Lee HK. 2014. Differential roles of lung dendritic cell subsets against respiratory virus infection. *Immune Netw* 14: 128-37
25. Beaty SR, Rose CE, Sung SsJ. 2007. Diverse and Potent Chemokine Production by Lung CD11bhigh Dendritic Cells in Homeostasis and in Allergic Lung Inflammation. *The Journal of Immunology* 178: 1882-95
26. Shortman K, Naik SH. 2007. Steady-state and inflammatory dendritic-cell development. *Nat Rev Immunol* 7: 19-30
27. Liu K, Waskow C, Liu X, Yao K, Hoh J, Nussenzweig M. 2007. Origin of dendritic cells in peripheral lymphoid organs of mice. *Nat Immunol* 8: 578-83
28. Holt PG, Haining S, Nelson DJ, Sedgwick JD. 1994. Origin and steady-state turnover of class II MHC-bearing dendritic cells in the epithelium of the conducting airways. *J Immunol* 153: 256-61
29. Cook PC, MacDonald AS. 2016. Dendritic cells in lung immunopathology. *Semin Immunopathol* 38: 449-60
30. Manh TP, Alexandre Y, Baranek T, Crozat K, Dalod M. 2013. Plasmacytoid, conventional, and monocyte-derived dendritic cells undergo a profound and convergent genetic reprogramming during their maturation. *Eur J Immunol* 43: 1706-15
31. Lin KL, Suzuki Y, Nakano H, Ramsburg E, Gunn MD. 2008. CCR2+ Monocyte-Derived Dendritic Cells and Exudate Macrophages Produce Influenza-Induced Pulmonary Immune Pathology and Mortality. *The Journal of Immunology* 180: 2562-72
32. Geissmann F, Jung S, Littman DR. 2003. Blood monocytes consist of two principal subsets with distinct migratory properties. *Immunity* 19: 71-82
33. Tacke F, Alvarez D, Kaplan TJ, Jakubzick C, Spanbroek R, Llodra J, Garin A, Liu J, Mack M, van Rooijen N, Lira SA, Habenicht AJ, Randolph GJ. 2007. Monocyte subsets differentially employ CCR2, CCR5, and CX3CR1 to accumulate within atherosclerotic plaques. *J Clin Invest* 117: 185-94
34. Molon B, Gri G, Bettella M, Gomez-Mouton C, Lanzavecchia A, Martinez AC, Manes S, Viola A. 2005. T cell costimulation by chemokine receptors. *Nat Immunol* 6: 465-71
35. Ito T, Carson WFt, Cavassani KA, Connett JM, Kunkel SL. 2011. CCR6 as a mediator of immunity in the lung and gut. *Exp Cell Res* 317: 613-9
36. Pendl GG, Robert C, Steinert M, Thanos R, Eytner R, Borges E, Wild MK, Lowe JB, Fuhlbrigge RC, Kupper TS, Vestweber D, Grabbe S. 2002. Immature mouse dendritic cells enter inflamed tissue, a process that requires E- and P-selectin, but not P-selectin glycoprotein ligand 1. *Blood* 99: 946-56
37. Schneeberger EE, Vu Q, LeBlanc BW, Doerschuk CM. 2000. The accumulation of dendritic cells in the lung is impaired in CD18-/- but not in ICAM-1-/- mutant mice. *J Immunol* 164: 2472-8
38. Maddaluno L, Verbrugge SE, Martinoli C, Matteoli G, Chiavelli A, Zeng Y, Williams ED, Rescigno M, Cavallaro U. 2009. The adhesion molecule L1 regulates transendothelial migration and trafficking of dendritic cells. *J Exp Med* 206: 623-35

39. Robays LJ, Maes T, Lebecque S, Lira SA, Kuziel WA, Brusselle GG, Joos GF, Vermaelen KV. 2007. Chemokine receptor CCR2 but not CCR5 or CCR6 mediates the increase in pulmonary dendritic cells during allergic airway inflammation. *J Immunol* 178: 5305-11
40. Vermaelen K, Pauwels R. 2003. Accelerated airway dendritic cell maturation, trafficking, and elimination in a mouse model of asthma. *Am J Respir Cell Mol Biol* 29: 405-9
41. Grayson MH, Ramos MS, Rohlfing MM, Kitchens R, Wang HD, Gould A, Agapov E, Holtzman MJ. 2007. Controls for Lung Dendritic Cell Maturation and Migration during Respiratory Viral Infection. *The Journal of Immunology* 179: 1438-48
42. Swartz MA, Hubbell JA, Reddy ST. 2008. Lymphatic drainage function and its immunological implications: from dendritic cell homing to vaccine design. *Semin Immunol* 20: 147-56
43. Schraufnagel DE. 2010. Lung lymphatic anatomy and correlates. *Pathophysiology* 17: 337-43
44. Nakano H, Burgents JE, Nakano K, Whitehead GS, Cheong C, Bortner CD, Cook DN. 2013. Migratory properties of pulmonary dendritic cells are determined by their developmental lineage. *Mucosal Immunol* 6: 678-91
45. Dieu MC, Vanbervliet B, Vicari A, Bridon JM, Oldham E, Ait-Yahia S, Briere F, Zlotnik A, Lebecque S, Caux C. 1998. Selective recruitment of immature and mature dendritic cells by distinct chemokines expressed in different anatomic sites. *J Exp Med* 188: 373-86
46. Ricart BG, John B, Lee D, Hunter CA, Hammer DA. 2011. Dendritic cells distinguish individual chemokine signals through CCR7 and CXCR4. *J Immunol* 186: 53-61
47. Willimann K, Legler DF, Loetscher M, Roos RS, Delgado MB, Clark-Lewis I, Baggiolini M, Moser B. 1998. The chemokine SLC is expressed in T cell areas of lymph nodes and mucosal lymphoid tissues and attracts activated T cells via CCR7. *Eur J Immunol* 28: 2025-34
48. Gunn MD, Tangemann K, Tam C, Cyster JG, Rosen SD, Williams LT. 1998. A chemokine expressed in lymphoid high endothelial venules promotes the adhesion and chemotaxis of naive T lymphocytes. *Proc Natl Acad Sci U S A* 95: 258-63
49. Yen JH, Khayrullina T, Ganea D. 2008. PGE2-induced metalloproteinase-9 is essential for dendritic cell migration. *Blood* 111: 260-70
50. Mandala S, Hajdu R, Bergstrom J, Quackenbush E, Xie J, Milligan J, Thornton R, Shei GJ, Card D, Keohane C, Rosenbach M, Hale J, Lynch CL, Rupprecht K, Parsons W, Rosen H. 2002. Alteration of lymphocyte trafficking by sphingosine-1-phosphate receptor agonists. *Science* 296: 346-9
51. Clatworthy MR, Aronin CE, Mathews RJ, Morgan NY, Smith KG, Germain RN. 2014. Immune complexes stimulate CCR7-dependent dendritic cell migration to lymph nodes. *Nat Med* 20: 1458-63
52. Belz G, Mount A, Masson F. 2009. Dendritic cells in viral infections. In *Dendritic Cells*, pp. 51-77: Springer
53. Mihret A. 2012. The role of dendritic cells in Mycobacterium tuberculosis infection. *Virulence* 3: 654-9
54. Barnes PJ. 2008. Immunology of asthma and chronic obstructive pulmonary disease. *Nature Reviews Immunology* 8: 183
55. Neyt K, Lambrecht BN. 2013. The role of lung dendritic cell subsets in immunity to respiratory viruses. *Immunol Rev* 255: 57-67
56. Yoo J-K, Kim TS, Hufford MM, Braciale TJ. 2013. Viral infection of the lung: Host response and sequelae. *The Journal of allergy and clinical immunology* 132: 10.1016/j.jaci.2013.06.006
57. Gill MA. 2012. The role of dendritic cells in asthma. *J Allergy Clin Immunol* 129: 889-901
58. Lambrecht BN, Hammad H. 2003. Taking our breath away: dendritic cells in the pathogenesis of asthma. *Nat Rev Immunol* 3: 994-1003

59. Lambrecht BN, Hammad H. 2009. Biology of lung dendritic cells at the origin of asthma. *Immunity* 31: 412-24
60. van Helden MJ, Lambrecht BN. 2013. Dendritic cells in asthma. *Curr Opin Immunol* 25: 745-54
61. Vassallo R, Ryu JH, Colby TV, Hartman T, Limper AH. 2000. Pulmonary Langerhans'-cell histiocytosis. *N Engl J Med* 342: 1969-78
62. Vassallo R, Ryu JH, Schroeder DR, Decker PA, Limper AH. 2002. Clinical outcomes of pulmonary Langerhans'-cell histiocytosis in adults. *N Engl J Med* 346: 484-90
63. Arico M, Girschikofsky M, Genereau T, Klersy C, McClain K, Grois N, Emile JF, Lukina E, De Juli E, Danesino C. 2003. Langerhans cell histiocytosis in adults. Report from the International Registry of the Histiocyte Society. *Eur J Cancer* 39: 2341-8
64. Elia D, Torre O, Cassandro R, Caminati A, Harari S. 2015. Pulmonary Langerhans cell histiocytosis: a comprehensive analysis of 40 patients and literature review. *Eur J Intern Med* 26: 351-6
65. Badalian-Very G, Vergilio JA, Degar BA, MacConaill LE, Brandner B, Calicchio ML, Kuo FC, Ligon AH, Stevenson KE, Kehoe SM, Garraway LA, Hahn WC, Meyerson M, Fleming MD, Rollins BJ. 2010. Recurrent BRAF mutations in Langerhans cell histiocytosis. *Blood* 116: 1919-23
66. Kamionek M, Ahmadi Moghaddam P, Sakhdari A, Kovach AE, Welch M, Meng X, Dresser K, Tomaszewicz K, Cosar EF, Mark EJ, Fraire AE, Hutchinson L. 2016. Mutually exclusive extracellular signal-regulated kinase pathway mutations are present in different stages of multi-focal pulmonary Langerhans cell histiocytosis supporting clonal nature of the disease. *Histopathology* 69: 499-509
67. Chakraborty R, Hampton OA, Shen X, Simko SJ, Shih A, Abhyankar H, Lim KP, Covington KR, Trevino L, Dewal N, Muzny DM, Doddapaneni H, Hu J, Wang L, Lupo PJ, Hicks MJ, Bonilla DL, Dwyer KC, Berres ML, Poulikakos PI, Merad M, McClain KL, Wheeler DA, Allen CE, Parsons DW. 2014. Mutually exclusive recurrent somatic mutations in MAP2K1 and BRAF support a central role for ERK activation in LCH pathogenesis. *Blood* 124: 3007-15
68. Mourah S, How-Kit A, Meignin V, Gossot D, Lorillon G, Bugnet E, Mauger F, Lebbe C, Chevret S, Tost J, Tazi A. 2016. Recurrent NRAS mutations in pulmonary Langerhans cell histiocytosis. *Eur Respir J* 47: 1785-96
69. Tazi A, Moreau J, Bergeron A, Dominique S, Hance AJ, Soler P. 1999. Evidence that Langerhans cells in adult pulmonary Langerhans cell histiocytosis are mature dendritic cells: importance of the cytokine microenvironment. *J Immunol* 163: 3511-5
70. Fleming MD, Pinkus JL, Fournier MV, Alexander SW, Tam C, Loda M, Sallan SE, Nichols KE, Carpentieri DF, Pinkus GS, Rollins BJ. 2003. Coincident expression of the chemokine receptors CCR6 and CCR7 by pathologic Langerhans cells in Langerhans cell histiocytosis. *Blood* 101: 2473-5
71. Cantwell-Dorris ER, O'Leary JJ, Sheils OM. 2011. BRAFV600E: implications for carcinogenesis and molecular therapy. *Mol Cancer Ther* 10: 385-94
72. Jinih M, Foley N, Osho O, Houlihan L, Toor AA, Khan JZ, Achakzai A, Redmond HP. 2016. BRAF V600E mutation as a predictor of thyroid malignancy in indeterminate nodules: A systematic review and meta-analysis. *European Journal of Surgical Oncology (EJSO)*
73. Bracke KR, D'Hulst A I, Maes T, Moerloose KB, Demedts IK, Lebecque S, Joos GF, Brusselle GG. 2006. Cigarette smoke-induced pulmonary inflammation and emphysema are attenuated in CCR6-deficient mice. *J Immunol* 177: 4350-9
74. Van Pottelberge GR, Bracke KR, Joos GF, Brusselle GG. 2009. The role of dendritic cells in the pathogenesis of COPD: liaison officers in the front line. *Copd* 6: 284-90

75. Tsoumakidou M, Demedts IK, Brusselle GG, Jeffery PK. 2008. Dendritic cells in chronic obstructive pulmonary disease: new players in an old game. *Am J Respir Crit Care Med* 177: 1180-6
76. Givi ME, Redegeld FA, Folkerts G, Mortaz E. 2012. Dendritic cells in pathogenesis of COPD. *Curr Pharm Des* 18: 2329-35
77. Wang B, Shi L, Sun X, Wang L, Wang X, Chen C. 2016. Production of CCL20 from lung cancer cells induces the cell migration and proliferation through PI3K pathway. *J Cell Mol Med* 20: 920-9
78. Wang GZ, Cheng X, Li XC, Liu YQ, Wang XQ, Shi X, Wang ZY, Guo YQ, Wen ZS, Huang YC, Zhou GB. 2015. Tobacco smoke induces production of chemokine CCL20 to promote lung cancer. *Cancer Lett* 363: 60-70
79. Demedts IK, Bracke KR, Van Pottelberge G, Testelmans D, Verleden GM, Vermassen FE, Joos GF, Brusselle GG. 2007. Accumulation of dendritic cells and increased CCL20 levels in the airways of patients with chronic obstructive pulmonary disease. *Am J Respir Crit Care Med* 175: 998-1005
80. Vassallo R, Walters PR, Lamont J, Kottom TJ, Yi ES, Limper AH. 2010. Cigarette smoke promotes dendritic cell accumulation in COPD; a Lung Tissue Research Consortium study. *Respir Res* 11: 45
81. Suri HS, Yi ES, Nowakowski GS, Vassallo R. 2012. Pulmonary langerhans cell histiocytosis. *Orphanet J Rare Dis* 7: 16
82. Givi ME, Peck MJ, Boon L, Mortaz E. 2013. The role of dendritic cells in the pathogenesis of cigarette smoke-induced emphysema in mice. *Eur J Pharmacol* 721: 259-66
83. Sawahata M, Sugiyama Y. 2016. An epidemiological perspective of the pathology and etiology of sarcoidosis. *Sarcoidosis Vasc Diffuse Lung Dis* 33: 112-6
84. Ungprasert P, Crowson CS, Matteson EL. 2016. Seasonal variation in incidence of sarcoidosis: a population-based study, 1976-2013. *Thorax*
85. Forman JD, Klein JT, Silver RF, Liu MC, Greenlee BM, Moller DR. 1994. Selective activation and accumulation of oligoclonal V beta-specific T cells in active pulmonary sarcoidosis. *J Clin Invest* 94: 1533-42
86. Baughman RP, Culver DA, Judson MA. 2011. A concise review of pulmonary sarcoidosis. *Am J Respir Crit Care Med* 183: 573-81
87. Ten Berge B, Kleinjan A, Muskens F, Hammad H, Hoogsteden HC, Hendriks RW, Lambrecht BN, Van den Blink B. 2012. Evidence for local dendritic cell activation in pulmonary sarcoidosis. *Respir Res* 13: 33
88. Ota M, Amakawa R, Uehira K, Ito T, Yagi Y, Oshiro A, Date Y, Oyaizu H, Shigeki T, Ozaki Y, Yamaguchi K, Uemura Y, Yonezu S, Fukuhara S. 2004. Involvement of dendritic cells in sarcoidosis. *Thorax* 59: 408-13
89. Zaba LC, Smith GP, Sanchez M, Prystowsky SD. 2010. Dendritic cells in the pathogenesis of sarcoidosis. *Am J Respir Cell Mol Biol* 42: 32-9
90. Lommatzsch M, Bratke K, Bier A, Julius P, Kuepper M, Luttmann W, Virchow JC. 2007. Airway dendritic cell phenotypes in inflammatory diseases of the human lung. *European Respiratory Journal* 30: 878-86
91. Spiteri MA, Clarke SW, Poulter LW. 1988. Phenotypic and functional changes in alveolar macrophages contribute to the pathogenesis of pulmonary sarcoidosis. *Clin Exp Immunol* 74: 359-64
92. Moller DR, Forman JD, Liu MC, Noble PW, Greenlee BM, Vyas P, Holden DA, Forrester JM, Lazarus A, Wysocka M, Trinchieri G, Karp C. 1996. Enhanced expression of IL-12 associated

with Th1 cytokine profiles in active pulmonary sarcoidosis. *The Journal of Immunology* 156: 4952
93. Wahlstrom J, Berlin M, Skold C, Wigzell H, Eklund A, Grunewald J. 1999. Phenotypic analysis of lymphocytes and monocytes/macrophages in peripheral blood and bronchoalveolar lavage fluid from patients with pulmonary sarcoidosis. *Thorax* 54: 339-46
94. Ziegenhagen MW, Müller-Quernheim J. 2003. The cytokine network in sarcoidosis and its clinical relevance. *Journal of Internal Medicine* 253: 18-30
95. Doty JD, Mazur JE, Judson MA. 2005. Treatment of sarcoidosis with infliximab. *Chest* 127: 1064-71
96. Selman M, Pardo A, King TE. 2012. Hypersensitivity Pneumonitis. *American Journal of Respiratory and Critical Care Medicine* 186: 314-24
97. Agache IO, Rogozea L. 2013. Management of hypersensivity pneumonitis. *Clin Transl Allergy* 3: 5
98. Myers JL. 2012. Hypersensitivity pneumonia: the role of lung biopsy in diagnosis and management. *Modern Pathology* 25: S58-S67
99. Greer AM, Matthay MA, Kukreja J, Bhakta NR, Nguyen CP, Wolters PJ, Woodruff PG, Fahy JV, Shin JS. 2014. Accumulation of BDCA1(+) dendritic cells in interstitial fibrotic lung diseases and Th2-high asthma. *PLoS One* 9: e99084
100. Girard M, Israel-Assayag E, Cormier Y. 2009. Mature CD11c(+) cells are enhanced in hypersensitivity pneumonitis. *Eur Respir J* 34: 749-56
101. Gudmundsson G, Hunninghake GW. 1997. Interferon-gamma is necessary for the expression of hypersensitivity pneumonitis. *Journal of Clinical Investigation* 99: 2386-90
102. Blanchet MR, Bennett JL, Gold MJ, Levantini E, Tenen DG, Girard M, Cormier Y, McNagny KM. 2011. CD34 is required for dendritic cell trafficking and pathology in murine hypersensitivity pneumonitis. *Am J Respir Crit Care Med* 184: 687-98
103. Daito H, Kikuchi T, Sakakibara T, Gomi K, Damayanti T, Zaini J, Tode N, Kanehira M, Koyama S, Fujimura S. 2011. Mycobacterial hypersensitivity pneumonitis requires TLR9–MyD88 in lung CD11b+ CD11c+ cells. *European Respiratory Journal* 38: 688-701
104. Girard M, Israel-Assayag E, Cormier Y. 2009. Mature CD11c+ cells are enhanced in hypersensitivity pneumonitis. *European Respiratory Journal* 34: 749-56
105. Hwang SJ, Kim HS, Chung DH. 2010. Fas/Fas Ligand–mediated Apoptosis Promotes Hypersensitivity Pneumonitis in Mice by Enhancing Maturation of Dendritic Cells. *American journal of respiratory and critical care medicine* 181: 1250-61
106. Travis WD, Costabel U, Hansell DM, King Jr TE, Lynch DA, Nicholson AG, Ryerson CJ, Ryu JH, Selman M, Wells AU. 2013. An official American Thoracic Society/European Respiratory Society statement: update of the international multidisciplinary classification of the idiopathic interstitial pneumonias. *American journal of respiratory and critical care medicine* 188: 733-48
107. Collard HR, King TE. 2003. Demystifying idiopathic interstitial pneumonia. *Archives of internal medicine* 163: 17-29
108. Shimizu S, Yoshinouchi T, Ohtsuki Y, Fujita J, Sugiura Y, Banno S, Yamadori I, Eimoto T, Ueda R. 2002. The appearance of S-100 protein-positive dendritic cells and the distribution of lymphocyte subsets in idiopathic nonspecific interstitial pneumonia. *Respiratory medicine* 96: 770-6
109. Raghu G, Collard HR, Egan JJ, Martinez FJ, Behr J, Brown KK, Colby TV, Cordier JF, Flaherty KR, Lasky JA, Lynch DA, Ryu JH, Swigris JJ, Wells AU, Ancochea J, Bouros D, Carvalho C, Costabel U, Ebina M, Hansell DM, Johkoh T, Kim DS, King TE, Jr., Kondoh Y, Myers J, Muller NL, Nicholson AG, Richeldi L, Selman M, Dudden RF, Griss BS, Protzko SL, Schunemann HJ. 2011.

An official ATS/ERS/JRS/ALAT statement: idiopathic pulmonary fibrosis: evidence-based guidelines for diagnosis and management. *Am J Respir Crit Care Med* 183: 788-824
110. Ley B, Collard HR. 2013. Epidemiology of idiopathic pulmonary fibrosis. *Clinical Epidemiology* 5: 483-92
111. Marchal-Sommé J, Uzunhan Y, Marchand-Adam S, Valeyre D, Soumelis V, Crestani B, Soler P. 2006. Cutting edge: nonproliferating mature immune cells form a novel type of organized lymphoid structure in idiopathic pulmonary fibrosis. *The Journal of Immunology* 176: 5735-9
112. Tsoumakidou M, Karagiannis KP, Bouloukaki I, Zakynthinos S, Tzanakis N, Siafakas NM. 2009. Increased Bronchoalveolar Lavage Fluid CD1c Expressing Dendritic Cells in Idiopathic Pulmonary Fibrosis. *Respiration* 78: 446-52
113. Marchal-Somme J, Uzunhan Y, Marchand-Adam S, Kambouchner M, Valeyre D, Crestani B, Soler P. 2007. Dendritic cells accumulate in human fibrotic interstitial lung disease. *Am J Respir Crit Care Med* 176: 1007-14
114. Nuovo GJ, Hagood JS, Magro CM, Chin N, Kapil R, Davis L, Marsh CB, Folcik VA. 2012. The distribution of immunomodulatory cells in the lungs of patients with idiopathic pulmonary fibrosis. *Mod Pathol* 25: 416-33
115. Freynet O, Marchal-Somme J, Jean-Louis F, Mailleux A, Crestani B, Soler P, Michel L. 2016. Human lung fibroblasts may modulate dendritic cell phenotype and function: results from a pilot in vitro study. *Respir Res* 17: 36
116. Bantsimba-Malanda C, Marchal-Sommé J, Goven D, Freynet O, Michel L, Crestani B, Soler P. 2010. A role for dendritic cells in bleomycin-induced pulmonary fibrosis in mice? *American journal of respiratory and critical care medicine* 182: 385-95
117. Trujillo G, Hartigan AJ, Hogaboam CM. 2010. T regulatory cells and attenuated bleomycin-induced fibrosis in lungs of CCR7-/-mice. *Fibrogenesis & tissue repair* 3: 18
118. Vassallo R, Ryu JH, Colby TV, Hartman T, Limper AH. 2000. Pulmonary Langerhans'-cell histiocytosis. *New England Journal of Medicine* 342: 1969-78
119. Vassallo R, Ryu JH, Schroeder DR, Decker PA, Limper AH. 2002. Clinical outcomes of pulmonary Langerhans'-cell histiocytosis in adults. *New England Journal of Medicine* 346: 484-90
120. Arico M, Girschikofsky M, Genereau T, Klersy C, McClain K, Grois N, Emile J-F, Lukina E, De Juli E, Danesino C. 2003. Langerhans cell histiocytosis in adultsReport from the International Registry of the Histiocyte Society. *European Journal of Cancer* 39: 2341-8
121. Roden AC, Hu X, Kip S, Castellar ERP, Rumilla KM, Vrana JA, Vassallo R, Ryu JH, Eunhee SY. 2014. BRAF V600E expression in Langerhans cell histiocytosis: clinical and immunohistochemical study on 25 pulmonary and 54 extrapulmonary cases. *The American journal of surgical pathology* 38: 548-51
122. Chakraborty R, Burke TM, Hampton OA, Zinn DJ, Lim KPH, Abhyankar H, Scull B, Kumar V, Kakkar N, Wheeler DA. 2016. Alternative genetic mechanisms of BRAF activation in Langerhans cell histiocytosis. *Blood* 128: 2533-7
123. Badalian-Very G, Vergilio J-A, Degar BA, MacConaill LE, Brandner B, Calicchio ML, Kuo FC, Ligon AH, Stevenson KE, Kehoe SM. 2010. Recurrent BRAF mutations in Langerhans cell histiocytosis. *Blood*: blood-2010-04-279083
124. Kamionek M, Ahmadi Moghaddam P, Sakhdari A, Kovach AE, Welch M, Meng X, Dresser K, Tomaszewicz K, Cosar EF, Mark EJ. 2016. Mutually exclusive extracellular signal-regulated kinase pathway mutations are present in different stages of multi-focal pulmonary Langerhans cell histiocytosis supporting clonal nature of the disease. *Histopathology* 69: 499-509

125. Berres M-L, Lim KPH, Peters T, Price J, Takizawa H, Salmon H, Idoyaga J, Ruzo A, Lupo PJ, Hicks MJ. 2014. BRAF-V600E expression in precursor versus differentiated dendritic cells defines clinically distinct LCH risk groups. *Journal of Experimental Medicine* 211: 669-83
126. Dauriat G, Mal H, Thabut G, Mornex J-F, Bertocchi M, Tronc F, Leroy-Ladurie F, Dartevelle P, Reynaud-Gaubert M, Thomas P. 2006. Lung transplantation for pulmonary langerhans' cell histiocytosis: a multicenter analysis. *Transplantation* 81: 746-50
127. Davies H, Bignell GR, Cox C, Stephens P, Edkins S, Clegg S, Teague J, Woffendin H, Garnett MJ, Bottomley W. 2002. Mutations of the BRAF gene in human cancer. *Nature* 417: 949
128. Cantwell-Dorris ER, O'Leary JJ, Sheils OM. 2011. BRAFV600E: implications for carcinogenesis and molecular therapy. *Molecular cancer therapeutics* 10: 385-94
129. Espinosa A, Porchia L, Ringel M. 2007. Targeting BRAF in thyroid cancer. *British journal of cancer* 96: 16
130. McCain J. 2013. The MAPK (ERK) pathway: investigational combinations for the treatment of BRAF-mutated metastatic melanoma. *Pharmacy and Therapeutics* 38: 96
131. Cravens PD, Lipsky PE. 2002. Dendritic cells, chemokine receptors and autoimmune inflammatory diseases. *Immunology & Cell Biology* 80: 497-505
132. Liu H, Osterburg AR, Flury J, Huang S, McCormack FX, Cormier SA, Borchers MT. 2018. NKG2D is Required for Regulation of Lung Pathology and Dendritic Cell Function Following RSV Infection. *The Journal of Infectious Diseases*
133. Lommatzsch M, Bratke K, Knappe T, Bier A, Dreschler K, Kuepper M, Stoll P, Julius P, Virchow JC. 2010. Acute effects of tobacco smoke on human airway dendritic cells in vivo. *European Respiratory Journal* 35: 1130-6
134. Botelho FM, Nikota JK, Bauer CM, Morissette MC, Iwakura Y, Kolbeck R, Finch D, Humbles AA, Stämpfli MR. 2012. Cigarette smoke-induced accumulation of lung dendritic cells is interleukin-1α-dependent in mice. *Respiratory research* 13: 81
135. Demedts IK, Bracke KR, Van Pottelberge G, Testelmans D, Verleden GM, Vermassen FE, Joos GF, Brusselle GG. 2007. Accumulation of dendritic cells and increased CCL20 levels in the airways of patients with chronic obstructive pulmonary disease. *American journal of respiratory and critical care medicine* 175: 998-1005
136. Tsoumakidou M, Demedts IK, Brusselle GG, Jeffery PK. 2008. Dendritic cells in chronic obstructive pulmonary disease: new players in an old game. *American journal of respiratory and critical care medicine* 177: 1180-6
137. Milne P, Bigley V, Bacon CM, Néel A, McGovern N, Bomken S, Haniffa M, Diamond EL, Durham BH, Visser J. 2017. Hematopoietic origin of Langerhans cell histiocytosis and Erdheim-Chester disease in adults. *Blood* 130: 167-75
138. Chilosi M, Facchetti F, Caliò A, Zamò A, Brunelli M, Martignoni G, Rossi A, Montagna L, Piccoli P, Dubini A. 2014. Oncogene-induced senescence distinguishes indolent from aggressive forms of pulmonary and non-pulmonary Langerhans cell histiocytosis. *Leukemia & lymphoma* 55: 2620-6
139. Probst HC, Lagnel J, Kollias G, van den Broek M. 2003. Inducible transgenic mice reveal resting dendritic cells as potent inducers of CD8+ T cell tolerance. *Immunity* 18: 713-20
140. Zaynagetdinov R, Sherrill TP, Kendall PL, Segal BH, Weller KP, Tighe RM, Blackwell TS. 2013. Identification of myeloid cell subsets in murine lungs using flow cytometry. *American journal of respiratory cell and molecular biology* 49: 180-9
141. Vassallo R, Harari S, Tazi A. 2017. Current understanding and management of pulmonary Langerhans cell histiocytosis. *Thorax*: thoraxjnl-2017-210125

142. Baqir M, Vassallo R, Maldonado F, Eunhee SY, Ryu JH. 2013. Utility of bronchoscopy in pulmonary Langerhans cell histiocytosis. *Journal of bronchology & interventional pulmonology* 20: 309-12
143. Jakubzick C, Tacke F, Ginhoux F, Wagers AJ, van Rooijen N, Mack M, Merad M, Randolph GJ. 2008. Blood monocyte subsets differentially give rise to CD103+ and CD103− pulmonary dendritic cell populations. *The Journal of Immunology* 180: 3019-27
144. Tazi A, Moreau J, Bergeron A, Dominique S, Hance AJ, Soler P. 1999. Evidence that Langerhans cells in adult pulmonary Langerhans cell histiocytosis are mature dendritic cells: importance of the cytokine microenvironment. *The Journal of Immunology* 163: 3511-5
145. Satyamoorthy K, Li G, Gerrero MR, Brose MS, Volpe P, Weber BL, van Belle P, Elder DE, Herlyn M. 2003. Constitutive mitogen-activated protein kinase activation in melanoma is mediated by both BRAF mutations and autocrine growth factor stimulation. *Cancer research* 63: 756-9
146. Mitsutake N, Knauf JA, Mitsutake S, Mesa C, Zhang L, Fagin JA. 2005. Conditional BRAFV600E expression induces DNA synthesis, apoptosis, dedifferentiation, and chromosomal instability in thyroid PCCL3 cells. *Cancer research* 65: 2465-73
147. Cargnello M, Roux PP. 2011. Activation and function of the MAPKs and their substrates, the MAPK-activated protein kinases. *Microbiology and molecular biology reviews* 75: 50-83
148. Michaloglou C, Vredeveld LC, Soengas MS, Denoyelle C, Kuilman T, Van Der Horst CM, Majoor DM, Shay JW, Mooi WJ, Peeper DS. 2005. BRAF E600-associated senescence-like cell cycle arrest of human naevi. *Nature* 436: 720
149. Wajapeyee N, Serra RW, Zhu X, Mahalingam M, Green MR. 2008. Oncogenic BRAF induces senescence and apoptosis through pathways mediated by the secreted protein IGFBP7. *Cell* 132: 363-74
150. Worbs T, Hammerschmidt SI, Förster R. 2017. Dendritic cell migration in health and disease. *Nature Reviews Immunology* 17: 30
151. Lin CL, Suri RM, Rahdon RA, Austyn JM, Roake JA. 1998. Dendritic cell chemotaxis and transendothelial migration are induced by distinct chemokines and are regulated on maturation. *European journal of immunology* 28: 4114-22
152. Vermaelen K, Pauwels R. 2003. Accelerated airway dendritic cell maturation, trafficking, and elimination in a mouse model of asthma. *American journal of respiratory cell and molecular biology* 29: 405-9
153. Felouzis V, Hermand P, de Laissardière GT, Combadière C, Deterre P. 2016. Comprehensive analysis of chemokine-induced cAMP-inhibitory responses using a real-time luminescent biosensor. *Cellular signalling* 28: 120-9
154. Cheng JW, Sadeghi Z, Levine AD, Penn MS, von Recum HA, Caplan AI, Hijaz A. 2014. The role of CXCL12 and CCL7 chemokines in immune regulation, embryonic development, and tissue regeneration. *Cytokine* 69: 277-83
155. Lazennec G, Richmond A. 2010. Chemokines and chemokine receptors: new insights into cancer-related inflammation. *Trends in molecular medicine* 16: 133-44
156. Sahm F, Capper D, Preusser M, Meyer J, Stenzinger A, Lasitschka F, Berghoff A-S, Habel A, Schneider M, Kulozik A. 2012. BRAFV600E mutant protein is expressed in cells of variable maturation in Langerhans cell histiocytosis. *Blood* 120: e28-e34
157. Nucera C, Lawler J, Hodin R, Parangi S. 2010. The BRAFV600E mutation: what is it really orchestrating in thyroid cancer? *Oncotarget* 1: 751
158. Loscher CE, Draper E, Leavy O, Kelleher D, Mills KH, Roche HM. 2005. Conjugated linoleic acid suppresses NF-κB activation and IL-12 production in dendritic cells through ERK-mediated IL-10 induction. *The Journal of Immunology* 175: 4990-8

159. Aguilera-Montilla N, Chamorro S, Nieto C, Sánchez-Cabo F, Dopazo A, Fernández-Salguero PM, Rodríguez-Fernández JL, Pello OM, Andrés V, Cuenda A. 2013. Aryl hydrocarbon receptor contributes to the MEK/ERK-dependent maintenance of the immature state of human dendritic cells. *Blood* 121: e108-e17
160. Allen CE, Li L, Peters TL, Leung H-cE, Yu A, Man T-K, Gurusiddappa S, Phillips MT, Hicks MJ, Gaikwad A. 2010. Cell-specific gene expression in Langerhans cell histiocytosis lesions reveals a distinct profile compared with epidermal Langerhans cells. *The Journal of Immunology* 184: 4557-67
161. Nourshargh S, Alon R. 2014. Leukocyte migration into inflamed tissues. *Immunity* 41: 694-707
162. Yadav A, Saini V, Arora S. 2010. MCP-1: chemoattractant with a role beyond immunity: a review. *Clinica chimica acta* 411: 1570-9
163. Váradi Z, Bánusz R, Csomor J, Kállay K, Varga E, Kertész G, Csóka M. 2017. effective BraF inhibitor vemurafenib therapy in a 2-year-old patient with sequentially diagnosed Langerhans cell histiocytosis and erdheim–Chester disease. *OncoTargets and therapy* 10: 521
164. Haroche J, Cohen-Aubart F, Emile J-F, Arnaud L, Maksud P, Charlotte F, Cluzel P, Drier A, Hervier B, Benameur N. 2013. Dramatic efficacy of vemurafenib in both multisystemic and refractory Erdheim-Chester disease and Langerhans cell histiocytosis harboring the BRAF V600E mutation. *Blood* 121: 1495-500
165. Mattei P, Alora-Palli M, Kraft S, Lawrence D, Flaherty K, Kimball A. 2012. Cutaneous effects of BRAF inhibitor therapy: a case series. *Annals of oncology* 24: 530-7
166. Hogstad B, Berres M-L, Chakraborty R, Tang J, Bigenwald C, Serasinghe M, Lim KPH, Lin H, Man T-K, Remark R. 2017. RAF/MEK/extracellular signal–related kinase pathway suppresses dendritic cell migration and traps dendritic cells in Langerhans cell histiocytosis lesions. *Journal of Experimental Medicine*: jem. 20161881
167. Glotzbecker MP, Carpentieri DF, Dormans JP. 2004. Langerhans cell histiocytosis: a primary viral infection of bone? Human herpes virus 6 latent protein detected in lymphocytes from tissue of children. *Journal of pediatric orthopedics* 24: 123-9
168. Leahy MA, Krejci SM, Friednash M, Stockert SS, Wilson H, Huff JC, Weston WL, Brice SL. 1993. Human herpesvirus 6 is present in lesions of Langerhans cell histiocytosis. *Journal of investigative dermatology* 101: 642-5
169. Motz GT, Eppert BL, Wortham BW, Amos-Kroohs RM, Flury JL, Wesselkamper SC, Borchers MT. 2010. Chronic cigarette smoke exposure primes NK cell activation in a mouse model of chronic obstructive pulmonary disease. *The Journal of Immunology* 184: 4460-9
170. Jungblut M, Oeltze K, Zehnter I, Hasselmann D, Bosio A. 2009. Standardized preparation of single-cell suspensions from mouse lung tissue using the gentleMACS Dissociator. *Journal of visualized experiments: JoVE*
171. Wortham BW, Eppert BL, Flury JL, Garcia SM, Borchers MT. 2013. TLR and NKG2D signaling pathways mediate CS-induced pulmonary pathologies. *PloS one* 8: e78735
172. Inaba K, Inaba M, Romani N, Aya H, Deguchi M, Ikehara S, Muramatsu S, Steinman R. 1992. Generation of large numbers of dendritic cells from mouse bone marrow cultures supplemented with granulocyte/macrophage colony-stimulating factor. *Journal of Experimental Medicine* 176: 1693-702
173. Motz GT, Eppert BL, Wesselkamper SC, Flury JL, Borchers MT. 2010. Chronic cigarette smoke exposure generates pathogenic T cells capable of driving COPD-like disease in Rag2−/− mice. *American journal of respiratory and critical care medicine* 181: 1223-33
174. Osterburg AR, Nelson RL, Yaniv BZ, Foot R, Donica WR, Nashu MA, Liu H, Wikenheiser-Brokamp KA, Moss J, Gupta N. 2016. NK cell activating receptor ligand expression in lymphangioleiomyomatosis is associated with lung function decline. *JCI insight* 1

175. Borchers MT, Ansay T, DeSalle R, Daugherty BL, Shen H, Metzger M, Lee NA, Lee JJ. 2002. In vitro assessment of chemokine receptor-ligand interactions mediating mouse eosinophil migration. *Journal of leukocyte biology* 71: 1033-41
176. Masson F, Mount AM, Wilson NS, Belz GT. 2008. Dendritic cells: driving the differentiation programme of T cells in viral infections. *Immunology & Cell Biology* 86: 333-42
177. Manches O, Frleta D, Bhardwaj N. 2014. Dendritic cells in progression and pathology of HIV infection. *Trends in immunology* 35: 114-22
178. Didierlaurent A, Goulding J, Hussell T. 2007. The impact of successive infections on the lung microenvironment. *Immunology* 122: 457-65
179. Nair H, Nokes DJ, Gessner BD, Dherani M, Madhi SA, Singleton RJ, O'Brien KL, Roca A, Wright PF, Bruce N. 2010. Global burden of acute lower respiratory infections due to respiratory syncytial virus in young children: a systematic review and meta-analysis. *The Lancet* 375: 1545-55
180. Dawson-Caswell M, Muncie HL, Jr. 2011. Respiratory syncytial virus infection in children. *Am Fam Physician* 83: 141-6
181. Falsey AR, Walsh EE. 2000. Respiratory syncytial virus infection in adults. *Clinical microbiology reviews* 13: 371-84
182. Li F, Zhu H, Sun R, Wei H, Tian Z. 2012. Natural killer cells are involved in acute lung immune injury caused by respiratory syncytial virus infection. *Journal of virology* 86: 2251-8
183. Ebihara T, Masuda H, Akazawa T, Shingai M, Kikuta H, Ariga T, Matsumoto M, Seya T. 2007. Induction of NKG2D ligands on human dendritic cells by TLR ligand stimulation and RNA virus infection. *International immunology* 19: 1145-55
184. Bauer S, Groh V, Wu J, Steinle A, Phillips JH, Lanier LL, Spies T. 1999. Activation of NK cells and T cells by NKG2D, a receptor for stress-inducible MICA. *Science* 285: 727-9
185. Raulet DH. 2003. Roles of the NKG2D immunoreceptor and its ligands. *Nat Rev Immunol* 3: 781-90
186. Groh V, Smythe K, Dai Z, Spies T. 2006. Fas ligand-mediated paracrine T cell regulation by the receptor NKG2D in tumor immunity. *Nature immunology* 7: 755-62
187. Orr MT, Lanier LL. 2010. Natural killer cell education and tolerance. *Cell* 142: 847-56
188. Nice TJ, Coscoy L, Raulet DH. 2009. Posttranslational regulation of the NKG2D ligand Mult1 in response to cell stress. *Journal of Experimental Medicine* 206: 287-98
189. Andoniou CE, van Dommelen SL, Voigt V, Andrews DM, Brizard G, Asselin-Paturel C, Delale T, Stacey KJ, Trinchieri G, Degli-Esposti MA. 2005. Interaction between conventional dendritic cells and natural killer cells is integral to the activation of effective antiviral immunity. *Nature immunology* 6: 1011-19
190. Schwarze J. 2008. Lung dendritic cells in respiratory syncytial virus bronchiolitis. *Pediatr Infect Dis J* 27: S89-91
191. Zitvogel L. 2002. Dendritic and natural killer cells cooperate in the control/switch of innate immunity. *Journal of Experimental Medicine* 195: F9-F14
192. Benvenuti F. 2016. The dendritic cell synapse: a life dedicated to T cell activation. *Frontiers in immunology* 7: 70
193. Zitvogel L, Terme M, Borg C, Trinchieri G. 2006. Dendritic cell-NK cell cross-talk: regulation and physiopathology. In *Immunobiology of Natural Killer Cell Receptors*, pp. 157-74: Springer
194. Owczarczyk AB, Schaller MA, Reed M, Rasky AJ, Lombard DB, Lukacs NW. 2015. Sirtuin 1 Regulates Dendritic Cell Activation and Autophagy during Respiratory Syncytial Virus-Induced Immune Responses. *J Immunol* 195: 1637-46
195. Moore ML, Newcomb DC, Parekh VV, Van Kaer L, Collins RD, Zhou W, Goleniewska K, Chi MH, Mitchell D, Boyce JA, Durbin JE, Sturkie C, Peebles RS, Jr. 2009. STAT1 negatively regulates

lung basophil IL-4 expression induced by respiratory syncytial virus infection. *J Immunol* 183: 2016-26
196. Draghi M, Pashine A, Sanjanwala B, Gendzekhadze K, Cantoni C, Cosman D, Moretta A, Valiante NM, Parham P. 2007. NKp46 and NKG2D recognition of infected dendritic cells is necessary for NK cell activation in the human response to influenza infection. *Journal of Immunology* 178: 2688-98
197. Henry CJ, Ornelles DA, Mitchell LM, Brzoza-Lewis KL, Hiltbold EM. 2008. IL-12 Produced by Dendritic Cells Augments CD8(+) T Cell Activation through the Production of the Chemokines CCL1 and CCL17. *Journal of Immunology* 181: 8576-84
198. Wortham BW, Eppert BL, Motz GT, Flury JL, Orozco-Levi M, Hoebe K, Panos RJ, Maxfield M, Glasser SW, Senft AP, Raulet DH, Borchers MT. 2012. NKG2D mediates NK cell hyperresponsiveness and influenza-induced pathologies in a mouse model of chronic obstructive pulmonary disease. *J Immunol* 188: 4468-75
199. Rölle A, Mousavi-Jazi M, Eriksson M, Odeberg J, Söderberg-Nauclér C, Cosman D, Kärre K, Cerboni C. 2003. Effects of human cytomegalovirus infection on ligands for the activating NKG2D receptor of NK cells: up-regulation of UL16-binding protein (ULBP) 1 and ULBP2 is counteracted by the viral UL16 protein. *Journal of Immunology* 171: 902-8
200. Ruckwardt TJ, Malloy AM, Morabito KM, Graham BS. 2014. Quantitative and qualitative deficits in neonatal lung-migratory dendritic cells impact the generation of the CD8+ T cell response. *PLoS pathogens* 10: e1003934
201. Jang S, Smit J, Kallal LE, Lukacs NW. 2013. Respiratory syncytial virus infection modifies and accelerates pulmonary disease via DC activation and migration. *Journal of leukocyte biology* 94: 5-15
202. Lukens MV, Kruijsen D, Coenjaerts FE, Kimpen JL, van Bleek GM. 2009. Respiratory syncytial virus-induced activation and migration of respiratory dendritic cells and subsequent antigen presentation in the lung-draining lymph node. *Journal of virology* 83: 7235-43
203. Boogaard I, Van Oosten M, Van Rijt LS, Muskens F, Kimman TG, Lambrecht BN, Buisman AM. 2007. Respiratory syncytial virus differentially activates murine myeloid and plasmacytoid dendritic cells. *Immunology* 122: 65-72
204. Johnson TR, Johnson CN, Corbett KS, Edwards GC, Graham BS. 2011. Primary human mDC1, mDC2, and pDC dendritic cells are differentially infected and activated by respiratory syncytial virus. *PloS one* 6: e16458
205. Kallal LE, Schaller MA, Lindell DM, Lira SA, Lukacs NW. 2010. CCR6 deficiency enhances immunity to respiratory syncytial virus by impairing recruitment of T helper type II-skewing dendritic cells. *European journal of immunology* 40: 1042-52
206. Furuhashi K, Suda T, Hasegawa H, Suzuki Y, Hashimoto D, Enomoto N, Fujisawa T, Nakamura Y, Inui N, Shibata K. 2012. Mouse lung CD103+ and CD11bhigh dendritic cells preferentially induce distinct CD4+ T-cell responses. *American journal of respiratory cell and molecular biology* 46: 165-72
207. Moll H. 2003. Dendritic cells and host resistance to infection. *Cellular microbiology* 5: 493-500
208. Guan H, Moretto M, Bzik DJ, Gigley J, Khan IA. 2007. NK cells enhance dendritic cell response against parasite antigens via NKG2D pathway. *J Immunol* 179: 590-6
209. Wang SZ, Bao YX, Rosenberger CL, Tesfaigzi Y, Stark JM, Harrod KS. 2004. IL-12p40 and IL-18 modulate inflammatory and immune responses to respiratory syncytial virus infection. *J Immunol* 173: 4040-9

210. Guerra N, Tan YX, Joncker NT, Choy A, Gallardo F, Xiong N, Knoblaugh S, Cado D, Greenberg NR, Raulet DH. 2008. NKG2D-deficient mice are defective in tumor surveillance in models of spontaneous malignancy. *Immunity* 28: 571-80
211. Boukhvalova MS, Yim KC, Prince GA, Blanco JC. 2010. Methods for Monitoring Dynamics of Pulmonary RSV Replication by Viral Culture and by Real-Time Reverse Transcription–PCR In Vivo: Detection of Abortive Viral Replication. *Current Protocols in Cell Biology*: 26.6. 1-.6. 19
212. Weiss KA, Christiaansen AF, Fulton RB, Meyerholz DK, Varga SM. 2011. Multiple CD4+ T cell subsets produce immunomodulatory IL-10 during respiratory syncytial virus infection. *J Immunol* 187: 3145-54
213. Osterburg AR, Nelson RL, Yaniv BZ, Foot R, Donica WR, Nashu MA, Liu H, Wikenheiser-Brokamp KA, Moss J, Gupta N. 2016. NK cell activating receptor ligand expression in lymphangioleiomyomatosis is associated with lung function decline. *JCI insight* 1: e87270
214. Barber MA, Zhang T, Gagne BA, Sentman CL. 2007. NK cells negatively regulate antigen presentation and tumor-specific CTLs in a syngeneic lymphoma model. *J Immunol* 178: 6140-7
215. Molfetta R, Quatrini L, Santoni A, Paolini R. 2017. Regulation of NKG2D-Dependent NK Cell Functions: The Yin and the Yang of Receptor Endocytosis. *International journal of molecular sciences* 18: 1677
216. Bogunovic M, Ginhoux F, Helft J, Shang L, Hashimoto D, Greter M, Liu K, Jakubzick C, Ingersoll MA, Leboeuf M. 2009. Origin of the lamina propria dendritic cell network. *Immunity* 31: 513-25
217. Nakano H, Burgents J, Nakano K, Whitehead G, Cheong C, Bortner C, Cook D. 2013. Migratory properties of pulmonary dendritic cells are determined by their developmental lineage. *Mucosal immunology* 6: 678